BIOCHEMICAL ANALYSIS OF THE INTERACTION BETWEEN TRANSFER-RIBONUCLEIC ACID AND EXPORTIN-T

Dissertation

zur Erlangung des Grades Doktor der Naturwissenschaften
- Dr. rer. nat.-

der Fakultät für Biologie, Chemie und Geowissenschaften
der Universität Bayreuth

vorlegt von

Sheng Li

aus Liaoning

Bayreuth 2006

Die vorliegende Arbeit wurde in der Zeit von December 2002 bis Juni 2006 am Lehrstuhl für Biochemie der Universität Bayreuth unter der Leitung von Herrn Prof Dr. Mathias Sprinzl angefertigt.

Vollständiger Abdruck der von der Fakultät Biologie, Chemie und Geowissenschaften der Universität Bayreuth genehmigten Dissertation zu Erlangung des Grades eines Doktors der Naturwissenschaften

- Dr. rer. nat.-

Promotionsgesuch eingericht am:	2. August 2006
Tag des wissenschaftlichen Kolloquiums:	3. November 2006

Erster Gutachter:	Prof. Dr. M. Sprinzl
Zweiter Gutachter:	Prof. Dr. G. Krauss

Abbreviations

Amino acids are abbreviated with the three-letter abbreviation.

Å	Angstrom, 10^{-10} meter
A_{xyz}	Absorption at xyz nm
aaRS	Aminoacyl-tRNA synthetase
aa-tRNA	Aminoacyl-tRNA
AFM	Atomic force microscopy
Amp	Ampicilin
APS	Ammoniumperoxodisulfate
ATP	Adenosine-5′-triphosphate
BAP	Bacterial alkaline phosphatase
BP	Bromophenol blue
BSA	Bovine serum albumin
BTFK	3-Butylsulfanyl-1,1,1-trifluoro-propan-2-one
cpm	Count per minute
ddH_2O	Double distilled water
DEAE	Diethylaminoethyl-
DMF	N, N-dimethyl foramide
DNA	Deoxyribonucleic acid
DTE	Dithioerythritol
DTT	Dithiothreitol
E.coli	*Escherichia coli*
EDTA	Ethylenediaminetetraacetate
eEF1A	Eukaryotic elongation factor 1A
EF-Tu	Elongation factor Tu
EMSA	Electrophoretic mobility shift assay
FPLC	Fast performance liquid chromatography
GOPTS	Glycidyloxypropyl-trimethoxysilan
GDP	Guanosine-5′-diphosphate

GMP	Guanosine-5′-monophosphate
GppNHp	5′-Guanylyl-imido-diphosphate
GTP	Guanosine-5′-triphosphate
HPLC	High performance liquid chromatography
H.s.	*Homo sapiens*
IPTG	Isopropyl-β-D-thiogalactoside
K_D	Dissociation constant
kDa	Kilodalton
MDa	Megadalton
mRNA	Messenger RNA
NES	Nuclear export signal
Ni-NTA	Ni^{2+}-nitriloacetic acid
NLS	Nuclear localization signal
NPC	Nuclear pore complex
NTase	ATP(CTP):tRNA nucleotidyltransferase
PAGE	Polyacrylamide gel electrophoresis
PMSF	Phenylmethylsulfonylfluoride
RanGEF	Ran guanine nucleotide exchange factor
RanBP1	Ran binding protein 1
RCC1	Regulator of chromosome condensation
RNase	Ribonuclease
rpm	Revolution per minute
rRNA	Ribosomal RNA
Pu	Purine
Py	Pyrimidine
R_g	Radius of gyration
SAP	Shrimp alkaline phosphatase
SDS	Sodium dodecylsulfate
s^4U	4-thiouridine
$(s^4U)\ tRNA^{Phe}_{T.th}$	s^4U containing $tRNA^{Phe}_{T.th}$ transcript

S. c	*Saccharomyces cerevisiae*
TBE	Tris/Borate/EDTA
TEMED	N,N,N′,N′-Tetramethylenediamine
TFK	Trifluoromethyl ketone
TLC	Thin layer chromatography
T.th	*Thermus thermophilus*
Tris	Tris(hydroxymethyl)aminomethane
tRNA	Transfer RNA
uv	Ultraviolet light
XC	Xylene cyanol
Xpo-5	Exportin-5
Xpo-t	Exportin-t

Contents

1 Introduction

1.1 Nucleocytoplasmic transport in eukaryotic cells

Eukaryotes appeared 2 billion years later than prokaryotes on the earth and developed some decisive characteristics, one of which is the compartmentalization of the cell. Sequestering highly specific biochemical reactions to different membrane-enclosed regions leads to higher efficiency for eukaryotes, however also poses a serious problem: it requires material and informational communications among the compartments, especially between nucleus and cytoplasm. All nuclear proteins are made in the cytoplasm and must be imported to the nucleus. RNAs are transcribed in nucleus and most of them are exported to cytoplasm. Many proteins shuttle continuously between nucleus and cytoplasm. It was estimated that more than 1 million macromolecules per minute are transferred between them in a growing mammalian cell (Görlich *et al.,* 1996).

The barrier between nucleus and cytoplasm is a double lipid bilayer of membranes — nuclear envelope (NE) — embedded with nuclear pore complexes (NPC), the gateway of nucleocytoplasmic transport. Each of these giant complexes, about 125 MDa in vertebrates (Reichelt *et al*., 1990), consists of 50 to 100 distinct polypeptides called nucleoporins. The NPC displays eightfold symmetry perpendicular to the membrane, and is composed of 8 spoke-ring complexes sandwiched between nuclear and cytoplasmic rings with eight fibrils of about 50 nm into the cytoplasm and a nuclear basket-like structure stretching up to 100 nm on the nucleoplasmic side (Fahrenkrog *et al.*, 2001, Cullen *et al.,* 2003). The NPC forms an aqueous channel of 9 nm in diameter. Theoretically small proteins (≤40 kDa) and small RNAs can diffuse through the NPC, but this is not the case. Rather, most proteins and all known RNAs transport through NPCs via an active and signal-mediated process. NPC can expand itself to accommodate particles up to 40 nm during active transport (Kiseleva *et al*., 1998).

It is obvious that not all proteins produced in the cytoplasm are imported to the nucleus. There must be some recognizable difference between protein cargoes and other

proteins remaining in the cytoplasm. The pioneering analyses on two protein cargoes of nucleoplasmin and simian virus 40 (SV40) large-T antigen led to the discovery of a short sequence of basic amino acids (P***KKKKRK*** in SV40 large-T antigen, and ***KR***PAATKKAGQA***KKKK***LD in nucleoplasmin), which contribute crucially to nuclear import of the two proteins and are the archetypes for monopartite and dipartite nuclear localization signal (Dingwall *et al.*, 1982, Kalderon *et al.*, 1984). Now nuclear localization signal is known to be present in thousands of different proteins as the identification card for nuclear entry.

It was found that nuclear import required saturable carriers. After crosslinking of a nuclear localization signal (NLS) to human serum albumin, the conjugates, at high concentration, competitively inhibited nuclear import of NLS-bearing proteins (Goldfarb *et al*., 1986). A great technological advance in studying nuclear protein import has been the selective permeabilisation of the cholesterol-rich plasma membrane with digitonin (Adam *et al.*, 1990). After such treatment the cells were depleted of their soluble cytosol and intact nuclei were obtained *in vitro*. Fractionalized cytosol portions were added to the nuclei to identify the soluble factors required for NLS-protein import. The key players, namely Ran, importin α, importin ß were thus discovered (Görlich 1998, Mattaj *et al.*, 1998). In a classical import pathway, importin α binds the substrate protein through recognition of the NLS, then the complex is carried by importin ß (also known as karyopherin ß1) and docked at the cytoplasmic face of the NPC. After an energy-dependent NPC translocation, the complex enters into nucleus, where binding of Ran·GTP to importin ß disassembles the ternary complex.

In the subsequent studies a series of importin ß like proteins were identified. These importin ß homologs are categorized into a protein family called importin ß family (karyopherin ß family). There are 14 members in yeast and more than 20 in mammalian cells, which have similar molecular weights (90 – 150 kDa) and isoelectric points (4.0 – 5.0), and are composed of multiple tandem helical repeats termed HEAT repeats (proteins Huntington, Elongation Factor 3, PR65/A, TOR characterized with this typical helical repeat) (Chook *et al.*, 2001). Except the yeast karyopherin142/Msn5 (Karyopherin is another name for importin and exportin) and mammalian importin 13, all of the other carriers function exclusively either as importins or as exportins. Exportin 1 in budding

yeast (Crm1) was the first exportin to be identified (Fornerod *et al.*, 1997). It recognizes a short motif rich in leucine or related hydrophobic residues, which is found in the protein kinase A inhibitor and dozens of other proteins. **L**xxx**L**xx**L**x**L** is the prototypical nuclear export signal (NES) sequence (Macara 2001). In nucleus, Crm1 binds its cargoes with the help of Ran·GTP, the ternary complex then enters cytoplasm via NPC, where hydrolysis of Ran·GTP disassembles the complex (Askjaer *et al.*, 1998).

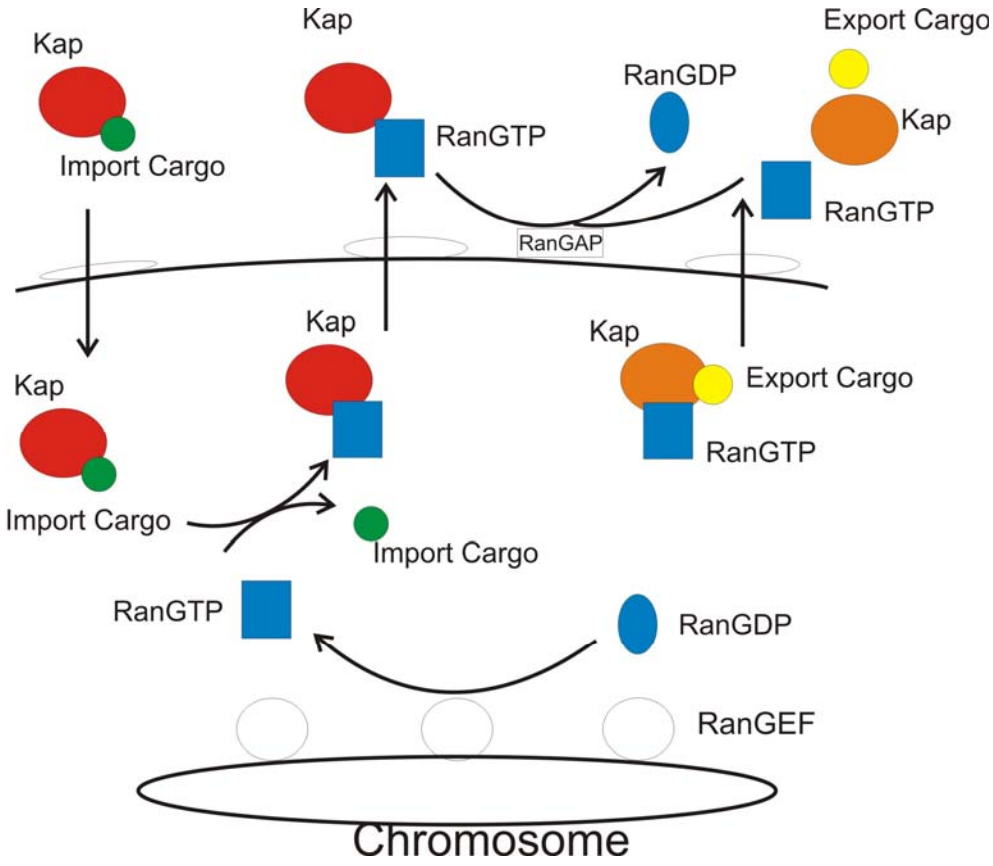

Fig. 1.1 The nuclear import and export cycle

During import, Kaps (importins) bind to their cargo in the cytoplasm and come across the nuclear pore complex (NPC). In the nucleus, binding of Ran·GTP to Kaps leads to release of the cargo, and the Kap–Ran·GTP complex recycles back to the cytoplasm. After hydrolysis Ran·GDP parts with Kaps. During export, Kaps (exportins) bind to their cargo and Ran·GTP in the nucleus. After arriving in cytoplasm, hydrolysis of Ran·GTP to Ran·GDP leads to disassembly of the complex. A gradient of Ran·GTP is produced by charging Ran with GTP by RanGEF in nucleus and hydrolysis of Ran·GTP by RanGAP in cytoplasm. Free Ran·GDP is imported by Ntf2 back into nucleus.

Ran·GTP plays a vital role in the nuclear transport by promoting the assembly of export complexes and disassembles the import complexes. The directionality of nuclear transport is maintained by the unbalanced distribution of Ran·GTP across the nuclear envelope. Charging Ran with GTP in nucleus requires a protein regulator named Ran nucleotide exchange factor RCC1 (regulator of chromosome condensation) which binds to chromatin through H2A and H2B (Nemergut *et al.*, 2001). To accelerate Ran·GTP hydrolysis in cytoplasm, Ran GTPase-activating protein (RanGAP) on the cytosolic face of the nuclear pore is involved (Quimby *et al.*, 2003). Another cytosolic protein regulator Ran binding protein 1(RanBP1) increases the rate of RanGAP1-mediated nucleotide hydrolysis *in vitro* (Schlenstedt *et al.*, 1995) and is essential for hydrolysis of Ran·GTP bound to nuclear transport receptors (Bischoff *et al.*, 1997). Not only deciding the transport direction, Ran system also pays for the energy cost required in this active process. One GTP is consumed per cycle. To complete the Ran·GTP cycle, cytosol-generated Ran·GDP is transported by an importin named Ntf 2 into the nucleus. Nucleocytoplasmic transport is depicted in Fig. 1.1 (Mosammaparast *et al.*, 2004).

RNAs, transcribed in nucleus, have to function or accept further modifications in cytoplasm, and are the major export cargoes (Cullen 2003, Rodriguez *et al.*, 2004). Exportin-1 was found to export late HIV-1 mRNAs, but not the major exportin for host mRNAs, because the mRNA export pathway cannot be influenced by leptomycin (LMB), the specific inhibitor of exportin-1 (Fornerod *et al.*, 1997). Quite interestingly, export of most mRNAs is independent of Ran and transportin systems. The key mediator of bulk mRNA export is a heterodimer of Tap and a small cofactor termed Nxt or p15 (Kang *et al.*, 1999), and their yeast homologs are Mex67p and Mtr2p respectively. Crm1 still plays a vital role in RNA export. The U snRNAs (critical to splicing pre-mRNAs), rRNAs in the form of 60S and 40S preribosomal units are exported in an exportin-1 dependent way (Ohno *et al.*, 2000, Gadal *et al.*, 2001, Moy TI *et al.*, 1999). It is worth noting that rRNA and snRNAs don't directly bind exportin-1, instead bind to the related protein cargoes that are exported by exportin-1 to their destination. tRNA was found to be exported by an exportin named exportin-t (Xpo-t), which is the first member of importin ß family to bind directly to a RNA molecule, hence receiving great attention.

However, as the research on nuclear transport is advancing, it is found that the events are far from such simplicity. Importin ß binds different protein cargoes by using different binding sites and adopting distinct conformations (Mosammaparast *et al.*, 2004). Several importins despite their low sequence similarity can recognize and import the same cargo. At least 4 import pathways are used to import core histone in both yeast and mammalians (Muhlhausser *et al.*, 2001). Furthermore, the latest observations suggest that transportins play important roles in cellular activities other than nuclear traffic. Biochemical approaches showed that importin α/ß heterodimer can inhibit microtubule polymerization (Wiese *et al.*, 2001). In *Xenopus* meiotic egg extracts, addition of Ran·GTP, which can dissociate importin α and ß, induces the formation of microtubule asters during mitosis (Carazo-Salas *et al.*, 1999). The opposing functions of Ran·GTP and Importin ß during mitosis were also seen in nuclear envelope and NPC assembly (Mosammaparast *et al.*, 2004). Crm1 has also been reported to display regulatory functions during S phase (Yamaguchi *et al.*, 2003). Transportins act beyond transport and are important regulators.

1.2 tRNA —— the translating molecules

Genetic information flows from nucleic acid to protein via translating nucleotide triplets in mRNA to amino acids in polypeptide. A kind of RNA molecules termed transfer RNA (tRNA) has evolved to bridge the structural incongruity between trinucleotides and amino acid. Consisting of 70 – 93 nucleotides, a tRNA molecule has five domains: acceptor stem, D-stem and loop, anticodon arm and loop, and TΨC-arm and loop, extra loop (Fig. 2). The acceptor stem and TΨC-arm stack each other forming a continuous A-helix, while the D-arm and anticodon arm form another continuous helix. The two helixes pose each other to an "L" shape. On one end of "L" is anticodon, which base pairs to the codon in mRNA; on the other end is an amino acid attached (Fig. 3).

Because there is no direct interaction between amino acid and anticodon, the tertiary structure of tRNA is of critical importance to fidelity of translation.

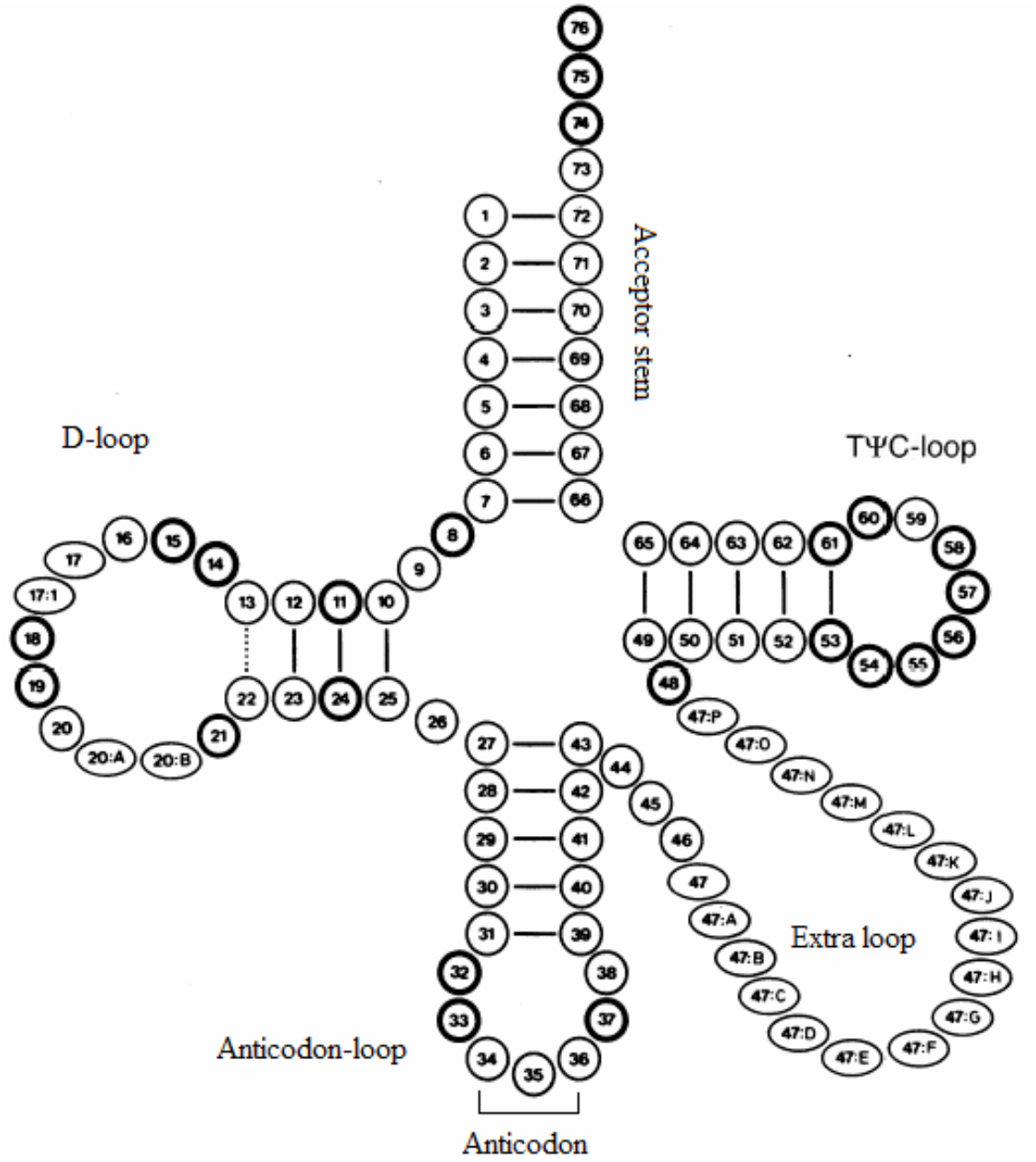

Fig. 1.2 Classical cloverleaf structure with numbering of nucleotides (Sprinzl *et al.*, 1984)

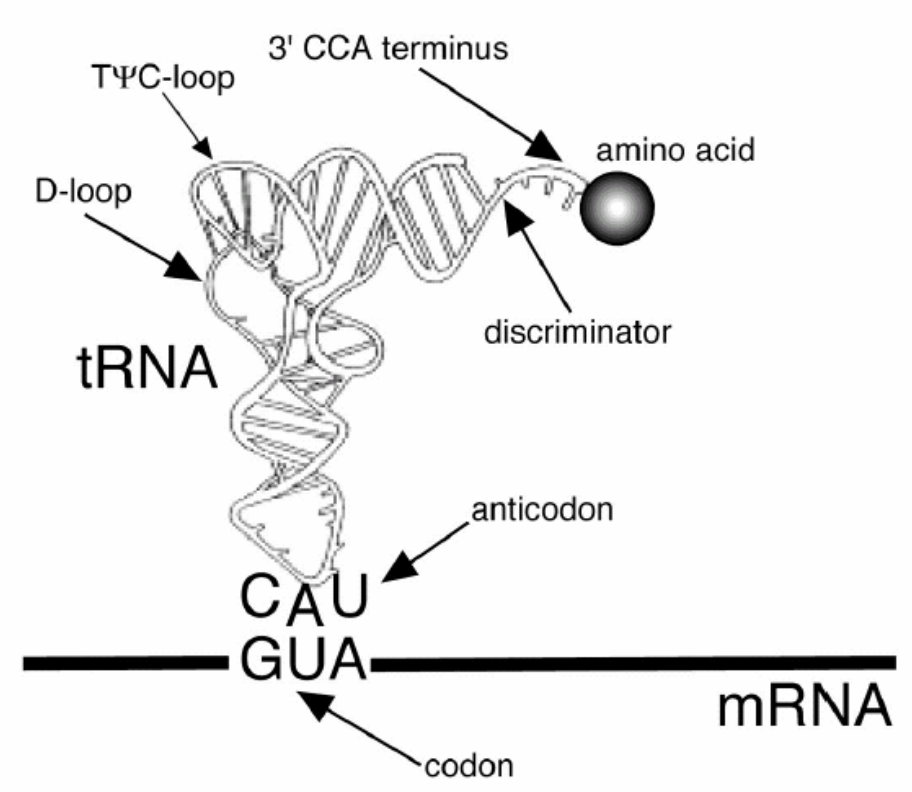

Fig. 1.3 The L-shaped tertiary structure of tRNA (adapted by Nakanishi *et al.*, 2005 from Kim *et al.*, 1973)

tRNA is initially transcribed by RNA polymerase III (in eukaryote) as functionless pre-tRNA with extra 5′ and 3′ sequence; some are even interrupted by introns. Maturation of tRNAs normally includes a series of processing steps, removal of 5′ and 3′ sequences, modification of specific nucleotide residues, and excision of introns, addition of CCA end (Nakanishi *et al.*, 2005). To date the primary structures of more than 3000 tRNAs from three kingdoms have been published (Sprinzl *et al.*, 2005) since the first tRNA was sequenced in 1965 (Holley *et al.*, 1965). Though tRNA functions in an extremely conservative way, comparison of tRNA sequences was not very informative. In the first 113 structures sequenced 108 are different. The biological significance of invariant and semi-invariant nucleotides at certain positions in tRNAs became evident only after the tertiary structure of tRNAs was discovered (Kim *et al.*, 1973). All cytoplasmic tRNAs are likely to assume the overall shape of an "L" with each arm being approximately 60 Å long and 20 Å thick. Most of the invariant and semi-invariant bases in all tRNAs are

involved in forming tertiary hydrogen bonds essential for maintaining the L-shaped three dimensional structure (Kim, 1979). In mammalian tRNAs, the nucleotides in which no exceptions were found are U9, Y11, G18-G19, Pu24, Py25, Py32, Pu37, G53, U55, C56, A58, and C74-C-A (Dirheimer *et al.*, 1995). The primary structure of tRNA is malleable to evolution and variation. However, after one change occurred in tRNA, other changes are often introduced to compensate the influence of the former change on the tertiary structure. In yeast $tRNA^{Phe}$, an A-U base pair in the acceptor stem is replaced in one of its isoacceptors by G-C pair ((Dirheimer *et al.*, 1995). Based on *in vivo* selection of effective suppressor tRNAs from two different combinatorial gene libraries in which several nucleotides in the D and T-loops were randomized, Zagryadskaya *et al.* showed that the position of the reverse-Hoogsteen base-pair of 54-58 in the T-loop covaried with the length of the D-domain (Zagryadskaya *et al.*, 2004).

tRNA is the most extensively modified nucleic acid in the cell, and has about 10% rare nucleotides. In general, modified nucleotides contribute to a compact native tRNA conformation. The level of tRNA modification influences the activity and specificity of tRNA in translation (Björk GR, 1992). However, most modified nucleosides in tRNA are not essential for the aminoacylation reaction. Unmodified tRNAs after aminoacylation were able to bind EF-Tu (Harrington *et al.*, 1993). The overall shapes of unmodified and native tRNAs are similar. Thermal denaturation studies indicated that the unmodified tRNAs generally required higher concentration of Mg^{2+} to achieve thermal stabilities comparable to the corresponding native sequences. Collectively, these results suggested that modified bases were not essential for tertiary folding, but instead modulated the stability of tertiary structure (Davonloo *et al.*, 1979, Maglott *et al.*, 1998).

tRNA requires protein binding at its functional sites at different steps. Some of them, i.e. elongation factor EF-Tu (Nissen *et al.*, 1995), the CCA-adding enzyme (Shi *et al.*, 1998), exportin-t takes all tRNAs as substrate, and recognizes universally conserved structural features of tRNAs, whereas others, for example, aminoacyl-tRNA synthetases (Giegé *et al.*, 1993) and some tRNA modifying enzymes (Edqvist *et al.*, 1993) function on a specific tRNA species and must distinguish one from other tRNAs.

The molecular recognition of tRNA and protein is vital to cell, thus interesting to us. EF-Tu, the elongation factor that brings aminoacylated tRNA to A site of ribosome,

interacts primarily with five regions of aa-tRNA, namely, the amino acid residue, the CCA end, the acceptor stem, the T stem, and the variable loop (Sprinzl *et al.*, 1993). The 3′ aminoacylated end of tRNA is the most important for the interaction with EF-Tu·GTP (Faulhamer *et al.*, 1987). EF-Tu can sharply discriminate aa-tRNA from free tRNA. An efficient chromatographic method has been developed based on this property to separate aminoacyl-tRNA from other uncharged tRNA (Derwenskus *et al.*, 1984). Sec-tRNA^{Sec} inserts the 21st amino acid selenocysteine on the UGA codon. tRNA^{Sec} is unusual to other 20 tRNA species. In *E.coli*, it is the longest tRNA (95 nucleotides), with 8 base pair acceptor arm (other tRNAs have 7 base pair acceptor arm) and a large extra loop. Unlike other tRNAs, in *E.coli* it is brought to A site in ribosome not by EF-Tu, but by a protein SELB (68 kDa), which shows significant sequence similarity with EF-Tu (43 kDa) (Forchhammer *et al.*, 1991). Ser-tRNA^{Sec} shows affinity to EF-Tu nearly 100 times lower than that of Ser-tRNA^{Ser} (Förster *et al.*, 1990). The reduction of the 8 bp aminoacyl-acceptor stem of tRNA^{Sec} to the standard length of 7 renders the tRNA mutant able to bind EF-Tu, but no more able to bind SELB (Baron *et al.*, 1991). The length of aminoacyl-acceptor stem is a major structural determinant of tRNA for binding EF-Tu. Another tRNA unable to bind EF-Tu is initiator tRNA, which doesn't enter A site in ribosome. Initiator tRNA has marked structural differences from other elongator tRNAs. It is worth noting that eubacterial initiator tRNA and tRNA^{Sec} have Pu11-Py24 base pair instead of Py11-Pu24 in other tRNAs (Dube *et al.*, 1968, Leinfelder *et al.*, 1988, Leibundgut *et al.*, 2005).

There are 20 aminoacyl-tRNA synthetases (aaRS), one for each amino acid and the corresponding tRNA. In each tRNA several specific nucleotides are crucial to tRNA recognition, and these residues are termed as determinants. If these specific residues were replaced by other nucleotides, the corresponding aa-RS would not recognize the tRNA any more. More interestingly, if the determinant nucleotides of one tRNA were introduced into another tRNA, the mutated tRNA would be misaminoacylated as the determinants determined. U73 and G2-C71 base pair are the determinants of *E.coli* tRNA^{Gly}. After introducing them into amber-suppressor tRNA^{Phe}, tRNA^{Arg}, tRNA^{Lys}, and tRNA^{Gln} these suppressor tRNAs are successfully charged by GlyRS with glycine (McClain *et al.*, 1991).

1.3 Distribution of tRNA species in a cell

There are 40 to 50 tRNA species in a cell. *Escherichia coli* has 79 tRNA genes coding for 46 amino acid acceptor species (Komine *et al.*, 1990). The situation is more complicate in eukaryotes, which have not only tRNAs transcribed in nucleus but also those produced by mitochondria and chloroplast themselves. In human cells 497 tRNA genes of nuclear origin have been found (Lander *et al.*, 2001), whereas in mitochondria, 22 tRNA genes are sufficient to decode 20 amino acids. Mitochondria tRNAs take different conformations from the canonical structure of cytoplasmic tRNAs. The absence of the complete D-arm was reported for several mammalian mt $tRNA^{Ser}_{AGY}$. More moderate deviations from the canonical cloverleaf, including changes in the number of nucleotides at the connectors as well as shortening of the D- and/or T-stems and loops, and/or elongated anticodon stems, have also been reported (Steinberg *et al.*, 1994). The concentrations of tRNA species and their aminoacyl synthetases have physiological importance. *E. coli* $tRNA^{Tyr}$, normally aminoacylated with tyrosine *in vivo*, is esterified by glutamine in response to an elevation of the intracellular concentration of GlnRS; this effect is reversed by the additional overproduction of either TyrRS or $tRNA^{Gln}$ (Sherman *et al.*, 1992).

Normally more than one tRNA isoacceptors are responsible for incorporation of one amino acid. What is the significance and function of multiple tRNA isoacceptors? This is an interesting topic. In *E.coli*, it has been found that one codon in each synonymous set of codons is predominantly used in genes and this codon is often read by the most abundant tRNA isoacceptors. This arrangement of biased codon usage and the matching tRNA abundance has been viewed as an optimal arrangement for bacteria to maximize the efficiency of translation (Dong *et al.*, 1996). Different tRNA isoacceptors and codons have different biological missions in *E.coli*. It has been shown that tRNA species with the smallest ratio between tRNA concentration and codon frequency are the most sensitive to amino acid starvation, and the codons they read are used in control loop that regulates the synthesis of the missing amino acid. Whereas those codons, read by tRNAs that retain high charging levels during starvation for their cognate amino acids, are the most used in

amino acid synthetase (Elf *et al.*, 2001, Dittmar *et al.*, 2005). It seems very likely that different tRNA species act differently in cells.

1.4 Nuclear export of tRNA

Born in nucleus, nuclear tRNAs have to go through the barrier of nuclear envelope to its destination in cytosol, and to deliver the proper amino acids to the growing peptide chain. Though tRNAs can diffuse across the nuclear envelope theoretically, it was found long ago that tRNA export was a saturable and thus a carrier-mediated process (Zasloff, 1983). Furthermore, injection of excess tRNA into nucleus only saturated tRNA export but not those of other RNAs suggesting that tRNA export was mediated by a class-specific carrier (Jarmolowski *et al.*, 1994). Microinjection of RanGAP into the nucleus depleted nuclear Ran·GTP and blocked tRNA export (Izaurralde *et al.*, 1997), indicating that the protein involved in tRNA export may be a member of importin ß family. Görlich's group identified Ran·GTP-binding proteins from HeLa cell extracts by systematically sequencing proteins that were isolated by affinity chromatography on immobilized Ran·GTP. One of the novel importin ß-like proteins turned out to be particularly interesting: it bound immobilized Ran·GTP in the presence of tRNA and was named as exportin-t. Microinjection experiments in *Xenopus* oocytes confirmed exportin-t as the rate-limiting factor for export of all tRNAs tested (Arts *et al.*, 1998a, Kutay *et al.*, 1998).

Kinetic analyses showed that binding of Ran·GTP and tRNA to exportin-t is highly cooperative. Ran·GTP increases the affinity of exportin-t for tRNA roughly 300 fold and *vice versa* (Kutay *et al.*, 1998). Although as a mammalian protein, exportin-t could also specifically bind to tRNAs from *E.coli* and yeast (Lipowsky *et al.*, 1999). Exportin-t preferentially binds mature tRNAs. Other premature tRNAs such as unmodified tRNA , tRNA with 10 nt 5′ extension, tRNA with 10 nt 3′ extension, with 10 nt 5′ extension and 10 nt 3′ extension, tRNA without 3′-CCA end showed 18%, 2.4%, 7.2%, 0.8%, 2.4% of binding affinity respectively, when compared with mature tRNA (Lipowsky *et al.*, 1999). End processing of tRNA is important for efficient tRNA export. However, $tRNA^{Ser}$

lacking the 3′ CCA end showed reduced, but not annulled binding ability to exportin-t. The presence of an intron in the anticodon loop did not affect tRNA·exportin-t·Ran·GTP interaction *in vitro*. Aminoacylation is not a prerequisite for tRNA transport either. A $tRNA^{Phe}$ mutant poorly aminoacylated was able to be exported, though the export rate was lower than wild type $tRNA^{Phe}$ (Arts *et al.*, 1998b). It was suggested that aminoacylation may increase export efficiency (Lund *et al.*, 1998).

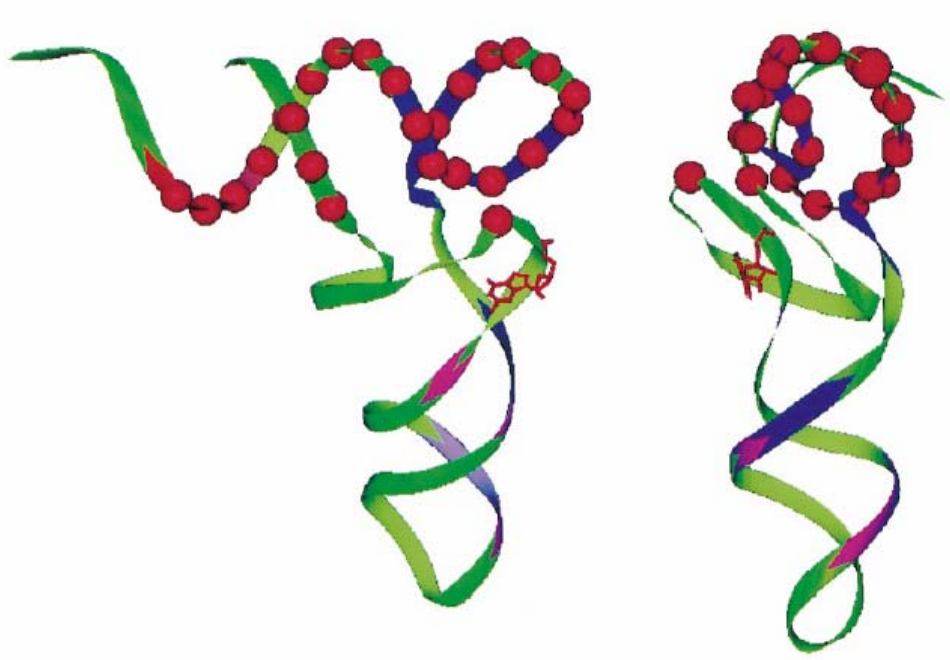

Fig. 1.4 The major contact sites of tRNA to exportin-t shown in protection experiments (Arts *et al.*, 1998b)
Riboses protected by Exportin-t and/or Ran·GTP are red spheres. Phosphates whose modification interferes with their binding are blue ribbons. The region protected against RNase T1 degestion is red, and purple ribbon represents increased accessibility to RNase V1.

Mattaj's group undertook a series of biochemical experiments to study the binding of tRNA to exportin-t (Arts *et al.*, 1998b). In footprinting experiment, Fe/EDTA was used to cleave the ribose rings and identify the accessible nucleotide residues in the exportin-t·tRNA·Ran·GTP complex. The riboses between 50 and 71 were significantly protected by exportin-t and/or Ran·GTP, positions 4 – 6 and 17 were also protected, positions 18, 47 – 49 and 72 were mildly protected. In contrast, riboses between 7 – 16 and 19 – 46

were cleaved equally whether there were exportin-t and Ran·GTP or not. Such results indicated that acceptor and T-domain might be the contact sites between exportin-t and tRNA. In RNase V1 (which cuts double-stranded helical regions in RNA) probing experiments, a partial protection of acceptor arm was demonstrated. Interestingly, the extent of cleavages occurred in the anticodon stem positions (28-30) and the D arm (position 22) were enhanced. This suggested that binding of tRNA and exportin-t results in a conformational change in tRNA. From phosphate ethylation-binding interference experiment, phosphates at positions 49, 56, 57, 59 and 62 in T domain might be in close contact with exportin-t/Ran·GTP. The major contact sites of tRNA and exportin-t in protection experiment are shown in Fig. 4. In another paper of Mattaj group (Kuersten *et al.*, 2002), a series of proteins with N- and C-terminal deletions were generated to test their ability to form an export complex with Ran·GTP and tRNA. Removal of the C-terminal of exportin-t eliminated the tRNA interaction but not the ability to bind Ran·GTP. Removal of the N-terminal affected both binding activities. Thus it is likely that tRNA binds to the C-segment of exportin-t.

Los1p is the homolog of exportin-t in *S. cerevisiae* and is likewise involved in the Ran·GTP dependent nuclear export of tRNA (Hellmuth *et al.*, 1998). However, disrupting the los1 gene did not cause any apparent growth defect (Hurt *et al.*, 1987), suggesting that other tRNA export pathways exist in yeast. It has been found later that a new tRNA export pathway in yeast is aminoacylation dependent (Grosshans *et al.*, 2000), and another protein carrier Msn5p can export aminoacylated tRNA (Yoshida *et al.*, 2001). Double mutation of msn5p and los1p genes is seriously defective in export of tRNA. It is proposed that the nuclear tRNA aminoacylation-dependent pathway may be the principal route used to export tRNA in *Saccharomyces cerevisiae* (Steiner-Mosonyi *et al.*, 2004). The mammalian homolog of Msn5P is exportin-5, an importin ß family member initially found to export minihelix containing RNAs (This structural motif are present in small RNA transcripts by RNA polymerase III, consisting of a double-stranded stem with a base-paired 5' end and a protruding 3' end). Xpo-5 exports tRNA and eEF1A (eukaryotic homolog of EF-Tu) simultaneously, and amioacylated tRNA is the bridge of these two proteins (Bohnsack *et al.*, 2004). But this aminoacylation-dependent pathway is not the major route in higher eukaryotes. Probably, the weight of tRNA export pathway has

shifted from aminoacylation dependent pathway by Msn5p in yeast gradually to the aminoacylation independent pathway by exportin-t in mammalians.

1.5 4-Thiouridine —— an ideal intrinsic photoaffinity crosslinking agent

Besides X-ray crystallography and nuclear magnetic resonance techniques, photocrosslinking is a powerful tool to resolving the structural questions over nucleic acid-protein interaction (Favre *et al.*, 1998). Intrinsic photoactivable probe, which ideally should be a base or amino acid analog incorporated within the RNA (or ribonucleoprotein) with a minimum of structural perturbation. The analog of uridine, 4-thiouridine (s^4U), discovered in 1965 as a rare nucleoside present at position 8 of *E. coli* tRNA (Lipsett, 1965), is a suitable agent for three reasons among photolabel candidates used in RNA structure study. Firstly, incorporation of 4-thiouridine into RNA is easily achieved through T7 *in vitro* transcription system. Secondly at a low ratio of 4-thiouridine to normal uridine it causes only minor changes over the RNA structure, thus not affecting its biological function too much (Kumar *et al.*, 1997). Thirdly, s^4U can be selectively excited between 330 nm and 370 nm thus keeping undesirable side reaction at a minimum.

In neutral aqueous medium, 4-thiouracil is essentially in the 2-keto-4-thione form. The thione group is expected to have larger polarizability and more steric hindrance than the 4-keto group of uridine. C—S bond is 0.4 to 0.8 Å than the C—O bond, and in the case of Watson-Crick A-U base pair the NH…O bond (2.9 Å) is replaced by an NH…S bridge of 3.4 Å. Mild oxidation efficiently converts s^4U into its disulfide form. Hydrolyzing s^4U at acidic or basic pH yields uridine, while treating s^4U with NH_3 produces cytidine. s^4U strongly absorbs light in the near-UV range (λ = 330 nm). Irradiation at this wavelength directly populates the singlet state S_2 ($\pi\pi^*$) which rapidly decays and efficiently converts to the corresponding lowest ($\pi\pi^*$) triplet state T_1. This state gives rise in solution to a room-temperature phosphorescence (λ_{max} = 550 nm, $\Phi \approx 3 \times 10^{-4}$) which decays with a lifetime (τ) of 200 ns in aerated solution at room temperature.

The high interconversion yield from singlet state to triplet state and the short singlet lifetime indicate that the triplet state T_1 is the photoreactive state. This triplet state is very sensitive to quenching in solution by halide ions, oxygen, and some amino acids and nucleotides. Because s^4U itself is a quencher, the quantum yield (Φ) can decrease substantially as the substrate concentration increases. s^4U can crosslink with groups in its close contact. The mechanism of s^4U photoaddition is schematically described in Fig. 1.5.

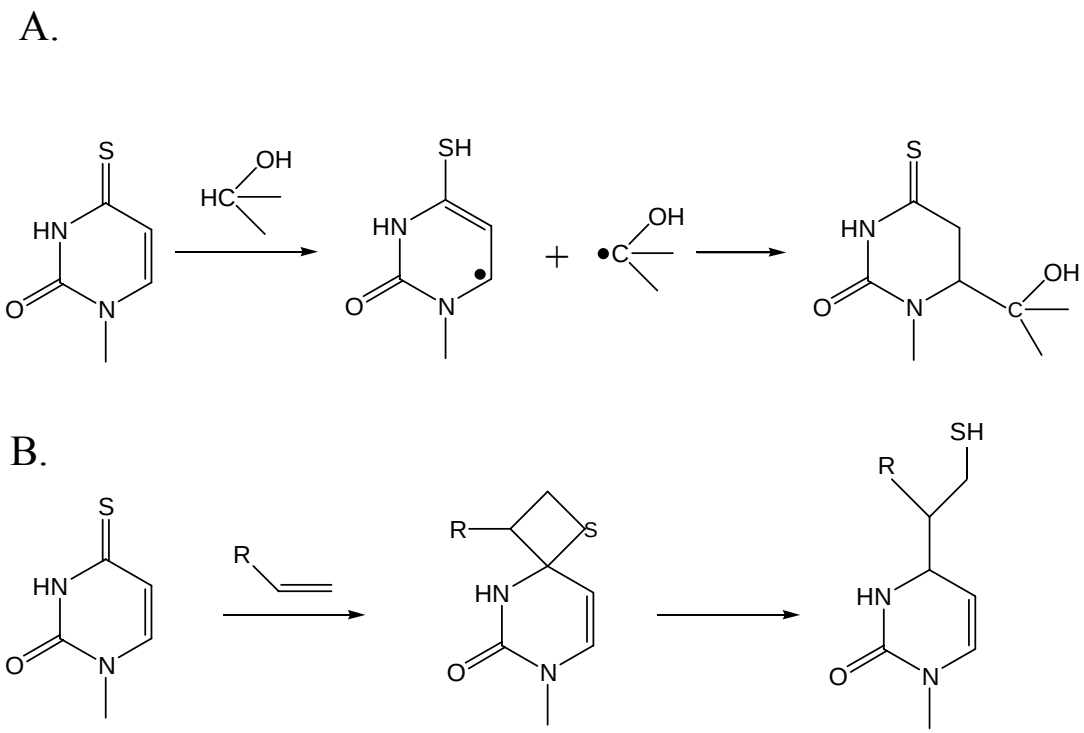

Fig. 1.5 Mechanism of model photoreactions of 4-thiouridine (Favre, 1990)
A. Photocoupling with hydrogen donor (amine, alcohols); B. cylcoaddition with electron-deficient olefins

In tRNA, the s^4U absorption spectrum is sensitive to the tRNA conformation on temperature, pH, and ionic strength. For native tRNA (at 300 K in neutral buffer plus Mg^{2+}) the s^4U π,π* transition shifts to the red ($\lambda_{max} \approx 340$ nm). The quantum yield (Φ) and lifetime (τ) of the 510 nm phosphorescence are sensitive to temperature and to changes of tRNA conformation mediated by cations. Increasing values of Φ and τ in native tRNA are strongly stabilized by divalent cations or spermidine. The efficiencies of quenching by O_2, or Cl^- are decreased by factors of 500 and 3000 in tRNA respectively (Favre, 1990 and references therein).

4-Thiouridine has been used in the study of splicesome (Sontheimer *et al.*, 1993), tRNA-aaRS interaction (Moor *et al.*, 2001), RNA – RNA interactions during translation (Wollenzien *et al.*, 1991) and other fields. In our lab it was used in study of tRNA·exportin-t·Ran·GppNHp interaction.

1.6 Atomic force microscopy — See molecules by touching

Atomic force microscopy (AFM) was invented by Binning, Quate and Gerber in 1986. The potential of atomic force microscopy for investigating biological samples on a scale ranging from living cells to single molecules has been recognized soon after its invention (Drake B *et al.*, 1989). In contrast to conventional biological imaging methods, specimens investigated by AFM can be in a native, unlabeled state and in their native environment for several hours – or even days –without damage.

Like all other scanning probe microscopes, the atomic force microscopy utilizes a sharp probe moving over the surface of a sample in a raster scan. The probe is a tip on the end of a cantilever which bends in response to the force between the tip and the sample. AFM operates by measuring attractive or repulsive forces between a tip and the sample. In its repulsive "contact" mode, the instrument lightly touches a tip at the end of a cantilever to the sample. As a raster scan drags the tip over the sample, a detection apparatus measures the vertical deflection of the cantilever, which indicates the local sample height. Thus, in contact mode the AFM measures hard-sphere repulsion forces between the tip and sample. As the vertical deflection of the cantilever is very small, a laser beam deflection method is used to magnify motions of the tip up to thousandfold. The magnified deflection can be precisely obtained by measuring the output voltage of the displace-detector circuit, which corresponds to the topography of the sample. The movement of the tip or sample is performed by an extremely precise positioning device made from piezo-electric ceramics, most often in the form of a tube scanner. The scanner is capable of sub-angstrom resolution in x-, y- and z-directions. The z-axis is conventionally perpendicular to the sample.

The AFM raster scans a sharp, cantilever-mounted stylus over the specimen, thereby creating a 3D surface map. The relative stiffness and mobility of the specimen is an important limiting factor in the sensitivity of AFM to surface position detection. Unfortunately biological specimens are soft and mobile. Thus, the force applied to the stylus must be kept very low to prevent sample deformation during AFM imaging. Likewise, topographs must be recorded in sufficiently short time ranges to prevent 'blurring' of the image caused by specimen movement.

Comparisons of AFM topographs with protein structures determined by electron microscopy and X-ray crystallography have shown excellent agreement within a lateral resolution of <1 nm and a vertical resolution of ca. 0.1 nm (Engel et al., 2000). It can be concluded that the protein structures were not influenced by their absorption to the supporting mica surface. The layered crystal mica is the most commonly used support for imaging of biological systems by AFM. It can be easily cleaved and by an adhesive tape can provide chemically inert and automatically flat surfaces over several hundreds of μm^2. In our lab, trifluoromethyl ketone (TFK), an esterase inhibitor that binds the enzyme with a K_D of 6 nM, was fixed to mica surface via covalent bond, which served as a platform to observe those proteins linked with esterase under AFM. Exportin-t-esterase was translated *in vitro* and its contour and its interaction between tRNA and Ran·GppNHp was studied by AFM.

2. Problem shooting

The pathway of tRNA export is still unclear. A research group in Japan found that having been microinjected into the HeLa S3 cells tRNA-conjugated Ribozymes (tRNA-Rz), which can be regarded as tRNA with extended 5′ and 3′ end, was exported to the cytoplasm. In marked contrast, in a *Xenopus* oocytes system tRNA-Rz was not exported even 6 hours after injection (Kuwabara T *et al.*, 2001). Is there any difference between somatic cells and oocytes upon the interaction of tRNA and exportin-t? Vigilin, a protein with extensive RNA-binding domains of the KH type, has been shown to accelerate tRNA export in human cells (Kruse *et al.*, 2000). Does exportin-t function solely on tRNA export or does it require other helper? Surprising findings came from publications of two groups. They independently discovered that in yeast mature tRNAs were not only exported out of nucleus into cytoplasm, but also were imported back to nucleus. tRNAs are not simply exported to nucleus, but shuttling between nucleus and cytoplasm (Takano *et al.*, 2005, Shaheen *et al.*, 2005). Obviously much more labor and time are required to understand the transport of tRNA and the function of its carrier – exportin-t.

In this thesis the interaction of tRNA·exportin-t·Ran·GTP is elucidated by biochemical and biophysical methods. The following questions are most interesting to us and studied in this thesis:

1. Which nucleotides of tRNA contact exportin-t and Ran in crosslinking experiment?
2. Which protein contacts the tRNA in the exportin-t·tRNA·Ran·GTP complex?
3. Do all mature tRNAs in cell bind to exportin-t with the same affinity?

3. Materials and Methods

3.1 Materials

3.1.1 Chemicals and radioactive chemicals

3.1.1.1 Chemicals

Acetontril	Arcos Organic (USA)
Acrylamide/Bisacrylamide Solution	Roth (Karlsruhe)
Agarose NEEO	Roth (Karlsruhe)
Amino acids	Sigma (Deisendorf)
Ammoniumperoxodisulfate (APS)	Serva (Heidelberg)
Ampicillin, Kanamycin, IPTG, Antifoam®	Gerbu (Gailberg)
ATP, CTP, GTP, GppNHp, UTP	Roche (Mannheim)
Bromophenolblue, Xylene cyanol	Serva (Heidelberg)
Coomassie Brilliant Blue G–250	Serva (Heidelberg)
Chloramphenicol	Sigma (Deisendorf)
dATP, dCTP, dGTP, dTTP, ddATP	Roth (Karlsruhe)
Dithiothreitol	Gerbu (Gailberg)
Ethidiumbromide	Roth (Karlsruhe)
Glycerol	Biesterfeld (Nürnberg)
2-Mercaptoethanol	Sigma (Deisendorf)
Peptone	Sigma (Deisendorf)
RNasIn® (RNase-Inhibitor)	Promega (Mannheim)
Spermidin	Fluka (Buchs, Schweiz)
TEMED	Merck (Darmstadt)
Tetrabutylammoniumhydrogensulfate	Aldrich (Steinheim)
4-thiouridine	LS Biochmie, Uni. Bayreuth
Tris, Na_2HPO_4, EDTA, PMSF	Roth (Karlsruhe)

Yeast extract	Serva (Heidelberg)

Other chemicals, if not mentioned, came from Merck (Darmstadt). The purity of all chemicals was all *pro analysis*.

For fermentation deionized water was used. For preparation of buffers and other solutions ddH_2O was used.

3.1.1.2 Radioactive material

[α^{32}P]ATP (3000 Ci/mol)	Hartmann Analytik (Braunschweig)
[α^{32}P]NTP mixture (3000 Ci/mol)	Hartmann Analytik (Braunschweig)
[γ^{32}P]ATP (3000 Ci/mol)	Hartmann Analytik (Braunschweig)
[γ^{32}P]pCp (3000 Ci/mol)	Hartmann Analytik (Braunschweig)

3.1.2 Chromatographic materials

DEAE-Cellulose	Pharmacia (Freiburg)
Fractogel SO_3-EMD	Pharmacia (Freiburg)
HPLC-column Supelcosil LC 18S	Supelco (Bellefonte, USA)
Ni^{2+}-NTA-Sepharose	Qiagen (Hilden)
Q-Sepharose FF	Pharmacia (Freiburg)
Sephacryl S200 HR	Pharmacia (Freiburg)

3.1.3 Enzymes and Proteins

Baterial alkaline phosphatase	Roche (Mannheim)
BSA	New England Biolabs, Frankfurt am Main
DNase I from calf pancreas, RNase free	Roche (Mannheim)

DNA polymerase from *Thermus aquaticus*	Peqlab (Erlangen)
Gel filtrations Standard for FPLC	BioRad (München)
Lysozyme	Amersham (Freiburg)
NTase from *E. coli* (6,65 mg/ml; 8880 U/mg)	Laboratorium für Biochemie, Bayreuth
pfu DNA polymerase	Promega (Mannheim)
Polynucleotide kinase	Roche (Mannheim)
Protein standard for SDS-PAGE	Pharmacia Biotech (Freiburg)
Protease K	Merck (Darmstadt)
Restriction enzymes	New England Biolabs, Frankfurt am Main
M-MLV (H^-) Reverse transcriptase	Promega (Mannheim)
RNase A from calf pancreas	Sigma (Deisendorf)
RNase P1	Roche (Mannheim)
RNase T_1, *Aspergillus Oryzae*	Roche (Mannheim)
RNase T_2	Sigma (Deisendorf)
SAP	Roche (Mannheim)
T4 DNA ligase	New England Biolabs, Frankfurt am Main
T4 RNA ligase	New England Biolabs, Frankfurt am Main
T7 RNA Polymerase (0.38 mg/ml)	Laboratorium für Biochemie, Bayreuth
Trypsin (sequencing grade)	Sigma (Deisendorf)

3.1.4 tRNAs

$tRNA^{Arg}_{E.\,c}$	Laboratorium für Biochemie, Bayreuth
$tRNA^{Val}_{E.\,c}$	Laboratorium für Biochemie, Bayreuth

3.1.5 Bacteria strains

Escherichia coli strains:

BL21(DE3)pLysS:	F^- omp T $hsdS_B((r_B\text{-}m_B\text{-})$ gal, dcm (DE3)pLys Novagen (Madison, USA)
DH5α:	*sup*E44, Δ*lac*U169, (Φ80*lac*ZΔM15), *hsd*R17, *rec*A1, *end*A1, *gyr*A96, *thi*-1, *rel*A (Hanahan, 1983)
XL1 blue:	*sup*E44, *hsd*R17, *end*A1, *gyr*A96, *rel*A1, *thi*-1, *rec*A1, lac^-, F′ [*pro*AB+, $lacI^q$, *lac*ZΔM15, Tn10] (Stratagene, Heidelberg)

3.1.6 Plasmids

pETran	Plasmid for overexpression of p24Ran in *E. coli* (AG Wittinghofer, Dortmund)
pQE30-Exportin-t	Plasmid for expression of Exportin-t in *E. coli* (D. Görlich, Heidelberg; Kutay *et al.*, 1998)
$ptRNA^{Phe}_{T.th.}$	Plasmid with $tRNA^{Phe}_{T.th.}$ gene (P. Hofmüller, Dissertation, Universität Bayreuth)

3.1.7 Oligonucleotides

PE-Phe	5′-GGCGAGAGGAGCCGUGGU-3′
Phe5F	5′-ACGCCAGGGTTTTCCCAGTCACG-3′
Phe47R	5′-TCGAACCGCCGTCACTGCGA-3′
Phe47F	5′-TCGCAGTGACGGCGGTTCGA-3′
Phe-3R	5′-CTCACTCATTAGGCACCCCAGGC-3′
Phe-3end	5′-TGGTGCCGAGGAGCGGAATCG-3′

Below are oligonucleotides used for fishing tRNAs on 2D gels by Northern

hybridization, the sequences and nominations are from tRNA gene database http://www.trna.uni-bayreuth.de (Sprinzl *et al.*, 2004)

Ser3009	5′-TGGCGTAGTCGGCAGGATTCG-3′
Ser3014	5′-TGGGCTGTGAGCAGGATTTGAAC-3′
Ser3019	5′-TGGGACGAGGGTGGGATTCGAAC-3′
Ser3023	5′-TGGCGCAGCGAGCAGGGTTCGA-3′
Leu2938	5′-TGGTGGCAGCGGTGGGATTTG-3′
Leu2941	5′-TGGGTTCCAAGACGGATTCGAAC-3′
Leu2943	5′-TGGGTCAGAAGTGGGATTCGAAC-3′
Leu2949	5′-TGGTGTCAGGAGTGGGATTCGAA-3′
Leu2952	5′-TGGGTTAAGAAGAGGAGTTGAAC-3′
Leu2953	5′-TGGACCGGGAGTGGGGCTCGAAC-3′
Leu2954	5′-TGGACCAGAAGTGGGGTTCGAAC-3′
Leu2955	5′-TGGACCGAGAGTGGGGTTCGAAC-3′
Leu2956	5′-TGGACCAGGAGTGGGGTTCGAAC-3′
Pro2999	5′-TGGGGGCTCGTCCGGGATTTGAA-3′
Arg2797	5′-TGGCGAGCCAGCCAGGAGTCGAAC-3′

3.1.8 Bacterial media and antibiotics

LB–Medium, Luria Bertani Broth	10 g Peptone
(Miller, 1972)	5 g yeas extract
	5 g NaCl, add 1 l H_2O, pH 7.2
2TY-Medium	16 g Peptone
	10 g yeast extract
	5 g NaCl, add 1 l H_2O, pH 7.2

Solution of antibiotics:

	Stock solution	Final concentration
Ampicillin (Sodium salt)	100 mg/ml (in ddH_2O)	100 µg/ml
Kanamycin (Sodium salt)	50 mg/ml (in ddH_2O)	50 µg/ml
Chloramphenicol	34 mg/ml (in ethanol)	34 µg/ml
IPTG	100 mg/ml (in ddH_2O)	
X-gal	20 mg/ml (in DMF)	

Bacterial media were autoclaved at 121°C (1 Bar) for 20 minutes. For preparation of solid media, 1.5% (w/v) agar was added to liquid media. Solutions of antibiotics were filter-sterilized.

3.1.9 Buffers and solutions

100 × Denhardt's solution	2.0 g BSA	
	2.0 g Ficoll 400	
	2.0 g polyvinylpyrrolidone	
Hybridization buffer	5 × SSC buffer	
	5 × Denhardt's solution	
	0.5% (w/v) SDS	
	100 µg/ml salmon sperm DNA	
1 × primer extension	50 mM Tris-HCl	pH 8.0
buffer	75 mM KCl	
	3 mM $MgCl_2$	
	10 mM DTT	
20 × SSC buffer	0.342 M Tri-sodium citrate	pH 7-8
	3 M NaCl	
1 × TBE buffer	89 mM Tris	pH 8.4
	89 mM Boric acid	
	2.5 mM EDTA	

1 × TE buffer	10 mM Tris-HCl 1 mM EDTA	pH8.0
Coomassie blue staining solution	0.2 % (v/v) Coomassie Brilliant Blue R-250, 10 % (v/v) acetic acid, 30 % (v/v) ethanol in H_2O	
Destaining buffer	10 % (v/v) acetic acid, 30 % (v/v) ethanol in H_2O	
SDS-PAGE loading buffer	100 mM Tris/HCl, pH 6.8 , 40 % (v/v) Glycerol, 2.5 % (w/v) SDS, 14.4 mM 2–mercaptoethanol, 0.05 % BP	
Urea-PAGE loading buffer	0.1g BP, 0.1 g XC, 0.1 g EDTA in 100 g formamide	
Running buffer for SDS-PAGE	25 mM Tris, 192 mM glycine, 0.1% (w/v) SDS, pH 8.3	

3.1.10 Instruments

AFM MultiMode	Veeco/Digital Instruments Inc. Santa Barbara, CA
Agarose gel apparatus	Pharmacia, Freiburg
Analysis Balance 1201 MP2	Sartorius, Göttingen
Autoclave FNR 4932E	Tecnomara, Fernwald
Autoclave Type 23	Melag, Würzburg
Centrifuge 5415C	Eppendorf, Hamburg
Cool centrifuge RC5B	Du Pont, Bad Homburg
Desk centrifuge	Heraeus Christ, Osterode
Digital pH Meter	WTW, Weilheim
Environmental Incubator Shaker	New Brunswick Scientific, Edison N.J., USA
FPLC system	Pharmacia, Freiburg
Gel dryer D61	Biometra, Göttingen
Hybridization oven	Bachofer, Reutlingen

HPLC system GOLD	Beckmann, München
Instant Imager 2024	Packard, Meriden, USA
Magnet mixer IKA-Combimag REO	IKA-Werke, Staufen
Mighty-Small-Gelsystem	Hoefer Scientific Instr., San Francisco, USA
Parr-Bomb	Parr Instruments, Moline, USA
Phosphoimager	Molecular Dynamics, Sunnyvale, CA, USA
Personal Cycler 20	Biometra, Göttingen
Power supplier EP C5 3000/150	Pharmacia, Freiburg
15 W-Quecksilberdampflamp	F8T5, Sankyo
Sigma-centrifuge 202 MK	Sigma, Osterode
Scintillation counter LS 1801	Beckmann, München
Speed Vac-centrifuge	Savant, New York, USA
Thermomixer 5436	Eppendorf, Hamburg
Thermostat heating block 5320	Eppendorf, Hamburg
Ultrasonic bath	Bandelin, Berlin
Ultracentrifuge OTB065B	Du Pont, Bad Homburg
UV-Spectral photometer UV 160A	Beckmann, München
UV-Spectral photometer UV 160A	Shimadzu, Kyoto, Japan
UV/Vis-Transllluminator with camera and computer	MWG, Ebersberg
Vortex-Genie	Bender & Holbein AG, Zürich
Waring commercial blendor	New Hartford, USA
Water bath	Kötternmann, Burgdorf

3.1.11 Other Materials

Cellulosefilter, 3MM	Whatman , Maidstone,

	England
Dialysis membrane	Serva, Heidelberg
Minisart Sterilfilter, 0.2 µM	Sartorius (Göttingen)
Sterile injector	Dispomed (Gelnhausen)
Vivaspin 20	Sartorius, Göttingen
Hybond-N^+ membrane	Amersham

3.2 Standard Methods

3.2.1 Spectrophotometric measurements

The A_{600} of bacterial suspensions was measured with a Beckmann DU-640 spectrophotometer in polystyrol cuvettes and one A_{600} unit corresponds to 6×10^8 cells.

Absorbance in UV region was measured with a Beckmann DU-640 spectrophotometer using 1 cm quartz cuvettes. Protein concentration was calculated according to Ehresmann *et al.*, (1973).

$$(A_{228.5} - A_{234.5})/3.14 = \text{mg/ml (protein)}$$

A_{260} of DNA, tRNA was measured to determine their concentration. One A_{260} unit corresponds to ca. 50 µg DNA, 1.5 nmol tRNA.

3.2.2 Centrifugations

If not mentioned otherwise, a standard centrifugation was carried out in desk centrifuge at 12000 rpm, or in Sigma centrifuge 202 MK at 12000 rpm, or in cool centrifuge RC5B at 15000 rpm in SS34 rotor, at 12000 rpm in GSA rotor, at 9000 rpm in GS-3 rotor (depending on sample volume), at 4°C for 20 min.

3.2.3 Ethanol and isopropanol precipitation of NA

Ethanol or isopropanol precipitation of DNA or tRNA was used for concentration or for changing buffer. Three volume of ice cold ethanol (in case of tRNA) or 0.6 volume of isopropanol (in case of DNA) was added to sample, and then NaOAc was added to a final concentration of 0.15 M.

After being mixed thoroughly, the sample was stored at -70°C for 2 h or -20°C overnight, and then subjected to centrifugation. The supernatant was decanted, and the pellets was washed with 70% cold ethanol, dried, and then dissolved in appropriate buffer or water.

3.2.4 Electrophoresis

3.2.4.1 SDS-polyacrylamide gel electrophoresis

The discontinuous pH SDS PAGE was performed according to Laemmli (1970) in the Mighty Small Vertical Slab Unit (Hoefer Scientific Instruments) with 25 mM Tris-HCl pH 8.3, 250 mM glycine, 0.1% (w/v) SDS, as the running buffer. The separating gel (10 – 15% acrylamide/N, N′-methylenebisacrylamide 29 : 1) contained 375 mM Tris-HCl 8.8, 0.1% (w/v) SDS. The 4% stacking gel (acrylamide/N, N′-methylenebisacrylamide 29 : 1) contained 125 mM Tris-HCl pH 6.8, 0.1% (w/v) SDS. Polymerization was started by addition of 0.05% (v/v) TEMED and 0.1% (v/v) APS. Two volumes of protein samples were mixed with one volume of SDS PAGE loading buffer and then heated at 95°C for 3 min. Electrophoresis was carried out at 15 V/cm, ca. 50 mA. The protein bands were visualized with Coomassie Brilliant Blue G250.

3.2.4.2 Agarose gel electrophoresis

Agarose gels (0.5 – 2% (w/v) agarose, 0.5 µg/ml ethidium bromide, 0.5 × TBE) were used for analysis and preparation of DNA. DNA samples were mixed with 1/3 volume of

loading buffer and loaded on a gel directly. Electrophoresis was run at 5-7 V/cm. The DNA bands were visualized with a UV lamp.

3.2.4.3 Urea-polyacrylamide gel electrophoresis

For normal analysis or preparation of tRNA, 10 - 20% polyacrylamide (acrylamide/N, N′-methylenebisacrylamide 19 : 1) gel of 20 × 20 × 0.1 cm or 40 × 20 × 0.1 cm containing 7 M urea in 1× TBE buffer were made. Polymerization was started by addition of 0.1 % (v/v) TEMED und 0.032 % (w/v) APS. Gels were prerun for at least 30 min at 35 W, and then samples mixed with 1/3 volume urea PAGE loading buffer were loaded onto the gel. Electrophoresis was run at 35 W. The tRNA bands were visualized by radioactivity detection in Instant Imager 2024 or with 0.5 µg/ml ethidium bromide staining.

For sequencing, thinner gels (40 × 20 × 0.02 mm) of 12% or 20% polyacrylamide containing 7 M urea in 1 × TBE buffer were made. Gels were prerun for 30 min at 1600 V, and then samples were loaded onto the gel. Electrophoresis was run at 1600 V. The gel was dried at 80°C for 1 h, and exposed to a Kodak BIomax MR-1 X-ray film (30 × 40 cm), or scanned by Phosphoimager (Molecular Dynamics).

3.2.4.4 Native polyacrylamide gel electrophoresis

For EMSA and for separation of crosslinked complex from free tRNA, a native 5% polyacrylamide gel of 20 × 20 × 0.1 cm containing 5 % (w/v) acrylamide, 0.25 % (w/v) N,N′-bisacrylamide, 5 % (v/v) glycerol in 1 × native gel buffer (200 mM glycine, 25 mM Tris, pH 8.3) was prepared. Polymerization was started by addition of 0.1 % (v/v) TEMED und 0.032 % (w/v) APS. In EMSA experiments, samples (3.2.8) were directly loaded onto the gel. Whereas the crosslinked complex plus 1/3 volume of SDS PAGE loading buffer was heated at 60°C for 5 min to disassemble uncrosslinked complex. The gel was precooled to 4°C, and the electrophoresis was run at 4°C, 12.5 V/cm.

3.2.4.5 Two dimensional urea PAGE

Two dimensional urea PAGE was used to fractionate tRNAs from calf liver, according to protocols of Dong *et al.* (1996), with a little modification. The acrylamide used here is premixed solution of acrylamide / N, N′ - methylenebisacrylamide 19:1 (w/v). The first dimension gel is 10% polyacrylamide gel containing 7 M urea (40 × 20 × 0.1 cm), and the second dimension gel is 20% polyacrylamide gel containing 4 M urea (20 × 20 × 0.1 cm). Twenty µl $tRNA^{Bulk}$ (0.2 to 1 A_{260}) in 10 M urea and 0.05% bromophenol blue and xylene cyanol was loaded and the electrophoresis was performed at 330 V for 43 h at 4°C. Having been visualized with ethidiumbromide staining, tRNA bands were cut out (about 8 cm in length and 0.5 cm in width) and moulded onto the second dimension gel after a 90° rotation. The second electrophoresis was run at 220 V for 26 h at room temperature. The gel was visualized with ethidiumbromide or with radioactivity detection.

3.2.5 Recovery of RNA from polyacrylamide gel

Visualized RNA bands or spots (through radioactivity detection or EB staining) were cut out, and smashed to powder, to which about 4 volumes of 0.3 NaOAc buffer pH 6 were added. The mixture was shaken mildly at 4°C over night and centrifuged. tRNA in the supernatant was precipitated by ethanol as described in 3.2.3.

3.2.6 Microbial fermentation

For the small-scale preparation of plasmid DNA, *E. coli* strains were grown in 5 ml LB-medium with the appropriate antibiotic. Single colonies were picked from LB-agar plates in Petri dishes. Cultures were incubated overnight at 37°C with agitation (170 rpm) in the Environmental Incubator Shaker (New Brunswick Scientific, Edison N.J., USA).

For preparation of recombinant proteins, *E. coli* strains were inoculated in 5 ml LB medium with appropriate antibiotics and grown overnight at 37°C with agitation. The culture was inoculated to 250 ml LB medium with appropriate antibiotics, and grown overnight at 37°C, 170 rpm for 4 h. Two flasks of 250 ml culture were then added to 10 l LB medium with appropriate antibiotics. This culture was grown at 37°C until A_{600} reached 0.8, at which point IPTG was added to a final concentration of 1 mM to start the overexpression of the target protein. The culture was grown further for 4 hours. Cells were harvested by centrifugation at 7,000 rpm for 10 minutes at 4°C in GSA rotor (Sorvall, DuPont).

3.2.7 Preparation of cell extracts

Bacterial (*E.coli*) cell extracts were prepared according to Leberman, *et al.* (1980) with some modifications. The whole procedure was carried out at 4 °C if not mentioned otherwise. 100 g cells were suspended in 200 ml disruption buffer (50 mM Tris-HCl pH 7.5, 5 mM EDTA, 1 mM 2-mercaptoethanol, 100 µM PMSF and 5% (v/v) glycerol). The cell suspension was treated with lysozyme (50 mg per 100 g cells) and stirred for 30 minutes. After addition of $MgCl_2$ to 30 mM, the cell suspension was treated with DNase I (5 mg per 100 g cells) for 30 minutes. The extraction of cells was achieved by high pressure of nitrogen decompression (after 40 minutes at 1,200 psi) using a cell-disruption bomb (Parr Instrument Co., Moline, USA). The cell homogenate was centrifuged at 30,000 g for 30 minutes to remove cell debris. The supernatant was further ultracentrifuged at 40,000 rpm for 4 hours and a ribosome-free S100 extract was obtained.

3.2.8 Formation of tRNA·exportin-t·Ran·GppNHp

tRNA was incubated with exportin-t and Ran·GppNHp in 20 mM Tris-HCl pH 7.5, 50 mM KCl, 5 mM $MgCl_2$, 1 mM DTT (complex forming buffer) .

For EMSA and crosslinking, the ratio of tRNA : exportin-t : Ran·GppNHp was 1 : 5 : 5. EMSA was carried on 5% native PAGE at 4°C, 12.5V /cm as described in 3.2.4.4.

3.3 Molecular cloning

3.3.1 Purification of DNA

Plasmid DNA was purified from *E.coli* cells with Qiagen Plasmid kit, and dissolved in appropriate volume of TE buffer.

Separated DNA fragments in agarose gel were purified with "QIAEX II Gel Extraction Kit" (Qiagen, Hilden), according to the manufacturer's instructions.

3.3.2 Digestion of DNA with restriction endonucleases

Digestion of DNA with restriction endonucleases was carried out under the conditions specified by the manufacturer. For analytical purposes, 0.1 – 0.2 µg of plasmid DNA was digested for 1 h in a volume of 10 µl, with 0.5 – 1 U of appropriate restriction endonucleases. Preparative digestion was carried out in a volume of 20 – 50 µl with 2 – 5 µg of plasmid DNA and 2 – 10 U of appropriate restriction endonucleases for at least 2 hours.

3.3.3 Polymerase chain reaction (PCR)

The polymerase chain reactions were performed in the DNA Thermal cycler (Perkin Elmer, Norwalk, USA). In a volume of 40 µl, the reaction mixture contained approximately 0.8 ng of plasmid DNA (template), 1 µM primers, 250 µM each dNTP and 2.5 U *pfu* DNA polymerase mixed with 0.12 U Taq DNA polymerase in 20 mM Tris-HCl

8.8, 10 mM KCl, 10 mM $(NH_4)_2SO_4$. For preparation of DNA template used in *in vitro* transcription, pure *pfu* polymerase was used.

Reaction samples were heated at first to 95ºC for 3 min, then entered into 20 cycles of 95ºC for 30s, 55ºC for 20s, 72ºC for 30s. In final the samples were kept at 72ºC for 3 min to complete reactions.

3.3.4 Cloning of PCR product

PCR products were directly ligated to pGEM®-T vector (Promega, Madison, USA) according to the manufacturer's instructions. The ligation samples were used to transform XL-1 blue competent cells.

3.3.5 Transformation of competent cells

Plasmids were transformed into the $CaCl_2$-treated competent cells, according to the protocol in *Molecular Cloning* (Sambrook).

3.3.6 Introduction of a point mutation (T47A) in $tDNA^{Phe}_{T.th}$

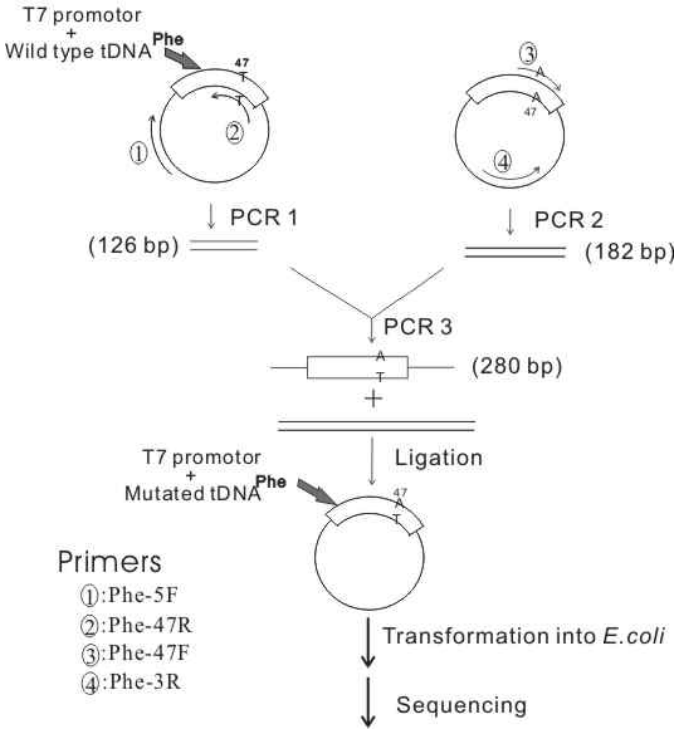

Fig. 3.1. Introduction of the point mutation of T47A in $tRNA^{Phe}_{T.th}$ gene

To mutate T47 of $tDNA^{Phe}_{T.th}$ to A, three PCR and two sets of primers (Phe-5F (1) and Phe-47R (2); Phe47F (3) and Phe3R (4)) were designed (the design line was outlined in Fig. 3.1). Phe47R contained an uncomplementary nucleotide of T47 (original is A47); and Phe47F contained also an uncomplementary nucleotide of A47 (original is T47). These two PCR products contained an A-T pair instead of T-A pair at the position of 47 in tDNA. Using these two PCR products as template and Phe-5F (1) and Phe-3R (4) as primers, we successfully obtained a PCR product of 280 bp. After ligation of this PCR product to pGEM T vector, the DNAs were transformed into *E.coli*. Clones on ampicilin resistant plates were picked out and incubated in 5 ml liquid LB media. Plasmid were purified and sent for sequencing. From the sequencing result we concluded that a point mutation of T to A was successfully introduced at the position of 47 in tDNA.

3.4 Preparation of exportin-t and Ran·GppNHp

3.4.1 Preparation of exportin-t

The S100 fraction of cells containing expressed exportin-t (3.2.7) was dialyzed against 50 mM sodium phosphate pH 6.0, 300 mM NaCl, 10 mM imidazol, 0.5 mM PMSF at 4°C overnight. The buffer was changed three times with an interval of at least 2 h. The S100 fraction was loaded onto a pre-equilibrated Ni-NTA column (2 × 4 cm) at room temperature (25°C). The flowout was monitored at 280 nm. After extensive wash of the column with buffer 50 mM sodium phosphate pH 6.0, 300 mM NaCl, 10 mM imidazol, 0.5 mM PMSF till base line reappeared, exportin-t was then eluted with the same buffer containing 200 mM imidazol. Based on results of 12.5% SDS-PAGE, appropriate fractions were collected and dialyzed against 100 mM NaOAc pH 6.0, 1 mM ß-Me, 5% glycerol at 4°C overnight.

The dialysate obtained (3.4.1.1) was loaded at 4°C onto an EMD-SO_3 Tentakel column (25 × 2 cm). Protein peaks were monitored at 280 nm. After extensive wash of the column with buffer 100 mM NaOAc pH 6.0, 1 mM ß-Me, 5% glycerol till base line reappeared, exportin-t was then eluted out with a linear gradient of KCl concentration. Based on results of 12.5% SDS-PAGE, appropriate fractions were collected, concentrated with Vivaspin 20 for further purification.

The concentrated exportin-t sample (less than 2 ml) was desalted on a Sephacryl S200 HR column (75 × 1.8 cm) at 4°C in buffer E (50 mM Tris-HCl pH 7.5, 100 mM NaCl, 5% glycerol). Protein peaks were monitored at 280 nm. Based on results of 12.5% SDS-PAGE, appropriate fractions were collected, concentrated to 11 mg/ml in 1.6 ml. The concentrated protein solution was shock frozen with dry ice, and stored at -20°C for further use.

3.4.2 Preparation of Ran·GppNHp

The cell extract (3.2.7) was loaded at 4°C onto an EMD-SO_3 Tentakel column (25 × 2 cm). Protein peaks were monitored at 280 nm. After extensive wash of the column with buffer 20 mM potassium phosphate pH 6.4, 50 mM KCl, 5 mM $MgCl_2$, 1 mM 2-mercaptomethanol, 20 µM PMSF, 10 µM GDP till base line reappeared, Ran·GDP was then eluted with a linear gradient of KCl concentration. Based on results of 15% SDS-PAGE, appropriate fractions were collected, concentrated with Vivaspin 20. Ran·GDP in it was further purified with gel filtration chromatography on a Sephacryl S200 HR column (75 × 1.8 cm) at 4°C in buffer 60 mM Tris-HCl 7.6, 1 mM $MgCl_2$, 1mM 2-mercaptoethanol, 10µM GDP, 20 µM PMSF. Protein peaks were monitored at 280 nm. Based on results of 15% SDS-PAGE, appropriate fractions were collected, concentrated to 8.8 mg/ml in 16 ml. The concentrated protein solution was shock frozen with dry ice, and stored at -20°C for further use.

For preparation of Ran·GppNHp, Ran-bound GDP was exchanged with free GppNHp. In 0.8 ml sample, 670 µM Ran·GDP and 3.4 mM GppNHp were mixed together in 25 mM potassium phosphate buffer pH 7.0 containing 0.1 M $(NH_4)_2SO_4$, 75 mM KCl, 10 mM EDTA, 5 mM $MgCl_2$, 5 mM DTE. The reaction was started by adding 130 U shrimp alkaline phosphatase. The sample was incubated at room temperature for 2 h, and then lat 4°C overnight.

The nucleotide exchange reaction sample was directly loaded on a Sephacryl S200 HR column (75 × 1.8 cm) at 4°C. Isocratic elution was performed with 50 mM Tris-HCl pH 7.5, 100 mM NaCl, 10 mM $MgCl_2$. Protein peaks were monitored at 280 nm. Based on results of 15% SDS-PAGE, appropriate fractions were collected, concentrated to 2.44 mg/ml in 1.5 ml. After addition of DTT to 1 mM, the concentrated protein solution was shock frozen with dry ice, and stored at -20°C for further use.

3.5 Preparation of tRNA

3.5.1 Preparation of $tRNA^{Phe}_{T.th}$ transcript

3.5.1.1 Preparation of tDNA template

Two methods were used to prepare tDNA template. Plasmid pT7TthF was linearized by BstN I digestion in order to produce a CCA end at 3′ terminus. 5.8 μg plasmid pT7TthF was incubated with 15 U BstN I in 20μl 10 mM Tris-HCl pH 7.9, 50 mM NaCl, 10 mM $MgCl_2$, 1 mM DTT at 60°C for 2 h. The digestion mixture was added directly to the *in vitro* transcription system.

Optionally, PCR was used to produce a fragment of dsDNA containing T7 promoter and tDNA gene ending with 3′ CCA end (3.3.3), for which 1 μM primer 5′-ACGCCAGGGTTTTCCCAGTCACG-3′ and 5′-TGGTGCCGAGGAGCGGAATCG-3′ were used. For synthesis of wild type $tRNA^{Phe}_{T.th}$, 2 ng plasmid pT7TthF was used as template; and for synthesis of 0.2 ng mutant $tRNA^{Phe}_{T.th}$ U47A, pGEM-T_T7TthF47A was used as template.

3.5.1.2 *in vitro* transcription

For transcription of normal $tRNA^{Phe}_{T.th}$, in 150 μl sample, 130 nM tDNA template, 4 mM NTPs, 40 mM Tris-HCl pH 8.1, 25 mM $MgCl_2$, 10 mM DTT, 2 mM spermidine, 0.16 U/μl RNasIn, 1.92 μM T7 RNA polymerase were mixed together and incubated at 37°C for 4 h. Two units DNase I (RNase free) were then added and the sample remained at 37°C for another 1 h to degrade the DNA in it. The tRNA produced was purified by gel electrophoresis (3.2.5).

For transcription of ^{32}P labeled $tRNA^{Phe}_{T.th}$, 1 mM cold ATP, and 11 nM [α-^{32}P] ATP (3000Ci/mmol) were present in the transcription system, while other conditions remained the same as in the first paragraph.

For transcription of s^4U containing $tRNA^{Phe}_{T.th}$, 2 mM s^4UTP, 0.5 mM UTP were present, while other conditions remained the same as those in the first two paragraphs.

3.5.2 Preparation of calf liver $tRNA^{Bulk}$

Two and half kg of fresh calf liver were cut to chunks and homogenized in 2 l buffer 140 mM NaOAc pH 4.5, 10 mM $MgCl_2$ and 2 l phenol using Waring commercial blendor (New Hartford, USA) . The slurry was filtered through cheesecloth and centrifuged at 8000 rpm in GSA rotor for 10 min (room temperature). The aqueous phase was drawn out and mixed with equal volume of chloroform, and then centrifuged again at 8000 rpm in GSA rotor for 10 min (room temperature). The supernatant was loaded onto a preequilibrated DEAE-Cellulose (50 × 5 cm) at room temperature. The column was extensively washed with buffer 140 mM NaOAc pH 4.5, 10 mM $MgCl_2$ till base line reappeared. The same buffer containing 200 mM NaCl washed the proteins and small RNA molecules out of column. tRNAs was then eluted with 650 mM NaCl in buffer 140 mM NaOAc pH 4.5, 10 mM $MgCl_2$. The peak was collected and mixed with 2.5 volume of ethanol. The tRNA precipitate was stored at -20°C overnight. After centrifugation tRNA pellets were dissolved in ddH_2O, and dialyzed against water. About 60 ml 1230 A_{260}/ml $tRNA^{Bulk}$ was obtained. The desalted tRNA solution was stored at -20°C for further use.

3.5.3 Preparation of deacylated $tRNA^{Bulk}$

In 1 ml sample, 700 A_{260} $tRNA^{Bulk}$ was deacylated in 100 mM Tris-HCl pH 7.6, 32.5 mM $CuSO_4$ at 37°C for 10 min (Schofield *et al.*, 1968). The reaction sample was then subjected to gel permeation chromatography of Sephacryl S200 HR with buffer 20 mM NaOAc pH 4.6, 100 mM NaCl, 10 mM $MgCl_2$ at 4°C.

The peak was collected and mixed with 2.5 volume of ethanol. The tRNA precipitate was stored at -20°C overnight. After centrifugation tRNA pellets were dissolved in ddH_2O, and dialyzed against water. The desalted tRNA solution was stored at -20°C for further use.

3.5.4 Preparation of tRNA with correct CCA end

In 100 µl sample, 450 µM deacylated $tRNA^{Bulk}$ was treated with 14 µM NTase in 100 mM Tris-HCl pH 9.0, 100 mM KCl, 10 mM $MgSO_4$, 1mM dithiothreitol, 1 mM ATP and CTP at 37°C for 4 h (Sprinzl *et al.*, 1979). The enzyme was removed by phenol/chloroform treatment and the tRNA was recovered by ethanol precipitation. The tRNA was purified with G50 column (0.4 ml) and subjected to ethanol precipitation as described in 3.2.3.

3.6 Radioactive labeling of tRNA and DNA

3.6.1 3′-end labeling of primer with [γ-^{32}P] ATP

Commercial primers had already been dephosphorylated at 5′ end, and were directly labeled by T4 polynucleotide kinase. In 10 µl sample, 50 µM primer and 10 µCi [γ-^{32}P] ATP were mixed together in 70 mM Tris-HCl pH 7.6, 10 mM $MgCl_2$, 5 mM DTT, and incubated at 37°C for 30 min after addition of 30 U T4 polynucleotide kinase. The enzyme in samples was inactivated at 65°C for 20 min. The labeled primer was stored at -20°C.

3.6.2 Incorporating ^{32}P into tRNA transcripts

^{32}P was incorporated into tRNA through in vitro transcription. For transcription of ^{32}P labeled tRNA, 1 mM cold ATP, and 11 nM [α-^{32}P] ATP (3000Ci/mmol) were added to transcription system, while other conditions remained the same as in the normal transcription (3.5.1.2).

3.7 Analysis of tRNA with HPLC

3.7.1 Degradation of tRNA to nucleosides

One A_{260}-unit tRNA (1.5 nmol) was lyophilized. The pellet was dissolved in 50 µl 100 mM NH_4OAc buffer, pH 5.3 and denatured at 95°C for 3 min. The sample was immediately cooled in ice bath for 5 min. 5 µl 20 mM ZnOAc and 3 U nuclease P1 were added and stored at 37°C for 1 h. Nuclease P1 splits phosphodiester bonds of tRNA and produces 5′-NMPs.

Then the pH of the sample was increased to pH 8.0 by addition of 15 µl 1 M Tris-HCl, pH 8.0, which is necessary for the subsequent alkaline phosphatase digestion. 2 U bacterial alkaline phosphatase (BAP) were added and the sample was further incubated at 37°C for 1 h, in which all 5′-NMPs were dephosphorylated to nucleosides.

3.7.2 HPLC analysis of nucleosides

Nucleosides were separated by reversed-phase HPLC (RP-HPLC) on a Supelcosil LC-18S column (25 cm × 4.6 mm). The nucleosides were monitored at 254 nm and 330 nm (for s^4U detection). The chromatography was performed at room temperature, and the flow rate was set to be 0.5 ml/min. HPLC buffer A: 100 mM NH_4OAc pH 5.3 with 2.5% methanol, HPLC buffer B: 100% methanol. The two buffers were degassed before use. The chromatography was programmed as below: From 0 to 5^{th} min, 100% A, 0% B; from 5^{th} -70^{th} min, linear gradient was run, 100% A, 0%B to 30% A, 70% B; from 70^{th} to 85^{th} min, 70%B was maintained; from 85^{th} to 95^{th} min, back to 100% A. The nucleosides were identified according to Gehrke *et al.* (1989, 1990).

3.8 Crosslinking experiments

3.8.1 Crosslinking of s^4U containing tRNA to exportin-t

After formation of ternary complex tRNA·exportin-t·Ran·GppNHp (3.2.8), the sample was transferred to a glass plate cooled on ice at a distance of 10 cm from uv light source of four 15 W mercury lamps (F8T5, Sankyo) and subjected to irradiation at 312 nm (4.5 mW/cm^2).

3.8.2 Competitive Inhibition of Crosslinking

In each of 10 µl sample, 0.4 µM tRNA and 2 µM exportin-t and 2 µM Ran·GppNHp and a series of $tRNA^{Arg}_{E.c}$ (from 0 µM to 10 µM) were mixed together in 20 mM Tris-HCl pH 7.5, 50 mM KCl, 5 mM $MgCl_2$ and 1 mM DTT. After formation of ternary complex (3.2.8), all samples were subjected to irradiation at 312 nm on ice for 1 min, and then subjected to PAGE analysis (3.2.4.4).

3.8.3 Primer extension analysis of crosslinked tRNA

3.8.3.1 Purification of crosslinked complex

In 200 µl sample, 6 µM s^4U containing $tRNA^{Phe}_{T.th}$, 30 µM exportin-t, 30 µM Ran·GppNHp were mixed together in complex forming buffer (3.2.8) and subjected to UV irradiation for 30 min. After addition of 50 µl SDS loading buffer, the sample was heated at 60°C and loaded onto a 5% native gel (3.2.4.4).

After visualization of bands on gel through radioactivity detection in Instant Imager 2024, the upper band containing crosslinked complex was cut out and incubated in 5 volumes of 0.3 M NaOAc pH 6.0 at 4°C overnight. After separation of gel pieces from solution by centrifugation, the crosslinked complex in the solution was precipitated with ethanol (3.2.3).

The crosslinked complex was dissolved in 150 µl 10 mM Tris-HCl 7.8, 5 mM EDTA, 0.5% SDS and digested by 0.25 U protease K at 37°C for 30 min.

3.8.3.2 Primer extension analysis

As a control, 2 pmol normal tRNA transcripts and 10 pmol 5′-labeled primer (3.6.1) in 10 µl were heated at 95°C for 1 min, and then cooled down slowly. A different annealing condition was used for s^4U containing tRNA and crosslinked tRNA: 2 pmol modified tRNA and 10 pmol 5′-labeled primer in 10 µl containing 1 mM EDTA, 1 mM phosphate buffer (pH 7.0) were heated at 80°C for 5 min, then cooled down slowly.

After annealing tRNA and primer, 1mM dNTP, 50 mM Tris-HCl (pH 8.3), 3 mM $MgCl_2$, 75 mM KCl, 5 mM DTT, 40 U RNasIn and 200U Superscript II reverse transcriptase were added. When ddATP used, 12.5 µM of dATP and 988 µM ddATP instead of 1mM dATP in reaction, other conditions remained the same as the former. The reaction samples were incubated at 50°C for 1 h. Subsequent electrophoresis was undertaken with 20% 7 M urea sequencing PAGE to analyze the reverse transcription reaction. The gel was dried at 80°C for 1 h and scanned with an image plate (3.2.4.3).

3.9 Affinity chromatography on immobilized exportin-t

3.9.1 Fractionation of $tRNA^{Bulk}$ by affinity chromatography on immobilized exportin-t

Recombinant protein exportin-t containing six histidine residues on its N-terminus was immobilized on Ni-NTA agarose column and used for fractionation of calf liver $tRNA^{Bulk}$ by affinity chromatography. tRNA·exportin-t·Ran·GppNHp ternary complexes were immobilized on Ni^{2+}-nitriloacetic acid agarose (Ni-NTA) and the exportin-t-bound tRNA was eluted at high ionic strength or with buffers containing 200 mM imidazol.

In each chromatography experiment, 500 µg exportin-t, 500 µg Ran·GppNHp, 13 A_{260} $tRNA^{Bulk}$ were incubated in 500 µl sample containing buffer 20 mM Tris-HCl pH 7.5, 50 mM KCl, 5 mM $MgCl_2$ (complex forming buffer) on ice for 10 min. The sample was then mixed with 0.4 ml Ni-NTA and incubated at room temperature for another 10 min. With a flow rate of 0.14 ml/min (achieved by gravity), the column was extensively

washed with complex forming buffer till A_{260} no longer sank down. Complex forming buffer containing 500 mM KCl was used to disrupt the ternary complex and elute exportin-t-bound tRNA out of column. Immobilized exportin-t was eluted by complex forming buffer containing 200 mM imidazol. Each fraction was subjected to phenol/chloroform treatment and tRNA in it was precipitated with ethanol (3.2.3) and subjected to two dimensional urea PAGE analysis (3.2.4.5).

An optional method is that after incubation of exportin-t with Ni-NTA beforehand, the column was washed with complex forming buffer till A_{280} decreased to zero (no unbound proteins in the column). Appropriate amounts of $tRNA^{Bulk}$ and Ran·GppNHp in 500 μl complex forming buffer were added and mixed with Ni-NTA and stored at room temperature for 10 min. The chromatography was performed the same as described in the former.

$tRNA^{Bulk}$, deacylated $tRNA^{Bulk}$, $tRNA^{Bulk}$ with correct 3′-CCA end from calf liver (3.5) were used as starting material.

3.9.2 Determination of tRNA by Northern analysis

3.9.2.1 Transblotting tRNAs from gel to Hybond-N^+ membrane

The second dimension polyacrylamide gel after being stained with ethidiumbromide and photographed, was immersed in 25 mM sodium phosphate (pH 6.5) for 30 min. The blotting was performed as described in *Molecular Cloning* (Sambrook). A corner of the gel was cut to simplify orientation for subsequent operations. The gel was laid onto a Hybond-N^+ membrane prewetted in 25 mM sodium phosphate (pH 6.5) and tRNAs in gel were transblotted to the Hybond-N^+ membrane for 12 h via capillary attraction. The membrane was put in an oven at 80ºC for 2 h to immobilize tRNA on it.

3.9.2.2 Northern hybridization

Northern hybridization reactions were carried on in sealed plastic tubes in hybridization oven (Bachofer, Reutlingen) at a temperature (T_{hy}) 5 to 10 degree below than the melting temperature (T_m), which was calculated as the sum of 4 × number of (G + C) bases and 2 × number of (A + T) bases. The prewetted membrane (normally 50 cm^2) was immersed in 10 ml hybridization buffer (5 × SSC buffer, 5 × Denhardt's solution, 0.5% (w/v) SDS, 100 µg/ml segmented and denatured salmon sperm DNA) at T_{hy} for 30 min (the details of buffers are in 3.1.9). Twenty µl 5′ end-labeled oligonucleotides (their sequences are listed in 3.1.7) after denaturation at 95ºC for 5 min was added directly into the tube containing membrane and hybridization buffer. Northern hybridization reaction was carried on at T_{hy} overnight. The unspecifically bound oligonucleotides were washed away with buffer 2 × SSC, 0.1% (w/v) SDS and buffer 0.1 × SSC, 0.1% (w/v) SDS sequentially at 25 to 30ºC. The radioactive dots, on which labeled DNA probes and tRNAs on membrane formed hybrid, were visualized in Instant Imager 2024. To disrupt the hybridization and to remove bound DNA labels, the membrane was immersed in 85 ºC 0.1% (w/v) SDS for 4 min, and then immediately soaked in 2 × SSC at room temperature. The membrane after such renewal could be repeatedly used.

3.10 AFM imaging on the TFK-modified mica surface

3.10.1 Preparation of HS-TFK

3-Bromo-1,1,1-trifluoroacetone (0.95 mmol in 0.1 ml) was dissolved in 20 ml of degassed CH_2Cl_2 under N_2 atmosphere, to which $NaHCO_3$ (3.6 mmol) was added and followed by 1,4-butanedithiol (0.81 mmol in 0.1 ml). The reaction mixture was stirred at ambient temperature for 5 days under N_2 atmosphere before diluted with CH_2Cl_2 (20 ml) and washed with aqueous H_2O (40 ml) and saturated NaCl solution (40 ml). Organic layer was dried over Na_2SO_4, filtered and concentrated. Excess of unreacted dithiol was disposed by evaporation on high vacuum pump. Because it was instable under flash column chromatography, the crude product was not purified and used directly for further reaction. Purity of HS-TFK was established by LC-EI-MS to be 50 %.

EI MS, *m/z* (%): 232 $[M]^+$ (25), 157 (34), 121 (30), 89 (100), 87 (92).

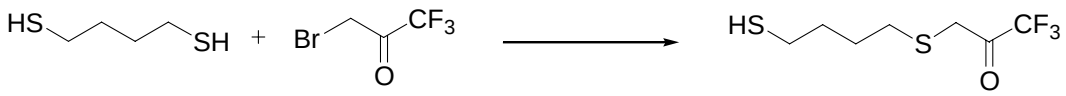

HS-TFK:
1,1,1-Trifluoro-3-(4-mercapto-butylsulfanyl)-propan-2-one

3.10.2 Preparation of BTFK

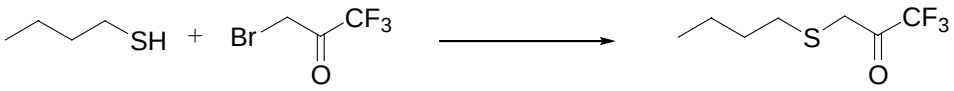

BTFK:
3-Butylsulfanyl-1,1,1-trifluoro-propan-2-one

3-Bromo-1,1,1-trifluoroacetone (BrTFK) (4.8 mmol in 0.5 ml) was dissolved in 15 ml of CH_2Cl_2 under N_2 atmosphere and mixed with butanethiol (4.3 mmol in 0.46 ml). Pyridine (4.3 mmol in 0.34 ml) in CH_2Cl_2 (10 ml) was added dropwise into ice-cooled solution of 3-Bromo-1,1,1-trifluoroacetone for 25 min. The reaction mixture was stirred further 1.5 h at 0°C before diluted with CH_2Cl_2 (20 ml) and washed with aqueous 1 M HCl (50 ml) and saturated NaCl (50 ml) solutions. Organic layer was dried over Na_2SO_4, filtered and concentrated. Flash column chromatography (hexane : ethylacetate = 5 : 1) afforded pure product as colorless oil in 74% yield (0.64 g).

For **BTFK** calculated $C_7H_{11}F_3OS$, Mol. Wt.: 200,22; ^{1}H-NMR (270 MHz, CDCl3): δ 0.90 (t, 3H), 1.38 (m, 2H), 1.55 (m, 2H), 2.49 (t, 1H), 2.69 (t, 1H), 2.88 (s, 1H), 3.46 (s, 1H); ^{13}C-NMR (90 MHz, CDCl3): δ 13.59, 21.82, 30.65, 33.37, 37.83, 92.72, 124.98; EI MS, *m/z* (%): 200 $[M]^+$ (65), 157 (8), 127 (12), 129 (14), 103 (53), 88 (35), 61 (100).

3.10.3 Modification of mica surface with HS-TFK

To the middle of a freshly cleaved mica sheet (0.4 cm^2) were put 4 µl of glycidyloxypropyl-trimethoxysilan (GOPTS), face to face (drop of GOPTS was put

between two mica sheets), for 70 minutes, and then the surface was rinsed with 3 ml of acetone and dried under nitrogen stream, according to Piehler *et al.* (2000). The dry mica sheets were immediately covered with 6 µl of 6 mM TFK in 0.1 M sodium hydrogen carbonate + methanol (in the rate of 1:1), pH 9.0 for 40 minutes. Then the surface was rinsed with 3 ml of ddH_2O and with 3 ml of ethanol and dried under nitrogen stream. For blocking of non-reacted free epoxy group on mica surface 10 µl of 0.1 M sodium hydrogen carbonate + methanol (in the ratio of 1:1), pH 9.0 were added for 60 minutes (rinsed with 3 ml of water and 3 ml of ethanol, dried under nitrogen stream). In the last step was repeated the second step of modification (2 mM TFK in 0.1 M sodium hydrogen carbonate + methanol (in the rate of 1:1), pH 9,0 for 30 minutes, rinsed with ddH_2O, ethanol and dried under nitrogen stream). Finally, the TFK-modified mica chip was stored under a drop of ddH_2O.

3.10.4 *in vitro* translation of exportin-t-esterase

Transcription/translation Kits were the gift from RiNA GmbH (Berlin, Germany) and the reaction was performed at 37 °C according to the manual provided by the supplier. The templates were added up to 5 nM.

3.10.5 Photometric measurement of esterase activity

Aliquots of 1 µl transcription/translation mixture were added to 1 ml of 50 mM phosphate buffer pH 7.5 containing 0.025 mM p-nitrophenyl acetate (Fluka). The production of p-nitrophenoxide was monitored at 405 nm in 1 cm path-length cells with UV-Spectral photometer DU 640 (Beckman, Fullerton, USA) at 25°C.

3.10.6 Immobilization of exportin-t-esterase to TFK-modified mica surface

TFK-modified mica was dried with nitrogen and immediately covered with 20 µl of 1 – 10 nM proteins in 1 mM Tris-HCl pH 7.5 for 15 minutes. The surface was washed with

200 µl 1 mM Tris-HCl pH 7.5 containing 0.3 M NaCl 3 times to remove non-specifically fixed biomolecules. Study of interaction exportin-t-esterase with tRNA and Ran·GppNHp was done by mixing 20 nM tRNA and 20 nM Ran·GppNHp in 20 µl 1 mM Tris-HCl pH 7.5 containing 25 µM KCl, 2.5 µM $MgCl_2$, 500 nM DTT for 10 minutes and was consequently washed with 200 µl of the same buffer. All these operations were done directly in the AFM.

3.10.7 Observing exportin-t-esterase under atomic force microscopy

For visualization of immobilized proteins on TFK-modified mica surface, tapping mode AFM in liquid was used, commercial equipment AFM MultiMode, with Nanoscope III control system and 13-µm scanner from Veeco/Digital Instruments Inc. Santa Barbara, CA. All images have been done around amplitude set-point 0.6, driving frequency 10 kHz, driving amplitude 180 mV and scanning rate 4 Hz at resolution 512 × 512 pixels. Measurements were realized by Silicon Nitride probes - DNP-S-NP series probes (with oxidation sharpened tips) purchased from Veeco/Digital Instruments Inc., Santa Barbara, CA. Probe with shape C Triangular and spring constant k = 0,32 N/m.

4 Results

4.1 Preparations of exportin-t and Ran·GppNHp

Exportin-t and p24Ran were prepared by overproduction in *E.coli*. The genes of these proteins were of human origin and introduced into *E. coli* via plasmids.

4.1.1 Expression and purification of exportin-t

Human exportin-t gene uses rare AAG and AGA codons for arginine, therefore, plasmid pUBS520 containing the gene of a $tRNA^{Arg}_{E.c}$ recognizing the two rare codons together with plasmid pQE30-Exportin-t were used for expression of exportin-t in *E. coli*. The gene of exportin-t was under the control of a *lac*-operon, and during fermentation IPTG was added after the culture had reached the mid-log phase of growth (A_{600} = 0.6 – 1.0) to inactivate the *lac*-repressor and to induce the production of exportin-t. Exportin-t could not be overexpressed to such extent as many other proteins in *E. coli*. No visible change of protein bands in SDS-PAGE was observed when analyzing the total cellular proteins before and after IPTG induction, implying that the yield of exportin-t after fermentation was low.

Six consecutive histidines residues adjacent to the N terminus of exportin-t were incorporated to facilitate the protein purification. Affinity chromatography of exportin-t on a Ni-NTA agarose column, in which Ni^{2+} ion bound the His_6 tag of exportin-t with its two ligand sites, was performed as the first purification step. The chromatographic profile is shown in Fig. 4.1, and the quantitative data are summarized in Tab. 4.1. Exportin-t was eluted as the main component of the 200 mM imidazol fraction. However there were still some protein impurities, which might contain high percentage of histidine and bound to Ni^{2+} ion. As the second step of purification a cation exchange chromatography on an EMD-SO_3 Tentakel column was used. At low salt concentration exportin-t together with some other proteins bound to the column, and as the ionic strength increased linearly,

exportin-t was eluted at 800 mM KCl. The chromatographic profile is shown in Fig. 4.2. The quantitative data are summarized in Tab. 4.1.

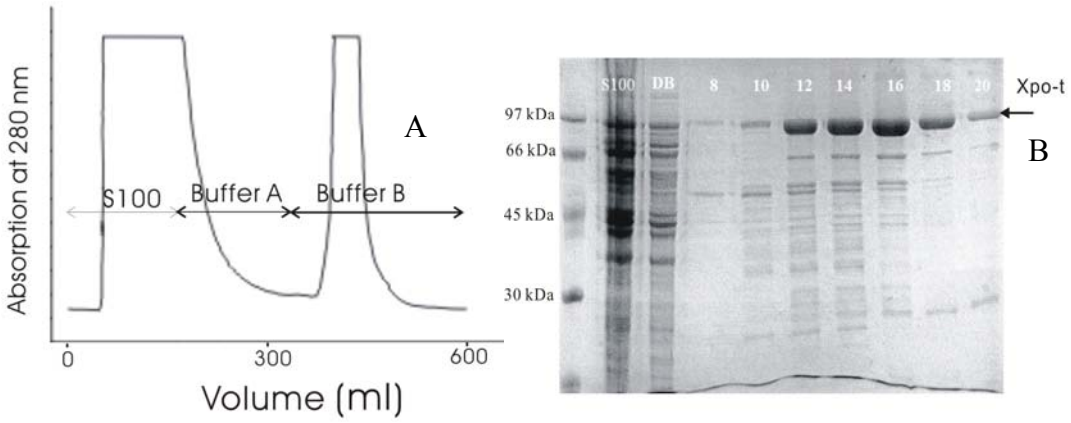

Fig. 4.1 Affinity chromatographic profile of His_6-exportin-t on a Ni-NTA column
The *E.coli* S100 supernatant containing exportin-t was loaded onto a Ni-NTA column (2 × 4 cm). After washing the column with buffer 50 mM sodium phosphate pH 6.0, 300 mM NaCl, 10 mM imidazol, 0.5 mM PMSF till base line reappeared, exportin-t was eluted with the same buffer containing 200 mM imidazol. The chromatographic profile is shown in (A). Based on results of 12.5% SDS-PAGE (B), fractions from 12 to 20 were pooled for further purification.

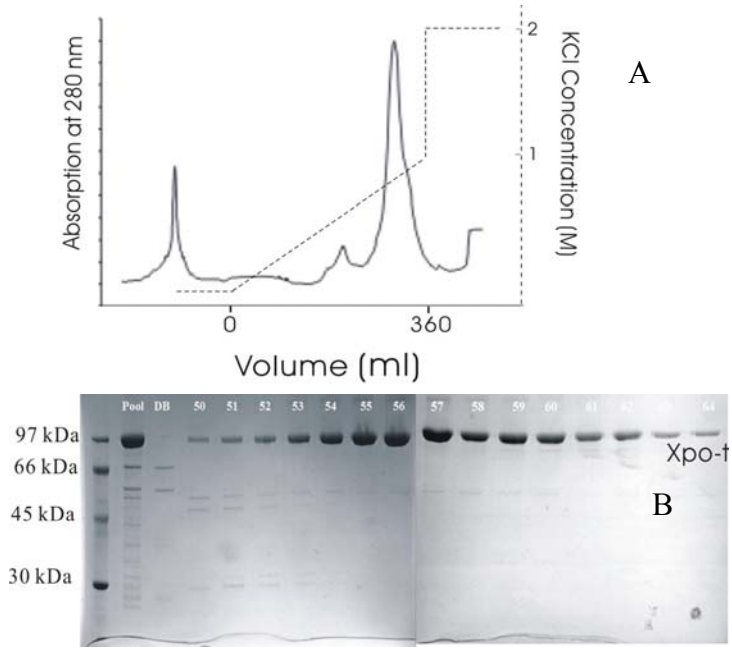

Fig. 4.2 Ion exchange chromatographic profile of exportin-t on an EMD-SO_3 Tentakel column
The protein pool containing exportin-t was loaded onto an EMD-SO_3 Tentakel column (25 × 2 cm). After extensive wash of the column till base line reappeared, exportin-t was eluted with a linear gradient of KCl (dotted line). The chromatographic profile is shown in (A). Based on results of 12.5% SDS-PAGE (B), fractions from 53 to 60 were collected.

After the second chromatography, the amount of impurities in the fractions containing exportin-t decreased remarkably (Fig. 4.2B). The third purification step was a gel

permeation chromatography on a Sephacryl S200 HR column. The elution profile is shown in Fig. 4.3. The quantitative data are summarized in Tab. 4.1. It is noteworthy that two protein peaks were observed in the gel permeation chromatographic profile, despite the fact that before this chromatography the protein sample contained exportin-t and little impurities. The first peak was probably due to the tendency of exportin-t to aggregate under the conditions used here.

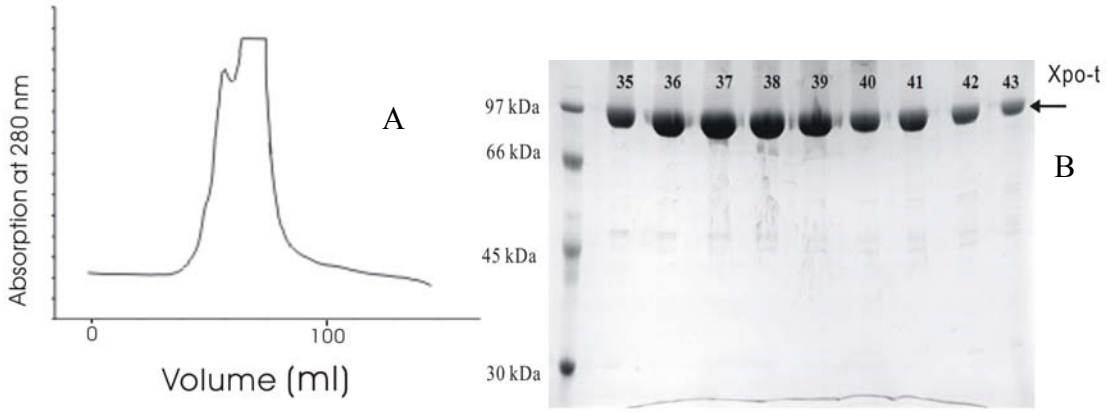

Fig. 4.3 Gel permeation chromatography profile of exportin-t on a Sephacryl S200 HR column
The concentrated exportin-t sample was loaded on a Sephacryl S200 HR column (75 × 1.8 cm) and eluted with 50 mM Tris-HCl pH 7.5, 100 mM NaCl, 5% glycerol. Based on results of 12.5% SDS-PAGE, fractions from 35 to 42 were collected.

Tab. 4.1 Purification of exportin-t

Purification step	Protein concentration (mg/ml)	Volume (ml)	Protein quantity (mg)	Protein Recovery (%)
S100 supernatant	22.4	85	1905.2	100
(1) Ni-NTA agarose	1.4	70	96.3	5.1%
(2) EMD-SO_3 Tentakel	0.9	48	42.1	2.2%
(3) Sephacryl S200 HR	1.7	16	27.7	1.4%

From quantitative data of the exportin-t purification listed in Tab. 4.1, it was noticed that the major purification effect was achieved in the first chromatography, 95% of total protein remained unbound to Ni-NTA agarose.

4.1.2 Preparation of Ran·GppNHp

4.1.2.1 Purification of Ran·GDP

Expression of p24Ran in *E.coli* was comparatively simpler than that of exportin-t. One plasmid pETran in *E.coli* expression strain BL21 (DE3) was sufficient for overexpression of the exogenous protein in *E.coli*.

Cation exchange chromatography on EMD-SO_3 Tentakel was performed as the first step of purification. As the ionic strength increased linearly, Ran·GDP was eluted in the first peak, at 280 mM KCl. The profile is shown in Fig. 4.4 and the quantitative data are summarized in Tab. 4.2.

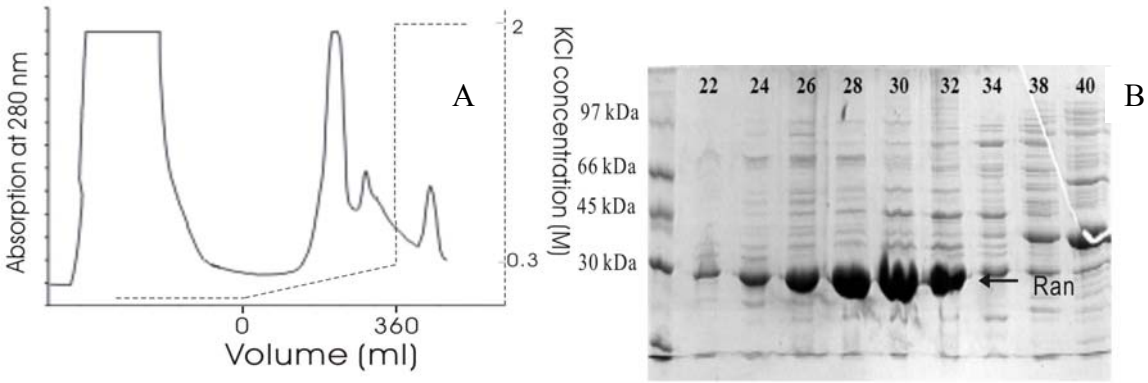

Fig. 4.4 Ion exchange chromatography profile of Ran·GDP on an EMD-SO_3 Tentakel column
The *E.coli* S100 supernatant containing Ran·GDP n was loaded onto EMD-SO_3 Tentakel (25 × 2 cm). After washing the column till base line reappeared, Ran·GDP n was eluted with a linear gradient of KCl (dotted line). The elution profile is shown in (A). Based on results of 15% SDS-PAGE (B), fractions from 25 to 32 were collected.

Since more than 80% of total protein in the eluted fraction was Ran·GDP (Fig. 4.4B), a simple gel permeation chromatography on Sephacryl S200 HR was sufficient for further purification, the profile of which is shown in Fig. 4.5. The quantitative data are summarized in Tab. 4.2. By gel permeation chromatography, the impurities, most of

which were of higher molecular mass than Ran·GDP and separated from Ran·GDP (Fig. 4.5B).

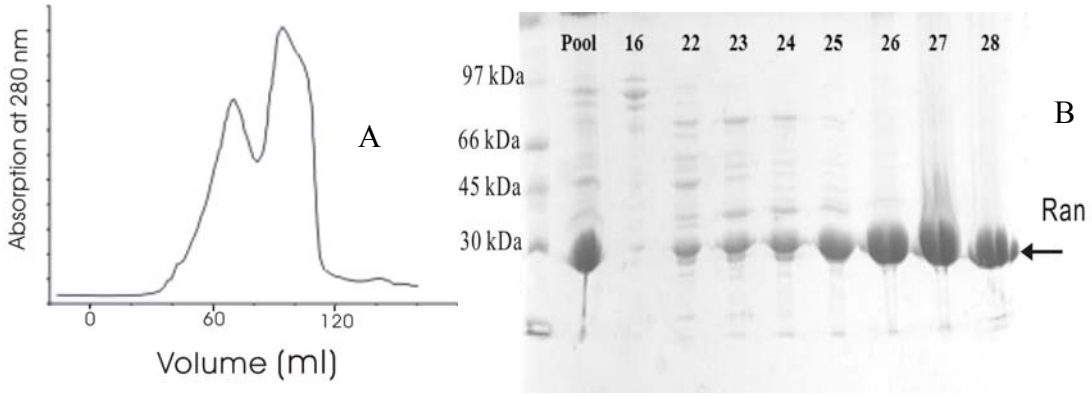

Fig. 4.5 Gel permeation chromatography profile of Ran·GDP on a Sephacryl S200 HR column
The concentrated protein sample containing Ran·GDP was loaded onto a Sephacryl S200 HR column (75 × 1.8 cm) and eluted with buffer 60mM Tris-HCl 7.6, 1 mM $MgCl_2$, 1 mM 2-mercaptoethanol, 10µM GDP, 20 µM PMSF. The elution profile is shown in (A). Based on results of 15% SDS-PAGE (B) fractions from 25 to 28 were collected.

Tab. 4.2 Purification of Ran·GDP

Purification step	Protein concentration (mg/ml)	Volume (ml)	Protein quantity (mg)	Protein recovery (%)
S100 supernatant	13.7	140	1918	100
(1) EMD-SO_3 Tentakel	9.9	60	591	30.8
(2) Sephacryl S200 HR	8.8	16	140.1	7.3

From quantitative data of Ran·GDP purification listed in Tab. 4.2, it can be concluded that the two chromatographies were efficient to obtain Ran·GDP which is overproduced in *E.coli*.

4.1.2.2 Preparation of Ran·GppNHp

Ran·GppNHp was used as a substitute of Ran·GTP and prepared by nucleotide exchange reaction of Ran·GDP (3.4.2.3). In the reaction sample, EDTA was added to deprive Ran·GDP of Mg^{2+} and to dissociate p24Ran from GDP. The free GDP was degraded by shrimp alkaline phosphatase and could not bind to p24Ran any more. GppNHp, resistant to the phosphatase degradation, was bound by the free p24Ran. A gel

permeation chromatography on Sephacryl S200 HR was performed to separate Ran·GppNHp from free GppNHp, the profile of which is shown in Fig. 4.6. Ran·GppNHp is in the first peak and free GppNHp in the second peak.

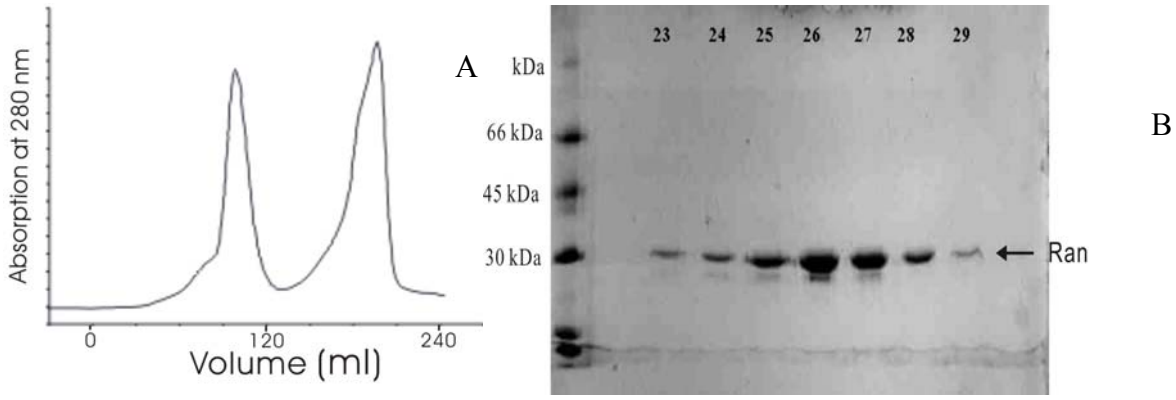

Fig. 4.6 Gel filtration chromatography profile of Ran·GppNHp on a Sephacryl S200 HR column
The nucleotige exchange reaction sample was directly loaded onto a Sephacryl S200 HR column (75 × 1.8 cm). Elution with buffer 50 mM Tris-HCl pH 7.5, 100 mM NaCl, 10 mM $MgCl_2$ was performed, the profile of which is in (A). Based on results of 15% SDS-PAGE (B) fractions from 25 to 28 were collected.

4.2 Preparation of s^4U containing tRNA

4.2.1 *in vitro* transcription of s^4U containing $tRNA^{Phe}_{T.th}$

To introduce the photoactive 4-thiouridine (s^4U) into tRNA transcript required for the photoaffinity crosslinking experiments, 4-thiouridine triphosphate (s^4UTP) and other 4 NTPs were used as substrates in *in vitro* transcription with bacteriophage T7 RNA polymerase, which initiates and terminates with high precision. Using a linear tDNA template with the complete 3′ end (which can be achieved by BstN I digestion or PCR), $tRNA^{Phe}_{T.th}$ transcripts were prepared *in vitro* (3.5.1.2). The ratio of s^4UTP to UTP in the reaction determined the incorporation rate of s^4U into tRNA transcripts. In my experiments this ratio was set to be 4 : 1. Unmodified $tRNA^{Phe}_{T.th}$ transcript was produced as control in the same way in the absence of s^4UTP. To increase the sensitivity for the

subsequent biochemical analyses, radioactivity was introduced into the transcripts by adding appropriate amount of radioactive [α^{32}P]ATP. The tRNA transcripts were separated from free [α^{32}P]ATP and other undesirable molecules by PAGE in the presence of 7M urea (Fig. 4.7), and recovered from the gel (3.2.5). The quantitative data are listed in Tab. 4.3.

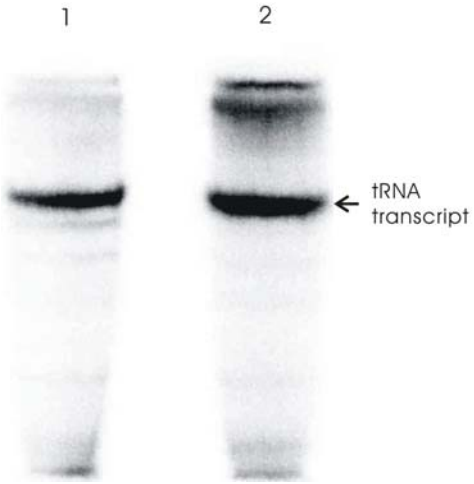

Fig. 4.7 Urea polyacrylamide gel analysis of the [^{32}P]tRNAs transcribed *in vitro*
1. (s^4U)tRNA$^{Phe}_{T.th}$; 2. unmodified tRNA$^{Phe}_{T.th}$. The two transcripts were labeled with [α^{32}P] ATP and visualized in Instant imager 2024.

Tab. 4.3 *In vitro* transcription of tRNA$^{Phe}_{T.th}$

	s^4U containing tRNA transcript	tRNA transcript without s^4U
Template used	19.5 pmol tDNA	19.5 pmol tDNA
Yield of tRNA	1.5 nmol tRNA	3.2 nmol tRNA

As shown in Tab. 4.3, using the same amount of template, the yield of tRNA$^{Phe}_{T.th}$ transcript is about 2.1 times higher than that of (s^4U)tRNA$^{Phe}_{T.th}$ (s^4U containing tRNA$^{Phe}_{T.th}$ transcript). However 1.5 nmol (45 µg) tRNA$^{Phe}_{T.th}$ out of 150 µl reaction system (3.5.1.2) was sufficient for the following crosslinking experiments.

4.2.2 Analysis of nucleoside components of tRNA$^{Phe}_{T.th}$ transcript by RP-HPLC

To test whether 4-thiouridine was successfully incorporated into the (s^4U)tRNA$^{Phe}_{T.th}$, reversed phase high performance liquid chromatography (RP-HPLC) was used (3.7.2).

Of normal $tRNA^{Phe}_{T.th}$ transcript, only four uv 254 nm-absorbing peaks were detected corresponding to cytidine, uridine, guanosine, and adenosine respectively (Fig. 4.8A). There was no detectable absorption at 330 nm (base line). It is clear that no nucleoside other than A, G, C, U existed in $tRNA^{Phe}_{T.th}$ transcript. When $(s^4U)tRNA^{Phe}_{T.th}$ was analyzed, a new peak appeared in the chromatographic profile at 19.3 ml besides the four known peaks of A, G, C, U (Fig. 4.8B). The eluted substance absorbed both at 254 nm and at 330 nm, which is typical for s^4U. The RP-HPLC was highly reproducible in different experiments, and the retention time of each nucleoside remained a constant. By calculating the peak areas of U and s^4U in Fig 4.8B, the incorporation ratio of s^4U is found to be 41%. Among 16 positions of Uridine in $tRNA^{Phe}_{T.th}$ transcript, about 6.5 were occupied by s^4U in average.

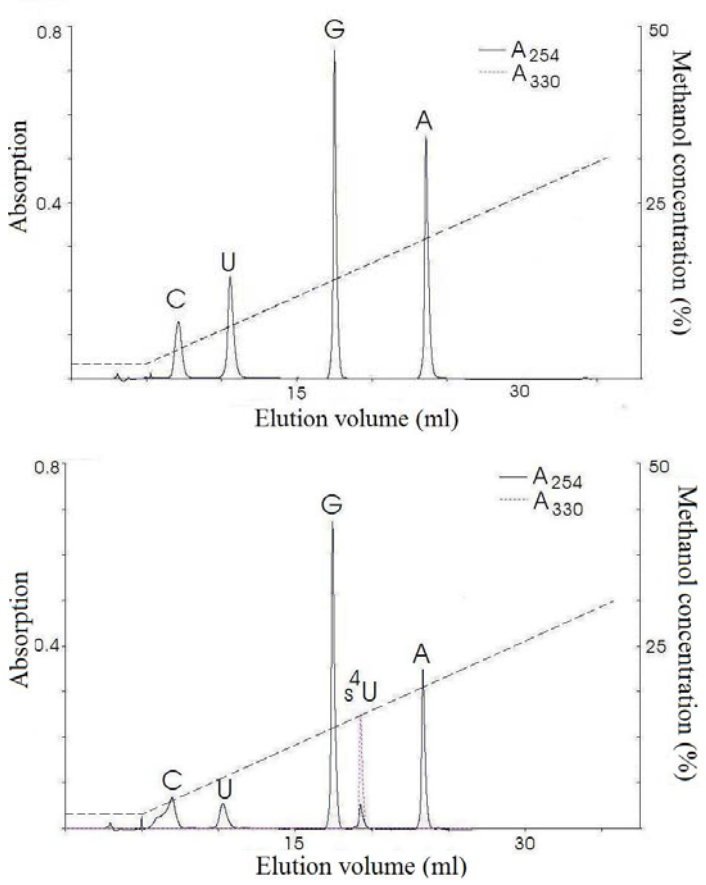

Fig. 4.8 Analysis of nucleoside components of $tRNA^{Phe}_{T.th}$ transcript by RP-HPLC
$tRNA^{Phe}_{T.th}$ transcript (A) and $(s^4U)tRNA^{Phe}_{T.th}$ (B) were degraded to nucleosides, and then subjected to RP-HPLC analysis on column Supelcosil LC 18S (25 cm × 4.6 mm). A methanol gradient (dotted line) was used to elute nucleosides.

4.3 Formation of a ternary complex of tRNA·exportin-t·Ran·GppNHp

The formation of complex exportin-t, Ran·GppNHp and (s^4U)tRNA$^{Phe}_{T.th}$ were tested by electrophoretic mobility shift assay (EMSA) (3.2.8, 3.2.4.4), in which the ternary complexes of tRNA·exportin-t·Ran·GppNHp can be separated from free tRNA molecules due to its enlarged size.

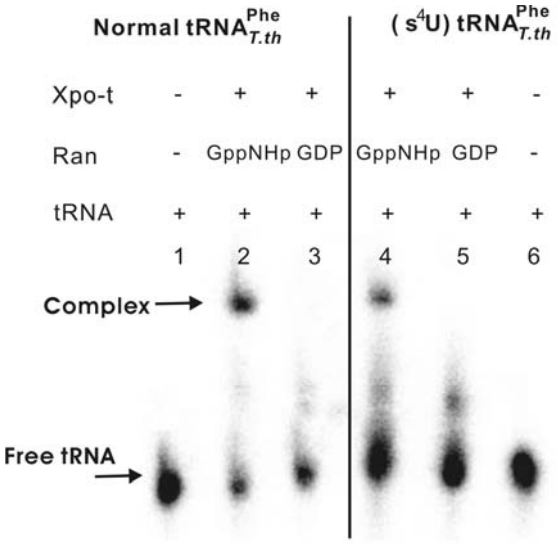

Fig. 4.9 Analysis of the interaction between exportin-t and [^{32}P]tRNA transcript by EMSA
[^{32}P] tRNA$^{Phe}_{T.th}$ transcript (left) and [^{32}P] (s^4U)tRNA$^{Phe}_{T.th}$ (right) were incubated with exportin-t, Ran·GppNHp or Ran·GDP in 20 mM Tris-HCl 7.5, 50 mM KCl, 5 mM $MgCl_2$, 1 mM DTT, 5% glycerol. The samples were loaded in 5% native polyacrylamide gel and run at 4°C, 250 V. The bands containing ^{32}P labeled tRNA were visualized in Instant Imager 2024.

From Fig. 4.9, it was found that both tRNA$^{Phe}_{T.th}$ transcript and (s^4U)tRNA$^{Phe}_{T.th}$ could bind exportin-t in the presence of Ran·GppNHp, suggesting that exportin-t, Ran·GppNHp and tRNA transcripts were biologically functional. The titration of exportin-t to the 1 μM normal tRNA$^{Phe}_{T.th}$ transcript and 5 μM Ran·GppNHp showed that 50% tRNA was found in complex as exportin-t concentration reached 3 μM, the result is shown in Fig. 4.16. It was observed that (s^4U)tRNA$^{Phe}_{T.th}$ bound exportin-t to a lesser extent than normal tRNA transcript. *in vitro* transcribed (s^4U)tRNA$^{Phe}_{T.th}$ was a mixture of tRNA molecules with s^4Us at every possible site. Some tRNAs in this mixture had too many s^4Us or s^4Us at certain sites that could impair its interaction with exportin-t. They did not bind exportin-t as good as the other tRNA transcripts with less s^4Us or with s^4Us at unimportant sites for exportin-t binding. In my experiments, only those (s^4U)tRNA$^{Phe}_{T.th}$ able to bind and crosslink to exportin-t were analyzed.

4.4 Photocrosslinking (s^4U)$tRNA^{Phe}_{T.th}$ to exportin-t

4.4.1 (s^4U)$tRNA^{Phe}_{T.th}$ crosslinked to exportin-t under uv irradiation

4-Thiouiridines in RNA can be photoactivated and covalently linked to groups in their neighborhood. Samples containing the ternary complex of exportin-t·Ran·GppNHp·(s^4U)$tRNA^{Phe}_{T.th}$ were irradiated at 312 nm (3.8.1). After a scheduled time period, the irradiated samples were analyzed by PAGE (Fig. 4.10).

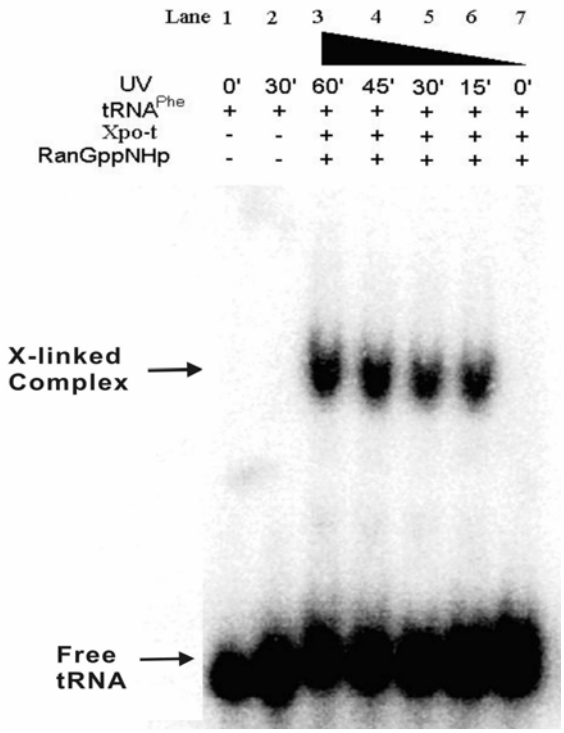

Fig. 4.10 PAGE analysis of photoaffinity crosslinking between exportin-t and [^{32}P] (s^4U)$tRNA^{Phe}_{T.th}$
The irradiated samples (the components in samples and irradiation time are listed on the upper part of the figure) were heated at 60°C for 5 min after addition of SDS loading buffer and loaded on a 5% polyacrylamide gel. The radioactive bands were visualized in Instant Imager 2024.

The crosslinked complex was a product of irradiation, and the yield increased as the amount of photons absorbed by the samples (correlated with irradiation time) increased. (s^4U)$tRNA^{Phe}_{T.th}$ in the absence of proteins did not form complexes after irradiation, implying that proteins were involved in the crosslinking.

Which protein crosslinked to tRNA, exportin-t, Ran or both? To answer this question, crosslinked complex was purified from gel (3.2.5) and subjected to 15% SDS PAGE analysis. The bands were visualized both by Coomassie brilliant blue staining and by ^{32}P detection (Fig. 4.11). The RNA (detected by radioactivity) was found at the same position of exportin-t (detected by Coomassie brilliant blue) but not at the position of Ran·GppNHp. In the purified crosslinked complex, only exportin-t, not Ran·GppNHp was observed. Ran·GppNHp was not crosslinked to tRNA, suggesting Ran·GppNHp did not contact tRNA, at least not to a noticeable extent.

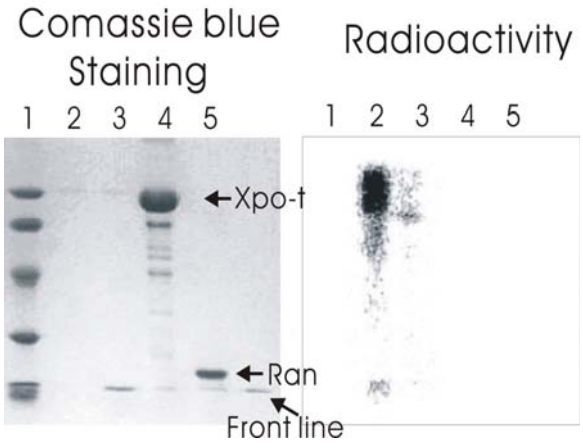

Fig. 4.11 SDS-PAGE analysis of purified crosslinked complex
The purified crosslinked complex (lane 2, 3) was subjected to 15% SDS PAGE analysis, and visualized with Coomassie brilliant blue (left) and ^{32}P detection (right). Exportin-t in lane 4 and Ran·GppNHp in lane 5 were used as control. In lane 3, crosslinked complex was digested with RNase A. There were bands visible in lane 2 and 3 at the position of exportin-t (compared with lane 4), whereas no bands at the position of Ran·GppNHp (compared with lane 5).

4.4.2 Formation of ternary complex is the prerequisite of crosslinking

4.4.2.1 The crosslinking is Ran·GTP dependent

Was this crosslinked complex only a random contact of tRNA with exportin-t or the product of the formation of ternary complex under irradiation? If the former was true, Ran·GppNHp, which was not found in the crosslinked complex, would be dispensable to this crosslinking. To test the role of Ran·GppNHp, $(s^4U)tRNA^{Phe}_{T.th}$ and exportin-t were subjected to irradiation in the presence of Ran·GDP and Ran·GppNHp, corresponding to relaxed and active conformation of Ran respectively. The results are shown in Fig. 4. 12.

Without exportin-t (s^4U)$tRNA^{Phe}_{T.th}$ did not bind Ran·GppNHp at all, and barely crosslinked to exportin-t in the absence of Ran. In the presence of Ran·GDP, crosslinking yield somewhat increased. In comparison, a bright band of crosslinked complex was observed in the sample containing (s^4U)$tRNA^{Phe}_{T.th}$, exportin-t and Ran·GppNHp. It is evident that the crosslinking between (s^4U)$tRNA^{Phe}_{T.th}$ and exportin-t was strongly stimulated by Ran·GppNHp.

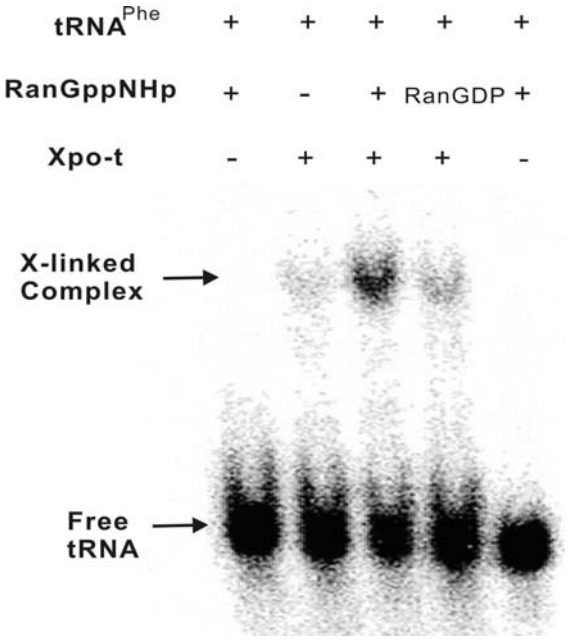

Fig. 4.12 PAGE analysis of crosslinking of [^{32}P] (s^4U)$tRNA^{Phe}_{T.th}$ with exportin-t in the presence of Ran·GDP and Ran·GppNHp
The composition of the irradiated samples is listed in the upper part of the figure. The samples after irradiation were heated in SDS loading buffer at 60°C for 5 min and loaded on a 5% polyacrylamide gel. The bands were visualized in Instant Imager 2024.

4.4.2.2 The crosslinking could be competitively inhibited by other tRNA species

If the crosslinking was dependent on formation of the ternary complex, other tRNA species would competitively inhibit the crosslinking. Unlabeled $tRNA^{Arg}_{E.c}$ of different concentrations was introduced in crosslinking samples containing (s^4U)$tRNA^{Phe}_{T.th}$, exportin-t, Ran·GppNHp. Irradiation time was set to be 1 min, so briefly that the amount of crosslinked tRNA was related to the crosslinking velocity. The yield of crosslinked complex was analyzed on a 5% polyacrylamide gel (Fig 4.13). As the amount of competitor $tRNA^{Arg}_{E.c}$ increased, the crosslinking yield decreased. $tRNA^{Arg}_{E.c}$ effectively inhibited the crosslinking. Other tRNA species were also tested; all of them produced the

same inhibition effect. These experiments revealed that specific tRNA/exportin-t recognition was the prerequisite for the crosslinking. The crosslinking can be viewed as a freezing of the tRNA: proteins interaction. The groups in tRNA crosslinked to exportin-t were the possible contact sites between them.

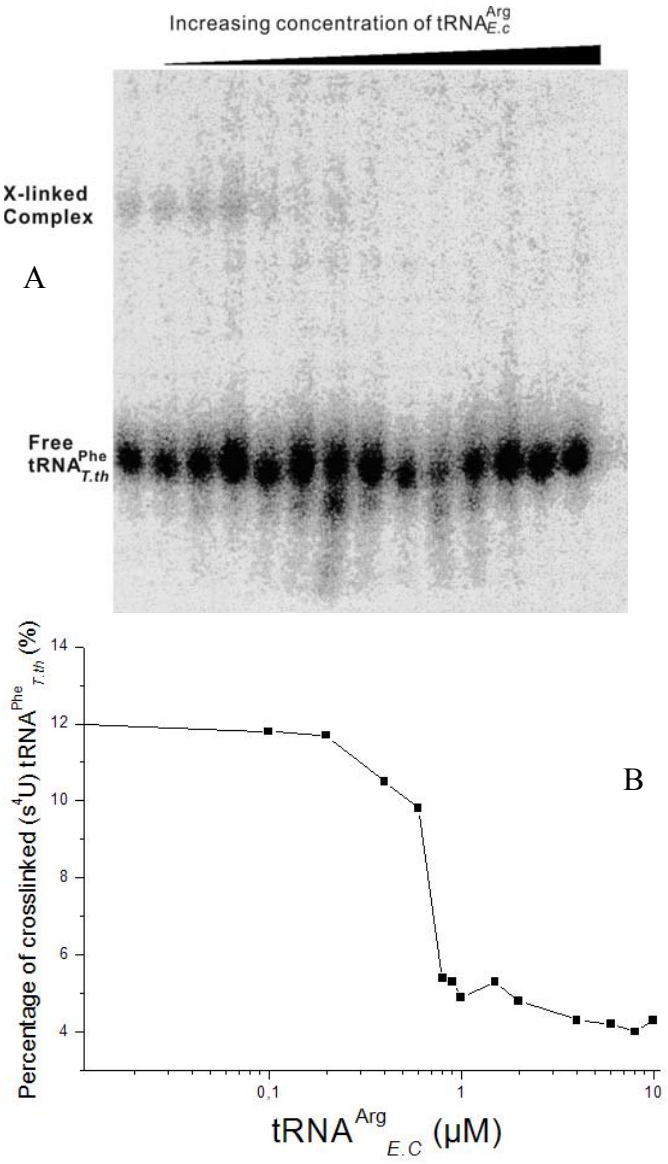

Fig. 4.13 PAGE analysis of the competitive inhibition of crosslinking [^{32}P] (s^4U)tRNA$^{Phe}_{T.th}$ by tRNA$^{Arg}_{E.c}$
The samples containing 0.4 μM [^{32}P] (s^4U)tRNA$^{Phe}_{T.th}$, 2 μM exportin-t, 2 μM Ran·GppNHp and a concentration series of tRNA$^{Arg}_{E.c}$ were irradiated for 1 min and subjected to a routine PAGE analysis (described in 3.2.4.4). The bands were detected in Instant imager 2024. The quantitative data was acquired from the calculation with the photoimager software.

4.4.3 U47 is the major contact site between (s^4U)tRNA$^{Phe}_{T.th}$ and exportin-t

To determine the contact site of (s^4U)tRNA$^{Phe}_{T.th}$ and exportin-t, crosslinked tRNA$^{Phe}_{T.th}$ was purified from gel and used as template in primer extension reaction after protease K treatment (3.8.3.3). tDNAs synthesized with this template would prematurely terminate at the crosslinking sites. The primer extension samples were analyzed in a sequencing gel (3.2.4.3), the results of which are shown in Fig. 4.14.

Because the primer covered the tRNA template from residue 76 to 61, it was only capable to analyze the tRNA region from residue 1 to 60. Primer extension with intact (s^4U)tRNA$^{Phe}_{T.th}$ as template was used as control (lane 2). Though, some weak bands were observed in lane 2, which might be due to accidental stops of the reverse transcriptase, the major product was the tDNA of full length, suggesting that most of the primer extension reactions came to completion and s^4U residues in tRNA template did not interfere with the DNA synthesis. In another control, ddATP was added to the primer extension reaction sample, and no nucleotides could be added to the tDNA chain having a ddA end, corresponding to U residue in tRNA template. An appropriate ratio of ddATP to dATP (80 : 1 here) was used to produce a DNA ladder stopping at every U position in tRNA (lane 1).

Using the crosslinked (s^4U)tRNA$^{Phe}_{T.th}$ as template, no tDNA of full length was observed (lane 4), suggesting that s^4U residues being crosslinked with peptide in the template formed a hindrance for the reverse transcriptase. The major DNA bands in lane 4 were stopped at U55 and at U47, which are probably the major crosslinking sites between (s^4U)tRNA$^{Phe}_{T.th}$ and exportin-t. The DNA bands at position U55 and below were the brightest, indicating the most efficient pausing of the reverse transcriptase at those positions. However, because they were too near of the primer, these bands might come from accidental stops. Besides, U55 located in TΨC loop, a well-known contact region of tRNA with exportin-t (Arts *et al.*, 1998b), the bright band at U47 showed that U47 in tRNA$^{Phe}_{T.th}$ was a major contact site to exportin-t. This indicates that the extra loop of the tRNA is also involved in contact with exportin-t. Besides them, weak bands were present in lane 4 at U20 and U33, which were possible contact sites between (s^4U)tRNA$^{Phe}_{T.th}$ and exportin-t, but not so important as U55 and U47. The DNA band at position U33 was the weakest. Other DNA bands in lane 4 were too weak and regarded as the noise of the primer extension reaction.

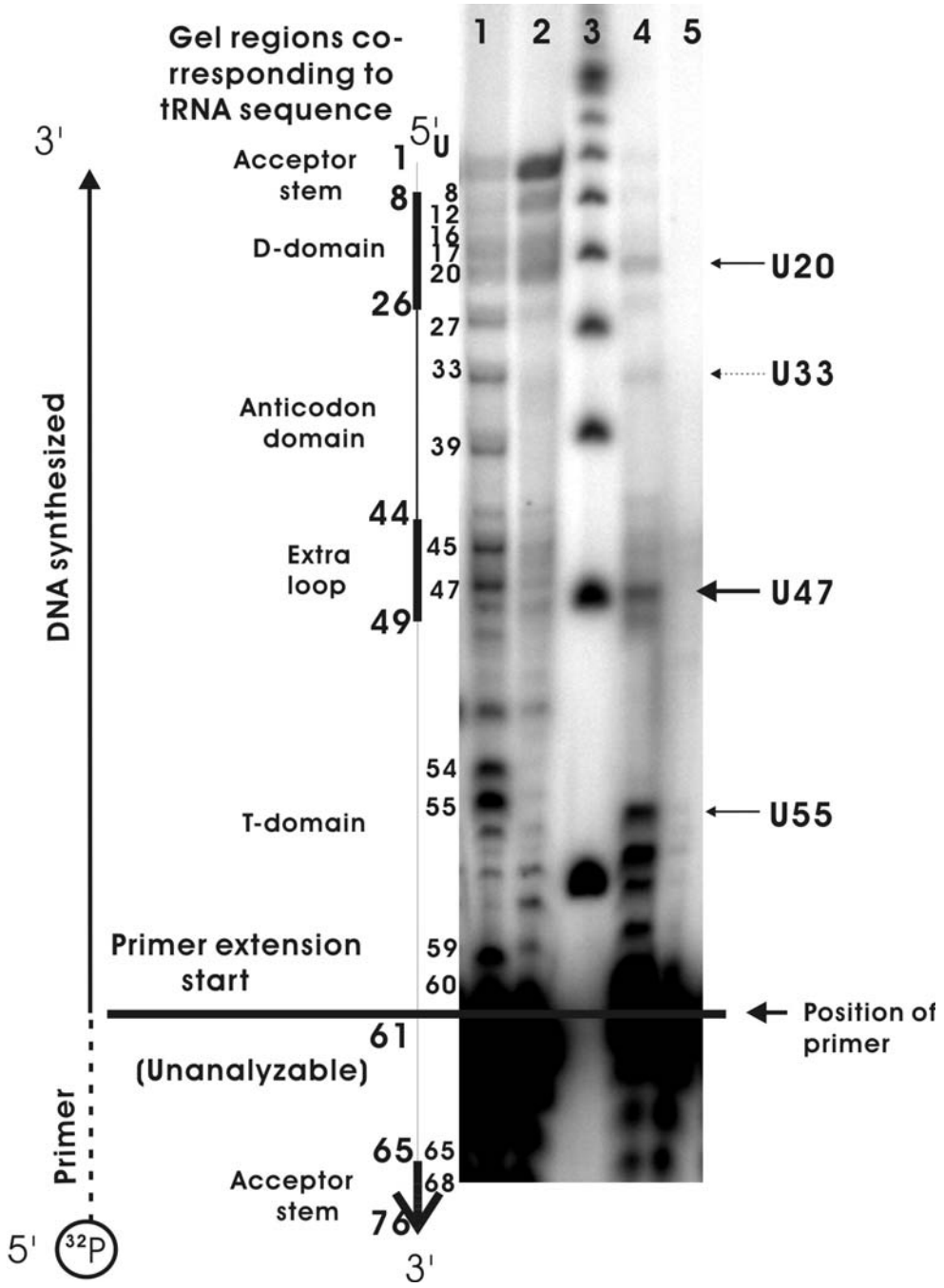

Fig. 4.14 Sequencing gel analysis of primer extension products using crosslinked tRNA as a template

With [^{32}P] 5′ labeled DNA primer, (lane 2) (s^4U)tRNA$^{Phe}_{T.th}$ and (lane 4) purified crosslinked (s^4U)tRNA$^{Phe}_{T.th}$ were used as templates in primer extension analysis. In lane 1, ddATP was added to produce a tDNA ladder stopping at each U of tRNA. ssDNAs with known molecular mass were used in lane 3 as a control. In lane 5, the [^{32}P] DNA primer of 16 nucleotides was used as the blank control. Uridine residues that lie in the region of primer (60-76) are not analyzable. Radioactive DNA bands were visualized in Instant Imager 2024.

The contact sites determined by primer extension analysis are marked out in the secondary and tertiary structure of tRNA (Fig. 4. 15).

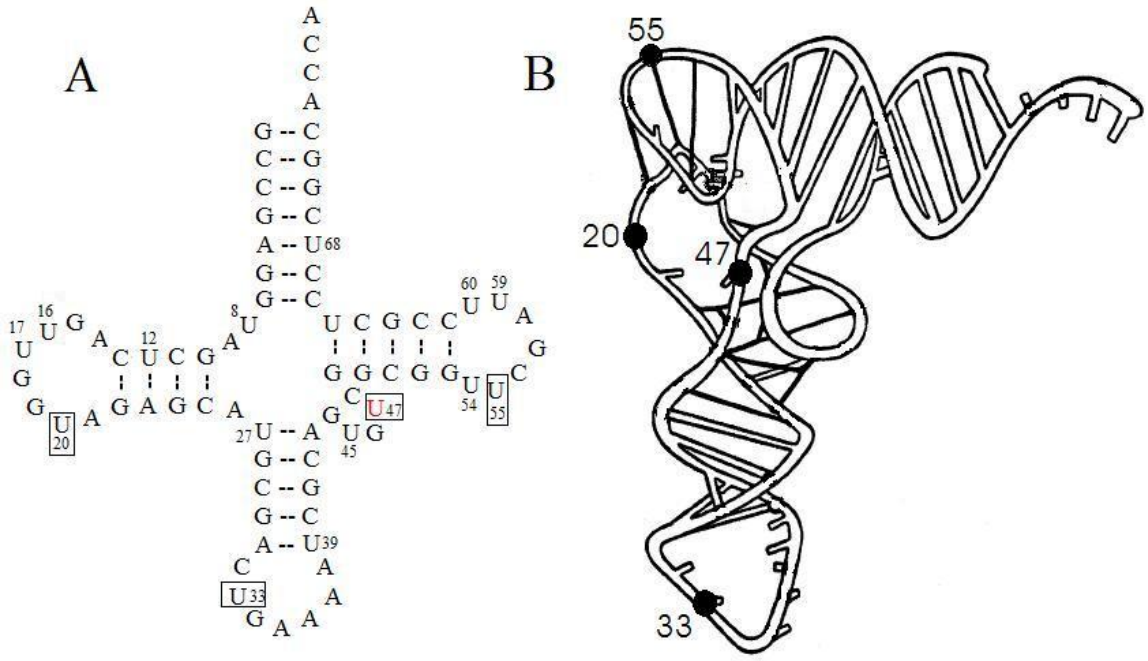

Fig. 4.15 Contact sites of tRNA$^{Phe}_{T.th}$ in crosslinking with exportin-t
(A). Sequence of tRNA$^{Phe}_{T.th}$ transcript, crosslinked sites are framed
(B). The tertiary structure of yeast tRNA^{Phe}, crosslinked sites are indicated by dots.

Since U47 in tRNA$^{Phe}_{T.th}$ appeared to be a major contact site of tRNA and exportin-t, its role in this interaction was further tested by mutation experiments. Routine methods were used to introduce a T47A mutation in tRNA$^{Phe}_{T.th}$ gene (3.3.6), which was confirmed by sequencing.

With mutant tDNA and wild type tDNA as template, mutant tRNA$^{Phe}_{T.th}$ U47A and wild type tRNA$^{Phe}_{T.th}$ were transcribed *in vitro* and labeled with ^{32}P. EMSA experiments were performed to test their abilities to bind exportin-t. The results are shown in Fig. 4. 16. Both normal and mutant tRNA$^{Phe}_{T.th}$ transcripts could bind exportin-t. The quantity of the ternary complex increased as the concentration of exportin-t increased. By rough

estimation of K_D (the concentration of exportin-t at which 50% tRNA was bound), it was found that mutant $tRNA^{Phe}_{T.th}$ transcript bound to exportin-t a little weaker (5 µM) than the normal tRNA transcript (3 µM). Thus, substitution of uridine 47 with adenosine did not substantially affect the tertiary structure of $tRNA^{Phe}_{T.th}$.

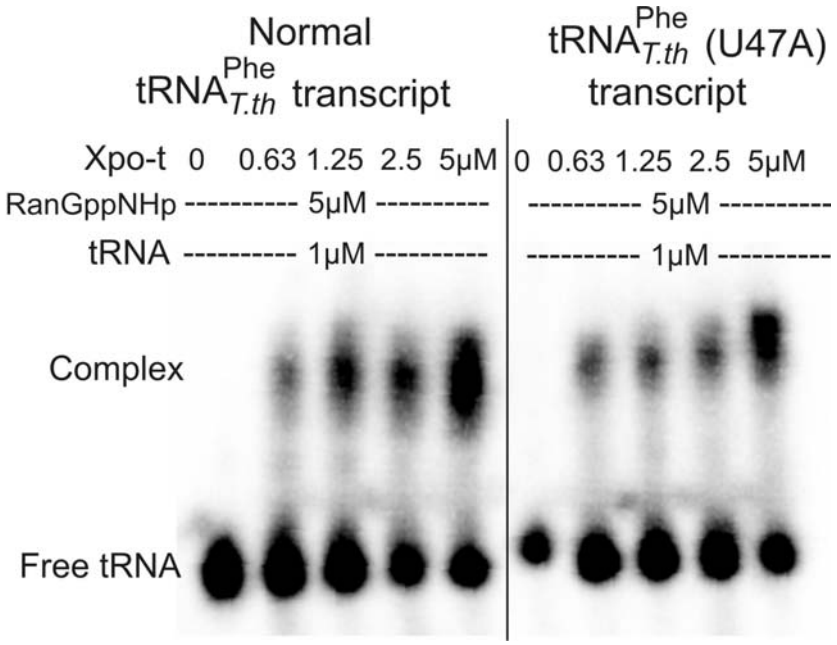

Fig. 4.16 EMSA analysis of the ability of mutant [^{32}P]$tRNA^{Phe}_{T.th}$ and normal [^{32}P]$tRNA^{Phe}_{T.th}$ transcripts to bind exportin-t
[^{32}P] normal $tRNA^{Phe}_{T.th}$ transcript (left) and [^{32}P] mutant $tRNA^{Phe}_{T.th}$ U47A(right) were incubated with exportin-t, Ran·GppNHp in 20 mM Tris-HCl 7.5, 50 mM KCl, 5 mM $MgCl_2$, 1 mM DTT, 5% glycerol. The samples were loaded in 5% native polyacrylamide gel and run at 4°C, 250 V. The bands were visualized in Instant Imager 2024.

To further study the role of U47 in the crosslinking experiment, s^4U was incorporated into the mutant $tRNA^{Phe}_{T.th}$U47A transcript, which was irradiated at 312 nm in the presence of Ran·GppNHp and exportin-t. The crosslinking results are shown in Fig. 4.17. It was found that mutant $tRNA^{Phe}_{T.th}$U47A crosslinked to exportin-t to a lesser extent. Though, U47 being replaced by A did not impede tRNA to bind exportin-t noticeably,

mutant (s^4U)$tRNA^{Phe}_{T.th}$ failed to crosslink exportin-t well. Therefore, it is suggested that U47 is a major contact site between $tRNA^{Phe}_{T.th}$ and exportin-t.

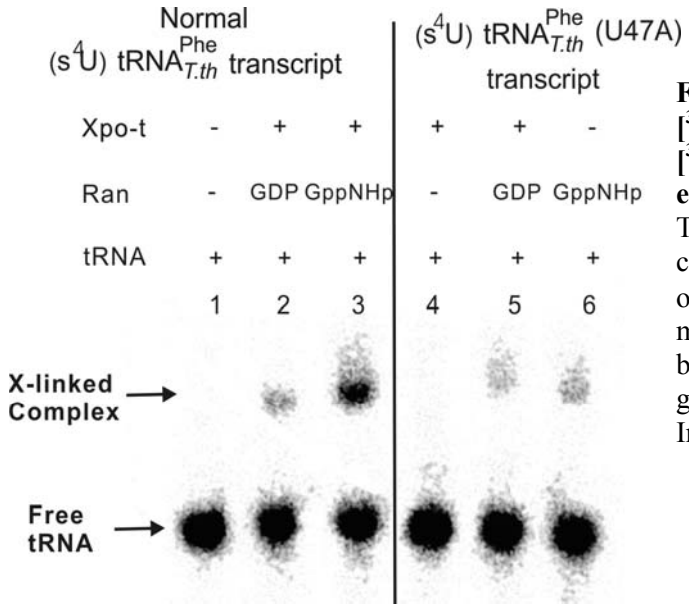

Fig. 4.17 PAGE analysis of mutant [^{32}P]$tRNA^{Phe}_{T.th}$ U47A and wild type [^{32}P]$tRNA^{Phe}_{T.th}$ crosslinking to exportin-t
The irradiated samples (The components are listed in the upper part of the figure) were heated at 60°C for 5 min after addition of SDS loading buffer and loaded on a 5% acrylamide gel. The bands were visualized in Instant Imager 2024.

4.5 Interaction of calf liver $tRNA^{Bulk}$ with immobilized exportin-t

In order to test the relative affinity of tRNA species in calf liver $tRNA^{Bulk}$ to exportin-t, exportin-t was immobilized on Ni-NTA agarose, and an affinity chromatography of $tRNA^{Bulk}$ was performed (3.10.1).

4.5.1 Preparation of calf liver $tRNA^{Bulk}$

From 2.5 kg calf liver, 73800 A_{260} (ca. 3.3 g) $tRNA^{Bulk}$ was obtained by anion-exchange chromatography, the profile of which is shown in Fig. 4.18.

The majority of tRNAs in $tRNA^{Bulk}$ purification were not aminoacylated due to instability of aminoacyl ester bond which could be hydrolyzed during purification.

However, to ensure all tRNAs in the deacylated form, $tRNA^{Bulk}$ was subjected to Cu^{2+} treatment (3.5.3), and then purified by gel permeation chromatography.

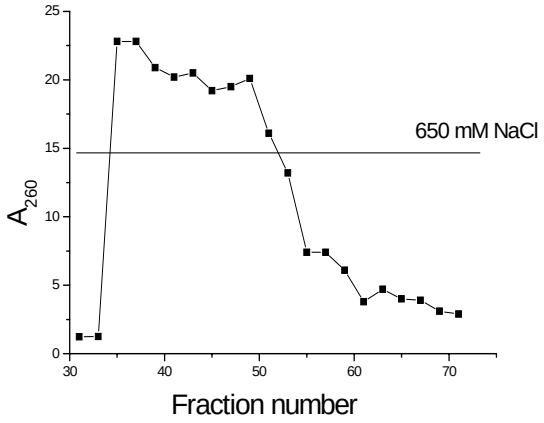

Fig. 4.18 Anion exchange chromatography of calf liver $tRNA^{Bulk}$ on DEAE-cellulose
The tRNA bound by the DEAE-cellulose column was eluted by 650 mM NaCl. Fractions from 34 to 70 were pooled and ethanol-precipitated.

4.5.2 Affinity Chromatography of $tRNA^{Bulk}$ on immobilized exportin-t

4.5.2.1 The affinity chromatography of $tRNA^{Bulk}$ on immobilized exportin-t is Ran·GTP dependent

Exportin-t was immobilized on Ni-NTA agarose column via the His_6 tag at its N terminus. The binding of $tRNA^{Bulk}$ to immobilized exportin-t is Ran·GTP dependent (Fig. 4.19), inferring that formation of ternary complex is the prerequisite of the affinity chromatography.

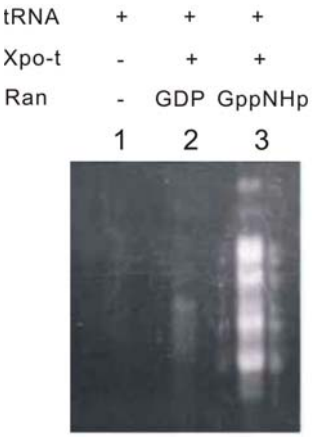

Fig. 4.19 Urea PAGE analysis of tRNA eluted from exportin-t·Ni-NTA agarose column
tRNA (lane 1), tRNA + exportin-t + Ran·GDP (lane 2), tRNA + exportin-t + Ran·GppNHp (lane 3) were loaded on three 0.4 ml Ni-NTA columns. The unbound molecules were eluted with 20 mM Tris-HCl pH 7.5, 50 mM KCl and 5 mM Mg^{2+}. The tRNA bound on the columns was eluted with the same buffer containing 500 mM KCl, ethanol-precipitated and analyzed by 10% PAGE containing 7 M urea. The bands were visualized with ethidiumbromide staining.

4.5.2.2 A mature 3′-CCA end of tRNA is critical for binding to exportin-t

The different tRNA species in a sample were separated by 2D urea polyacrylamide gel. It was found that the calf liver $tRNA^{Bulk}$ before and after the affinity chromatography produced the similar tRNA spot pattern on the 2D gel (Fig. 4.20 (A)). That is to say, most tRNAs in $tRNA^{Bulk}$ were able to bind immobilized exportin-t, supporting the published conclusion that aminoacylation is not a prerequisite to tRNA·exportin-t·Ran·GTP binding. On the other hand it was observed that some spots in $tRNA^{Bulk}$ disappeared after the chromatography, implying that these tRNAs or tRNA-like molecules in $tRNA^{Bulk}$ could not be recognized by exportin-t.

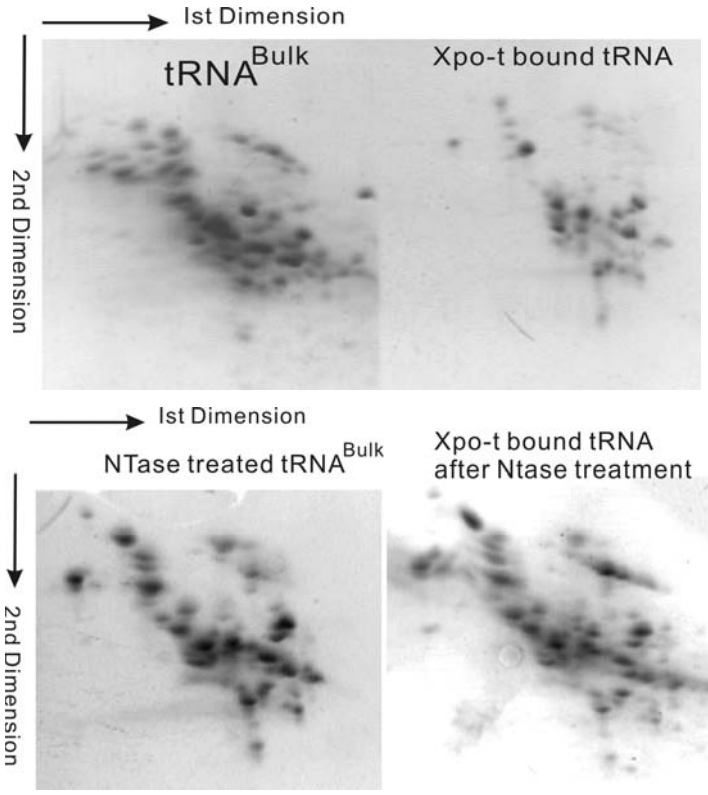

Fig. 4.20 2D urea PAGE analysis of tRNA eluted from exportin-t·Ni-NTA agarose column
$tRNA^{Bulk}$ (A) and NTase treated $tRNA^{Bulk}$ (B) were loaded on exportin-t·Ni-NTA agarose columns respectively. The tRNA bound on the columns was eluted with the 500 mM KCl, and analyzed by 2D urea PAGE. The tRNA spots were visualized with ethidiumbromide staining.

Then a question was raised: were there two groups of tRNAs, one can bind exportin-t, whereas the other not? It appeared to be so from the result above. But this claim is based on one premise that all tRNA molecules in the purified calf liver $tRNA^{Bulk}$ were mature and intact. This supposition was suspected, because tRNA has a 3′ extended end of CCA, which is vulnerable to degradation. So it is possible that $tRNA^{Bulk}$ used was a mixture of

intact tRNAs and truncated tRNAs lack of a complete 3′-CCA end. An enzyme, ATP(CTP):tRNA nucleotidyltransferase (NTase), is known to recover 3′-CCA end to truncated tRNAs. The $tRNA^{Bulk}$ was incubated with NTase, and then applied to an exportin-t·Ni-NTA agarose column. From 2D urea gel analysis (Fig. 4.20 (B)), it was observed that nearly all tRNA spots in the NTase $tRNA^{Bulk}$ were present in the exportin-t-bound tRNA fraction. When compared $tRNA^{Bulk}$ before (left part of Fig. 4.20 (A)) and after (left part of Fig. 4.20 (B)) NTase treatment, It was found that some tRNA molecules also disappeared after NTase treatment, inferring the existence of truncated tRNAs in the untreated $tRNA^{Bulk}$. This result showed that a mature 3′-CCA end is critical to tRNA·exportin-t·Ran·GTP interaction.

4.5.2.3 Not all tRNAs bind exportin-t with the same affinity

Are all mature deacylated tRNAs recognized by exportin-t indiscriminately? Or take it biochemically, do all mature deacylated tRNAs bind exportin-t with the same affinity? To answer this question, a step-wise increase of KCl concentration was applied to fractionate $tRNA^{Bulk}$. The chromatographic profile is shown in Fig. 4. 21.

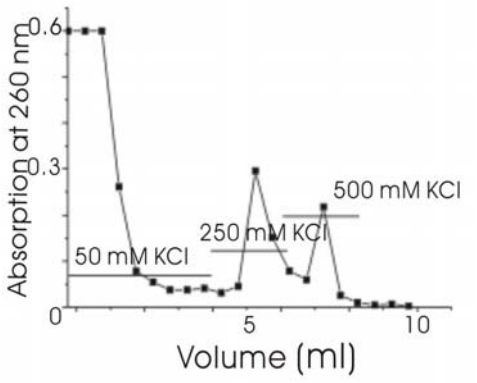

Fig. 4.21 Affinity chromatography of $tRNA^{Bulk}$ on exportin-t·Ni-NTA agarose column by step-wise elution
NTase treated $tRNA^{bulk}$ and Ran·GppNHp was loaded on an exportin-t·Ni-NTA agarose column (0.4 ml) in the environment of 20 mM Tris-HCl pH 7.5, 50 mM KCl and 5 mM Mg^{2+}. The bound tRNA was sequentially eluted with 250 mM KCl and 500 mM KCl.

Besides 250 mM and 500 mM KCl, elutions were performed also with 150 mM, 1M and 2 M KCl in the chromatography. 150 mM KCl was not concentrated enough to elute tRNA, and 500 mM KCl dissociated all bound-tRNA from the immobilized exportin-t so that the subsequent 1M KCl and 2M KCl, even 200 mM imidazol, which freed exportin-t

from the column, could not elute out any more tRNAs. The tRNAs in 250 mM KCl and 500 mM KCl fractions were pooled and subjected to 2D urea polyacrylamide gel analysis (Fig. 4.22).

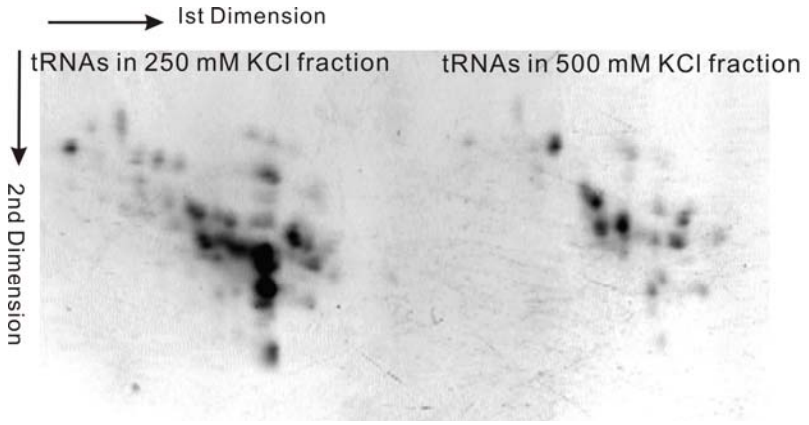

Fig. 4.22 2D urea PAGE analysis of tRNA fractions obtained by step-wise elution from exportin-t·Ni-NTA column
tRNAs in 250 mM KCl (the left part) and 500 mM KCl (the right part) fractions were analyzed by 2D urea PAGE. tRNA spots were visualized by ethidiumbromide staining.

The patterns of tRNA distribution of the two fractions on the 2D urea PAGE were remarkably different. Most tRNAs appeared in the 2D pattern of both fractions in Fig. 4.22. The difference is that some tRNA spots were brighter in the 250 mM KCl fraction than in the 500 mM KCl fraction. These early-eluted tRNAs probably have a lower affinity to exportin-t than those preferentially eluted in 500 mM KCl fraction.

4.5.3 Identification of the tRNAs on 2D urea PAGE by Northern hybridization

Northern hybridization was performed to identify the sequences of tRNAs on 2D PAGE. Oligonucleotides complementary to 3′end of $tRNA^{Ser,\ Leu,\ Pro,\ Arg}$ genes (these tRNAs were selected for analysis) were designed and labeled with ^{32}P at their 5′ ends. Since no complete bovine tRNA gene information is available, human tRNA gene

sequences (http://www.trna.uni-bayreuth.de/) were used to construct the hybridization probes. The sequences of oligonucleotides are listed in 3.1.7.

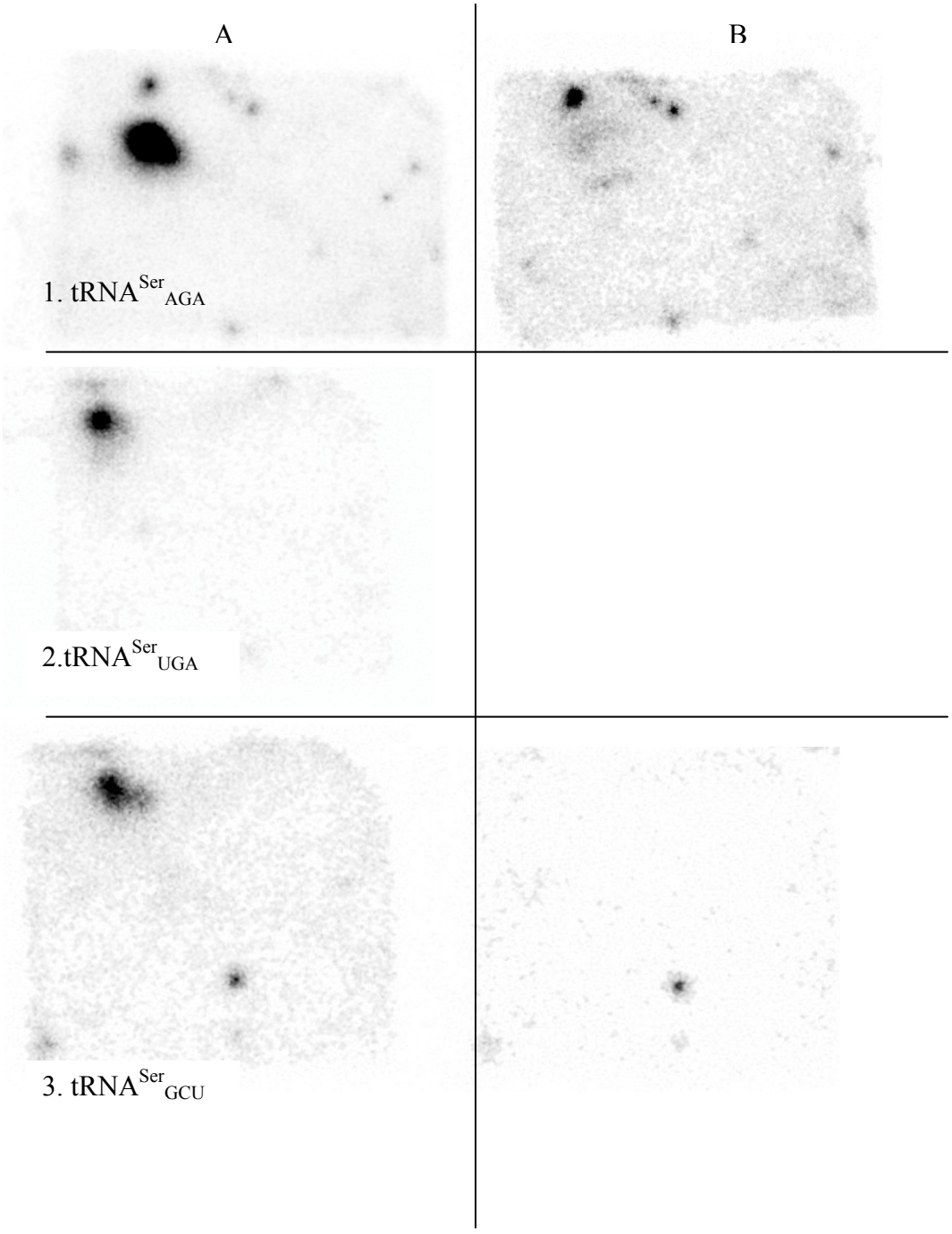

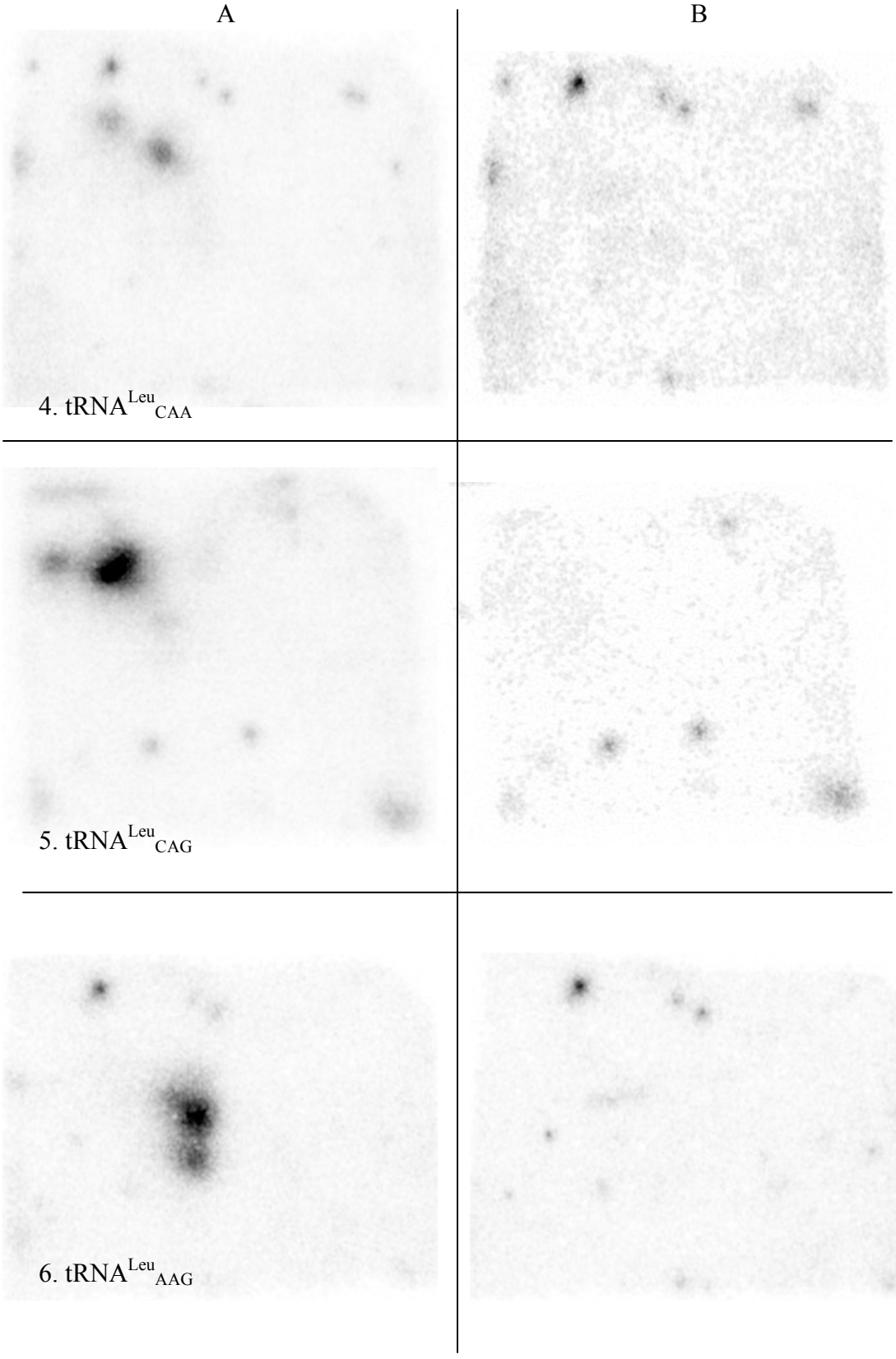
A
B
4. tRNA$^{Leu}_{CAA}$
5. tRNA$^{Leu}_{CAG}$
6. tRNA$^{Leu}_{AAG}$

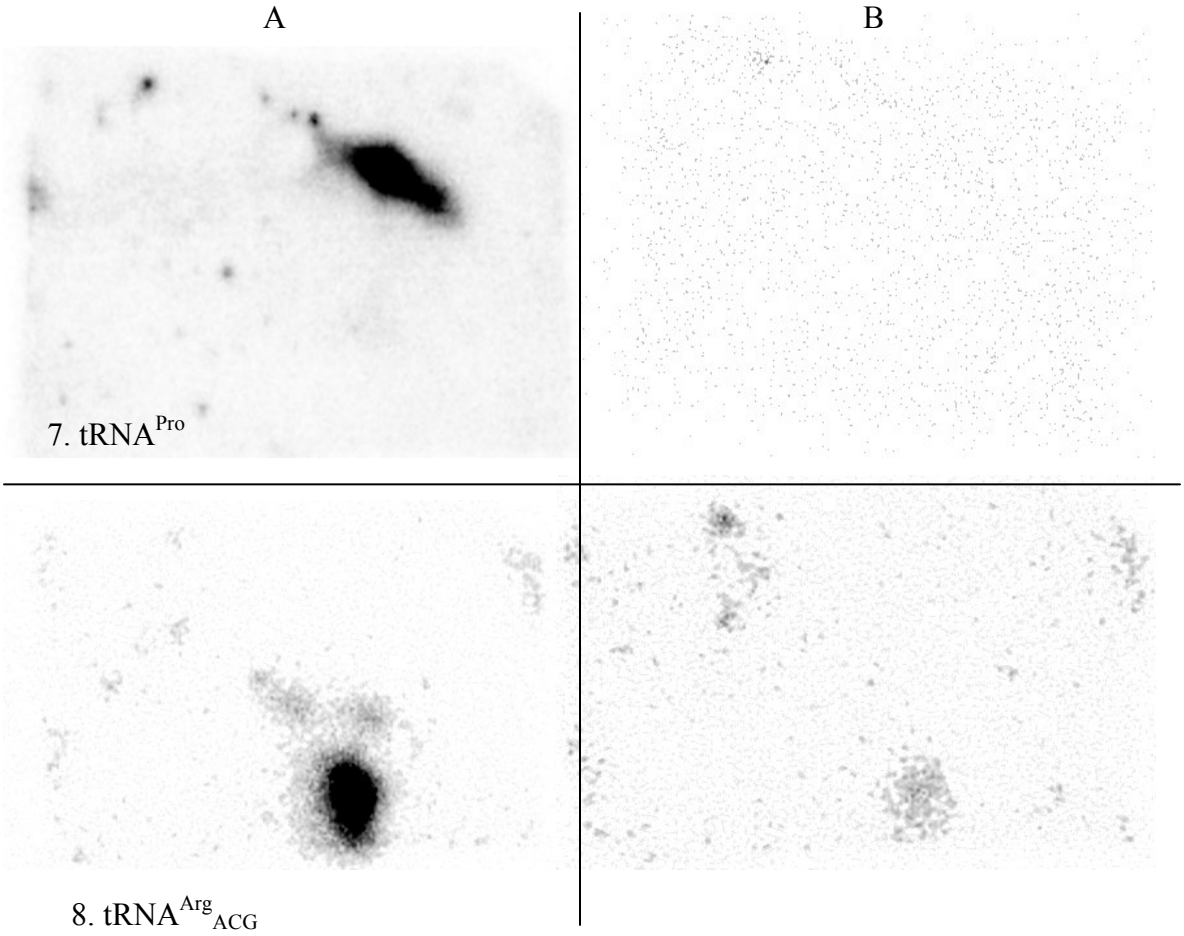

Fig. 4.23 Detecting tRNA by Northern hybridization with [^{32}P] 5′ labeled DNA probe s complementary to the tRNA sequences
(A) After hybridization (in 1M Na^+, 0.5%SDS) overnight and washing away unspecifically bound oliogonucleotides with low salt concentration (in 20 mM Na^+, 0.5% SDS), the tRNA·DNA hybrid of radioactivity was detected on the Hybond-N^+ membrane; (B) The tRNA·DNA hybrid was disrupted by soaking the membrane in 0.1% SDS at 85ºC for 4 min.

tRNAs on the 2D urea polyacrylamide gel were transblotted to Hybond-N^+ membrane (Amersham), on which northern hybridizations were carried on. In Fig. 4.23, tRNAs tested were radioactively detected on membrane (A) and the hybridization could be disrupted in 0.1% SDS at 85ºC (B).

After localization of the tRNAs on the membrane, it was not difficult to determine their positions on the original polyacrylamide gel image. Eight tRNA species were identified on the 2D polyacrylamide gel, which are indicated in Fig. 4.24 and Fig. 4.25. It is noteworthy that though all tRNA^{Arg} species were tested and found on 2D gel, only the

position of $tRNA^{Arg}_{ACG}$ was determined with exactness, while the other $tRNA^{Arg}$ spots overlapped with other tRNA spots, thus are not shown here.

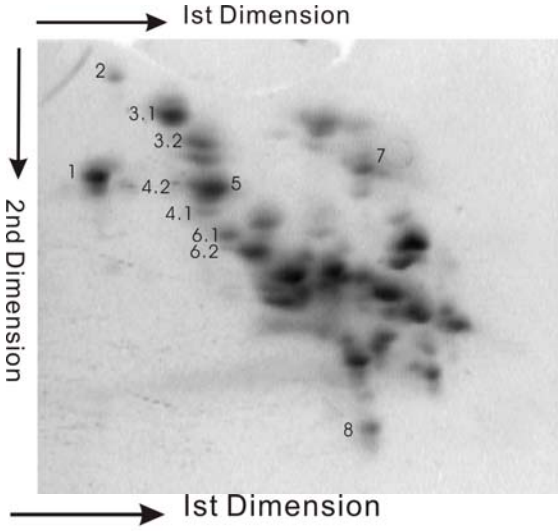

Fig. 4. 24 Based on Northern hybridization results the tRNAs were determined on the gel
1: $tRNA^{Ser}_{AGA}$; 2: $tRNA^{Ser}_{UGA}$; 3.1, 3.2: $tRNA^{Ser}_{GCU}$; 4.1, 4.2: $tRNA^{Leu}_{CAA}$; 5: $tRNA^{Leu}_{CAG}$; 6.1, 6.2: $tRNA^{Leu}_{AAG}$; 7*: $tRNA^{Pro}$; 8: $tRNA^{Arg}_{ACG}$;
*: All $tRNA^{Pro}$ genes are the same except the anticodon, thus it is unable to discriminate them by Northern Analysis.

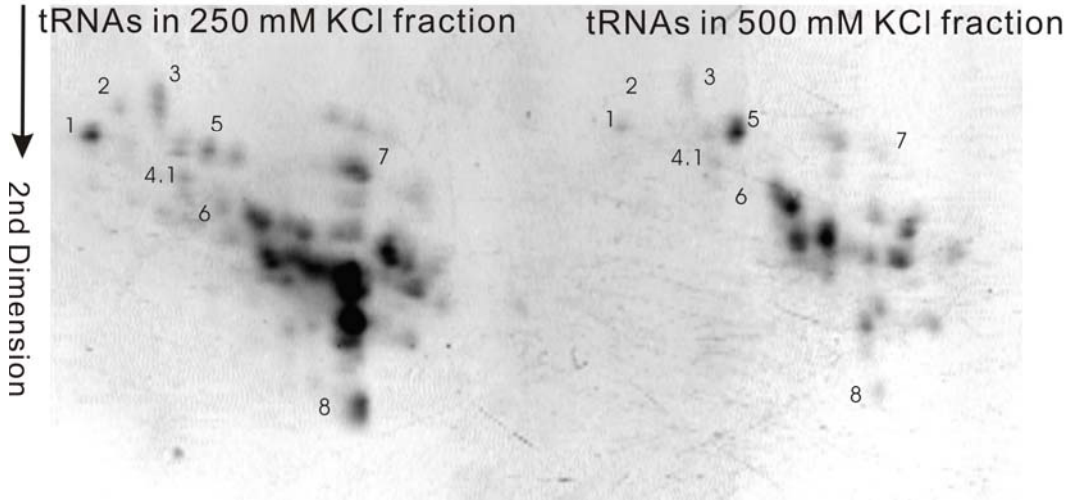

Fig. 4.25 tRNAs identified on 2D urea PAGE by elution with 250 mM KCl fraction (left) and 500 mM fraction (right)
The numbering of tRNA spots is adopted from Fig. 4.23. Because spots 3.1 and 3.2 are very close to each other on this gel, they are labeled here as one spot. The same case is for spot 6.1 and 6.2. It is hard to localize spot 4.2 on this gel.

From Fig. 4.25, it's evident that tRNA 1($tRNA^{Ser}_{AGA}$), 3 ($tRNA^{Ser}_{GCU}$) were more present in 250 mM KCl fraction than in 500 mM KCl fraction, while tRNA 5 ($tRNA^{Leu}_{CAG}$) was less present in 250 mM KCl fraction than in 500 mM KCl fraction. That is to say, $tRNA^{Leu}_{CAG}$ was eluted out from the column later than $tRNA^{Ser}_{AGA}$ and

$tRNA^{Ser}_{GCU}$. To better analyze the relative K_D of those tRNAs, software Quantity one (Bio-Grad) was applied to quantitate the tRNA spot density on the gel. The data are summarized in Tab. 4.4. The ratio of the tRNA spot density in 250 mM KCl fraction and in 500 mM KCl fraction is used as an indicator of the tRNA's affinity to exportin-t. The higher the ratio is, the earlier did the tRNA elute out, and lower the relative K_D is. Since $tRNA^{Pro}$ has three isoacceptors of close homology which cannot be distinguished by the oliognucleotide complementary to their 3′ ends, $tRNA^{Pro}$ (spot 7) was not taken into account.

Tab 4.4 Calculation of spot densities of selected tRNA in 250 mM and 500 mM fractions on the gel with the software Quantity One

Spot (tRNA)	Density in 250 mM KCl fraction (A)	Density in 500 mM KCl fraction (B)	Ratio of the two fractions (A/B)
1 ($tRNA^{Ser}_{AGA}$)	627785.9	211543.5	3.0
2 ($tRNA^{Ser}_{UGA}$)	312933.4	166573.1	1.9
3 ($tRNA^{Ser}_{GCU}$)	580609.1	375142.7	1.5
4 ($tRNA^{Leu}_{CAA}$)	468856.4	313669.1	1.5
5 ($tRNA^{Leu}_{CAG}$)	386784.9	935633.8	0.4
6 ($tRNA^{Leu}_{AAG}$)	534839.7	122883.3	4.6
8 ($tRNA^{Arg}_{ACG}$)	1037311.6	122787.3	8.4

From the result above, we obtained such information: among tRNAs tested, the affinity of tRNAs to exportin-t ranked as $tRNA^{Leu}_{CAG}$ > $tRNA^{Ser}_{GCU}$, $tRNA^{Leu}_{CAA}$, $tRNA^{Ser}_{UGA}$ > $tRNA^{Ser}_{AGA}$, $tRNA^{Leu}_{AAG}$ > $tRNA^{Arg}_{ACG}$. To explain the difference of tRNA's ability to bind exportin-t, a hypothesis is proposed and detailed in the Discussions (5.4.4).

4.6 AFM imaging of the interaction between exportin-t-esterase, tRNA and Ran·GppNHp on the modified mica surface

4.6.1 A mica surface covered with TFK could immobilize exportin-t-esterase conjugate

Mica is commonly used as a substrate for atomic force microscopy (AFM) imaging at molecular resolution due to its atomic flat surface. Partners of esterase and trifluoroemethyl ketone (TFK) (3.10) were used to immobilize proteins on the mica surface for AFM.

For comparison the gene of NADH oxidase (NADOX) was linked at its 3′ terminus with esterase gene in a plasmid, which was transformed into *E.coli*. The recombinant protein NADOX-esterase was overexpressed and purified. Its binding ability to the TFK-modified mica surface was tested. Hundred fmol NADOX-esterase was incubated with the TFK-modified mica surface and subjected to AFM observation (Fig. 4.26) (3.10.6, 3.10.7).

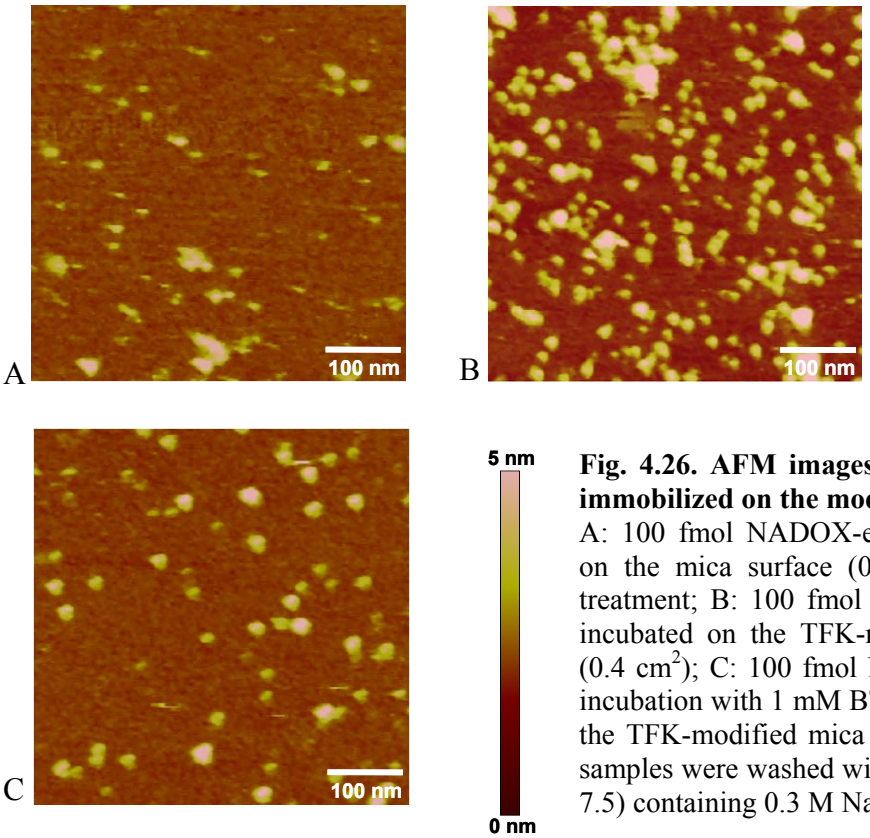

Fig. 4.26. AFM images of NADOX-esterase immobilized on the modified mica surface
A: 100 fmol NADOX-esterase was incubated on the mica surface (0.4 cm^2) without TFK treatment; B: 100 fmol NADOX-esterase was incubated on the TFK-modified mica surface (0.4 cm^2); C: 100 fmol NADOX-esterase after incubation with 1 mM BTFK for 90 minutes on the TFK-modified mica surface (0.4 cm^2). All samples were washed with 1 mM Tris-HCl (pH 7.5) containing 0.3 M NaCl.

On the mica surface without TFK coating (Fig. 4.26 A), little particles were present, suggesting NADOX-esterase was a poor substrate for mica surface via unspecific interaction. The images of particles on it are ill-defined due to lack of stable

immobilization and a possibility of mechanical movement during the experiment. On the TFK-modified mica surface (Fig. 4.26 B), many particles of 12 ± 2 nm were observed. Here the contours of the particles are sharp as the immobilization prevents movements. These particles could not be immobilized on the surface after 90 minute incubation with 3-butylsulfanyl-1,1,1-trifluoro-propan-2-one (BTFK) (Fig. 4.26 C). BTFK has no SH group, thus cannot be fixed on the mica surface and in a soluble form. It competitively binds the esterase part of the protein, thereby freeing the TFK-bound protein from the surface. It was proven that the immobilization of NADOX-esterase to the TFK-modified mica was via the binding of esterase to TFK. The success of immobilization NADOX-esterase on the TFK-modified mica surface showed that our experimental system for AFM study of exportin-t-esterase was competent.

4.6.2 Exportin-t-esterase was immobilized on the TFK-modified mica surface

Exportin-t gene (3899 bp) linked at its 3′ terminus with esterase gene (931 bp) in the plasmid was used as template in *in vitro* translation. The recombinant protein was produced successfully and showed esterase activity by photometric measurement (3.10.6), the results are shown in Tab. 4.5. Because the exportin-t-esterase could not be expressed in *E.coli* cells, the *in vitro* translation sample containing exportin-t-esterase (3.10.4) had to be used as the research subject. About 20 fmol exportin-t-esterase in *in vitro* translation system was incubated with the TFK-modified mica surface (0.4 cm^2). A blank *in vitro* translation system without protein production was incubated with another TFK-modified mica surface and used as a negative control. The mica chips were subjected to atomic force microscopy (AFM), the results of which are shown in Fig. 4.27. It is apparent that though some molecules in the blank *in vitro* translation system were bound to the modified mica surface, much more particles were present on the surface for the sample containing exportin-t-esterase. When BTFK was present together with exportin-t-esterase in *in vitro* translation sample, the number of particles on the TFK-modified mica surface decreased remarkably. These observations showed clearly that exportin-t-esterase

translated *in vitro* was successfully fixed to the modified mica surface and this binding was via the specific interaction between esterase and TFK.

Tab 4.5 Photometric measurement of esterase activity in the sample of in vitro translation

Sample	Esterase activity (U/ml)	Protein (pmol/ml)	Protein Concentration (mg/ml)
in vitro translation for 2 hours at 30°C	0.173	32.87	0.0047
in vitro translation for 2 hours at 37°C	0.432	82.08	0.012
in vitro translation for 4 hours at 37°C	0.668	126.92	0.0185

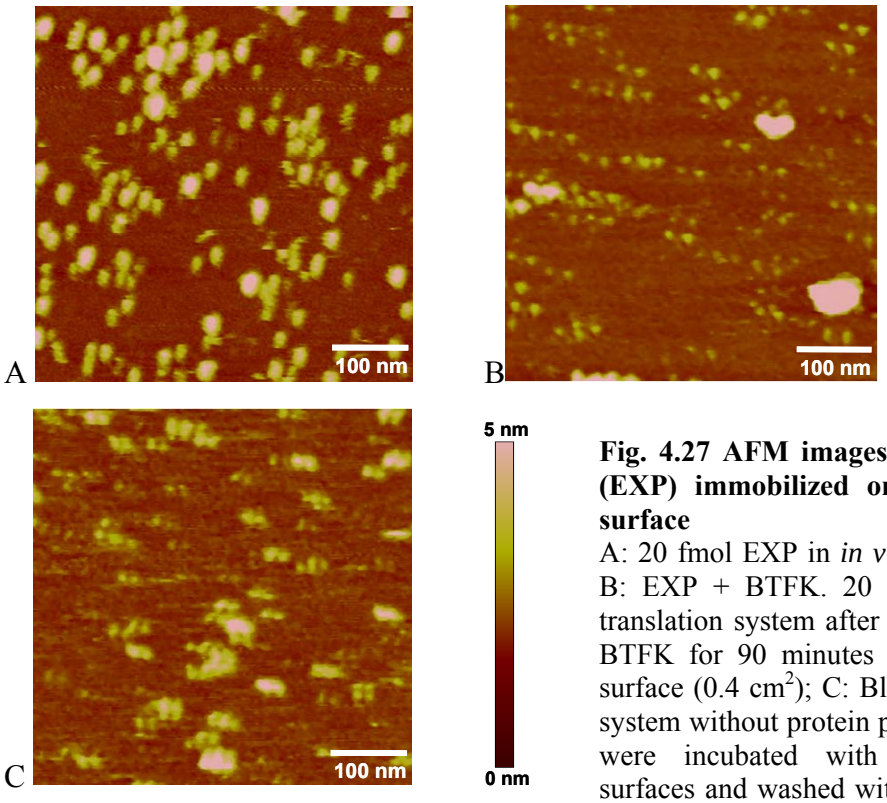

Fig. 4.27 AFM images of exporin-t-esterase (EXP) immobilized on the modified mica surface
A: 20 fmol EXP in *in vitro* translation system; B: EXP + BTFK. 20 fmol EXP in *in vitro* translation system after incubation with 1 mM BTFK for 90 minutes on the modified mica surface (0.4 cm^2); C: Blank *in vitro* translation system without protein production. All samples were incubated with TFK-modified mica surfaces and washed with 1 mM Tris-HCl (pH 7.5) containing 0.3 M NaCl.

The particles on mica surfaces were grouped according to their diameters, the number and proportion of which are listed in Tab. 4.6. Comparing the groups of different

particles in exportin-t-esterase and blank *in vitro* translation system, it was found that the proportion of particles of 13.1 to 17.0 nm in exportin-t-esterase sample increased most remarkably, while proportions of the other groups in exportin-t-esterase sample remained the similar or even decreased after exportin-t-esterase was produced in *in vitro* translation sample. When BTFK was added to inhibit the interaction between exportin-t-esterase and TFK, the particle number and proportion in group 13.1 to 17.0 nm decreased. These data strongly suggested that the exportin-t-esterase produced *in vitro* has a diameter between 13.1 to 17.0 nm. That is to say, the diameter of exportin-t-esterase in the photos is of 15 ± 2 nm.

Fukuhara *et al.* used x-ray scattering (SAXS) to study the shapes of some exportin and importins (Fukuhara *et al.*, 2004). In their experiments, the diameter of exportin-t is determined to be 16 ± 2 nm. Exportin-t-esterase (144kDa) was shown to be of the similar dimension, but not larger than the exportin-t (110 kDa) used by Fukuhara *et al.* as expected. The inconsistency may be caused by the difference of methods.

Tab. 4.6 Distribution of particles in exportin-t-esterase (EXP) and IVT on the TFK-modified mica surface of 2000 × 2000 nm

Diameter of Particles (nm)	Blank *in vitro* translation system (IVT)		EXP		EXP + BTFK	
	Number of the particles	Proportion of the particles (%)	Number of the particles	Proportion of the particles (%)	Number of the particles	Proportion of the particles (%)
5.1 – 9.0	667	43.8	528	24.3	446	49.6
9.1 – 13.0	321	21.1	515	23.6	267	29.7
13.1 – 17.0	**142**	**9.3**	**526**	**24.2**	**116**	**12.9**
17.1 – 21.0	108	7.2	256	11.7	19	2.1
21.1 – 25.0	95	6.2	159	7.3	10	1.1
25.1 – 29.0	96	6.3	109	5.0	17	1.9
29.1 – 33.0	62	4.1	63	2.9	15	1.7
33.1 – 36.0	32	2.1	21	1.0	9	1.0
Total	1524	100	2177	100	899	100

4.6.3 Interaction of tRNA, Ran·GppNHp with the immobilized exportin-t-esterase on the TFK-modified mica surface

To study the change in the dimension of exportin-t-esterase after its binding tRNA and Ran·GppNHp, 200 fmol $tRNA^{Arg}_{E.c}$, 200 fmol Ran·GDP, 200 fmol Ran·GppNHp was added step by step to the 20 fmol immobilized exportin-t-esterase on the modified mica surface (0.4 cm^2) in 1 mM Tris-HCl (pH 7.5) containing 25 µM KCl, 2.5 µM $MgCl_2$, 500 nM DTT. The mica chip was observed under AFM (Fig. 4.28). The distribution of particles in different diameters was analyzed and listed in Tab. 4.7.

Tab. 4.7 Distribution of particles in EXP in the presence of $tRNA^{Arg}_{E.c}$, Ran·GDP, Ran·GppNHp on the TFK-modified mica surface of 1000 × 1000 nm

Diameter of Particles (nm)	EXP		EXP + tRNA		EXP + tRNA + Ran·GDP		EXP + tRNA + Ran·GppNHp	
	Number of the particles	Proportion of the particles (%)	Number of the particles	Proportion of the particles (%)	Number of the particles	Proportion of the particles (%)	Number of the particles	Proportion of the particles (%)
5.1 – 9.0	117	27	100	30	72	18	63	15
9.1 – 13.0	129	30	79	24	96	23	76	18
13.1 – 17.0	**85**	**20**	**71**	**22**	**105**	**26**	**113**	**27**
17.1 – 21.0	**53**	**12**	**45**	**14**	**63**	**15**	**76**	**18**
21.1 – 25.0	22	5	17	5	40	10	42	10
25.1 – 29.0	9	2	10	3	15	4	28	7
29.1 – 33.0	8	2	3	1	14	3	13	3
33.1 – 36.0	3	1	3	1	4	1	1	0
Total	426	100	328	100	409	100	412	100

From Tab. 4.7, there was no remarkable changes in the distribution of particles in the samples except that the proportion of particles of 13.1 to 17.0 nm and 17.1 to 21.0 nm increased when tRNA and Ran·GppNHp were added, inferring that the diameter of the new particles shifted to right and was increased. Addition of tRNA only or tRNA plus Ran·GDP produced the similar effect, but to a lesser extent, suggesting that Ran·GppNHp played a role in it. From the data it is likely that after binding to tRNA and Ran·GTP, the

ternary complex of exportin-t·tRNA·Ran·GTP somewhat increased in diameter. Because the increase of particle proportion in the group of 17.0 to 21.0 nm was not very significant, and it is just a group neighboring the group 13.1 to 17.0 nm, in which exportin-t-esterase was supposed to be, it is suggested that after binding tRNA and Ran·GTP, the diameter of exportin-t does not change noticeably.

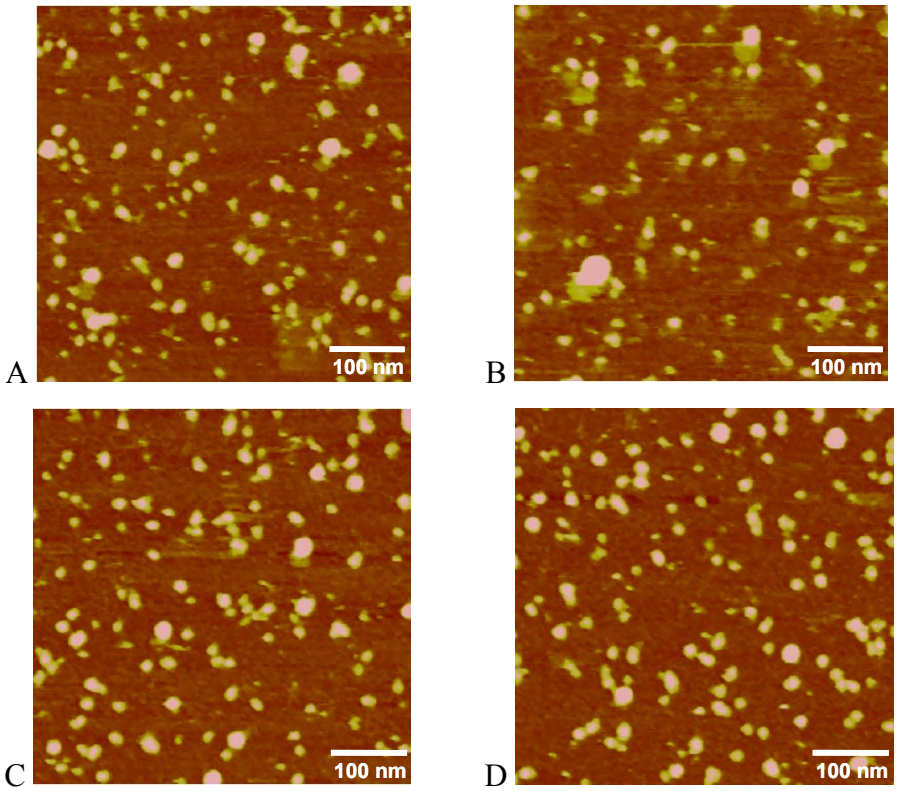

Fig. 4.28 AFM images of exportin-t-esterase (EXP) on the modified mica surface in the presence of tRNA, RanGDP, and RanGppNHp
A: EXP; B: EXP + $tRNA^{Arg}_{E.c}$; C: EXP + $tRNA^{Arg}_{E.c}$ + Ran·GDP; D: EXP + $tRNA^{Arg}_{E.c}$ + Ran·GppNHp. The experimental steps were performed on one mica chip from A to D. About 20 fmol EXP was immobilized on the modified mica surface (0.4 cm^2) and maintained in buffer 1 mM Tris-HCl (pH 7.5) containing 25 µM KCl, 2.5 µM $MgCl_2$, 500 nM DTT and observed in A. After 200 fmol $tRNA^{Arg}_{E.c}$, 200 fmol Ran·GDP, 200 fmol Ran·GppNHp was added step by step to the chip, which at each step was washed by the same buffer and observed in B, C and D respectively.

5 Discussions

5.1 Expression of exportin-t is detrimental to *E.coli* growth

Recombinant protein His_6-exportin-t was expressed in *E. coli* XL-1 blue, which was used mainly for DNA amplification instead of protein production. But our endeavors to express exportin-t in expression strains such as *E. coli* BL21 never succeeded. The quantity of exportin-t produced in *E. coli* XL-1 blue was very low. These two phenomena implied that exportin-t, which can bind tRNA in cells, was poisonous to its host *E. coli*.

5.2 (s^4U) $tRNA^{Phe}_{T.th}$ is qualified for complex formation

$tRNA^{Phe}_{T.th}$ transcript could form complex with exportin-t in the presence of Ran·GppNHp in EMSA experiments (Fig. 4.9). This is consistent with the observation that tRNA transcript devoid of modification is able to bind exportin-t (Lipowsky *et al.*, 1999). In their kinetic assays, it was found that *in vitro*-transcribed tRNA only had 18% of the affinity of the fully mature tRNA. However, the researchers were not confident with this conclusion, "Maybe we had by chance those tRNA transcripts that bind more weakly ". Their suspicion is reasonable, since *E.coli* tRNA binds to exportin-t with the same affinity as human tRNA (Lipowsky *et al.*, 1999) and intron containing tRNA can be exported by exportin-t (Arts et al., 1998b), modification of tRNA, which contributes mainly to codon recognition or to the stability of tRNA structure, should not play a significant role in this interaction.

In EMSA experiments, (s^4U) $tRNA^{Phe}_{T.th}$ also bound to exportin-t, but to a lesser extent when compared with normal $tRNA^{Phe}_{T.th}$ transcript. It is known that 4-thiouridine in RNA can induce the change of conformation, the extent of which depends on the incorporation ratio of s^4U to U in RNA (Kumar *et al.*, 1997). In the study of the interaction of $tRNA^{Phe}_{E.c}$ and PheRS, when only one U was replaced with s^4U in $tRNA^{Phe}_{E.c}$, the effect of s^4U is neglectable, whereas if all uridine positions were occupied by s^4U, the modified $tRNA^{Phe}_{E.c}$ transcript reduced the relative catalytic efficiency 14-

fold (Moor NA *et al.*, 1998). By HPLC analysis of the components of (s^4U) $tRNA^{Phe}_{T.th}$, the incorporation rate of s^4U is 41%. Among 16 Us in $tRNA^{Phe}_{T.th}$, about 6.5 were substituted s^4U in average. *in vitro*-transcribed (s^4U) $tRNA^{Phe}_{T.th}$ was a mixture of tRNAs with s^4Us at every possible site. (s^4U) $tRNA^{Phe}_{T.th}$ formed fewer complexes with exportin-t than normal $tRNA^{Phe}_{T.th}$ transcript, because some tRNA molecules in the (s^4U) $tRNA^{Phe}_{T.th}$ transcripts had too many s^4Us or s^4U at sites that could impede its interaction with exportin-t. In the present work, only (s^4U)$tRNA^{Phe}_{T.th}$ molecules able to crosslink to exportin-t (found in the complex) were analyzed.

5.3 Photoaffinity crosslinking of (s^4U)$tRNA^{Phe}_{T.th}$ to exportin-t

5.3.1 $tRNA^{Phe}_{T.th}$ crosslinked to protein successfully

4-Thiouridine can be activated at 365 nm, a wavelength at which there is no other photochemistry for the usual bases (Hajnsdorf *et al.*, 1986). s^4U containing RNA was usually irradiated at 337 nm or 350 nm (Moor *et al.*, 1998, Mcgregor *et al.*, 1996). In our lab crosslinking samples were irradiated at 312 nm, because tRNA transcripts used here have only four canonical nucleosides besides s^4U. They absorb at the wavelength no longer than 260 nm. When (s^4U)$tRNA^{Phe}_{T.th}$ was irradiated at 312 nm, neither degradation nor aggregation of tRNAs was observed (Fig. 4.10).

tRNA, exportin-t, Ran·GppNHp successfully formed a crosslinked complex after irradiation (Fig. 4.10). On the efficiency of crosslinking some comments are worth noting. The quality of s^4UTP is of the primary importance to the subsequent crosslinking experiments. If the s^4UTP had a poor quality, it would be hard to be incorporated into tRNA transcripts and crosslinking efficiency would be affected remarkably. Glycerol inhibited this photoaffinity crosslinking remarkably, and when the percentage of glycerol exceeded 10%, no crosslinking occurred. The efficiency of crosslinking varied among different batches of tRNA transcripts. Normally after 30 minutes of irradiation, 30% tRNA were crosslinked.

5.3.2 $tRNA^{Phe}_{T.th}$ crosslinked only to exportin-t

By analyzing the purified crosslinked complex on an SDS-PAGE (Fig. 4.11), it was found that tRNA crosslinked only to exportin-t.

In Mattaj's group, a series of exportin-t proteins with N- and C- terminal deletions were constructed to bind tRNA and Rap·GTP. The researchers concluded that Ran·GTP bound to the N- terminus of exportin-t, and tRNA binds to the C- terminus (Kuersten *et al.*, 2002). Importin ß family members share a common feature of binding Ran·GTP at their N terminus. From my experiment, it was likely that Ran·GTP might have no chance of contacting the cargo of exportin-t.

5.3.3 Formation of ternary complex is the prerequisite for the crosslinking

Crosslinking between tRNA to exportin-t was Ran·GppNHp stimulated and could be competitively inhibited by other tRNA species (Fig. 4.12, 4.13). That is to say, before it crosslinked to exportin-t, $(s^4U)tRNA^{Phe}_{T.th}$ had formed complex with exportin-t and Ran·GppNHp. Though $(s^4U)tRNA^{Phe}_{T.th}$ had the opportunity of randomly colliding with other molecules, such as exportin-t, Ran and other tRNAs in the solution, such accidental and rapid contacts did not lead to crosslinking. Maintaining a relative stable conformation by forming the ternary complex is the prerequisite for the crosslinking. Therefore, crosslinking can be viewed as freezing of the complex. Therefore, the crosslinking sites between $(s^4U)tRNA^{Phe}_{T.th}$ and exportin-t are the possible contact sites between them and can provide us with some valuable information.

5.3.4 U47 was found to be the major contact site of $(s^4U)\ tRNA^{Phe}_{T.th}$ and exportin-t

To determine the crosslinking sites of s^4U containing RNA to other biological molecules, several methods are available. An affinity electrophoresis system based on phenylmercuric substituted polyacrylamide (APM) gels was used to separate different s^4U containing RNA species according to their s^4U content. The RNAs containing single

s^4U at known positions were irradiated in the presence of protein of interest, by which the contact sites between RNA and proteins were determined (Moor *et al.*, 2001). It is the best method to study crosslinking between nucleic acids and proteins, but expensive and time-consuming. Another practical way to determine the crosslinking sites of s^4U containing RNA is primer extension analysis. Wollenzien *et al.* (1991) made use of reverse transcription experiments to determine the locations of crosslinking of s^4U containing mRNA with 16S rRNA and 23S rRNA. In primer extension analysis, the elongation of reverse transcriptase was obstructed by the peptide crosslinked to a s^4U residue, and a DNA band terminating at this point was thus produced.

By primer extension analysis, the contact sites of $tRNA^{Phe}_{T.th}$ and exportin-t were determined to be U55, U47, U20 and U33. Judged from band intensity at these positions, U55 and U47 are major contact sites of tRNA and exportin-t; U33 is the minor contact site. U20 is located in D loop; U55 in TΨC loop; U47 in extra loop; U33 in anticodon loop (Fig. 4.15). These regions seemed to have the opportunity to contact exportin-t.

Arts *et al*. (1998b) undertook a series of biochemical experiments to study the binding feature of tRNA and exportin-t. The riboses between 50 and 71 were significantly protected by exportin-t·Ran·GTP, positions 4 – 6 and 17 were also protected, positions 18, 47 – 49 and 72 were mildly protected. That is to say, the crosslinking sites of U55, U47, U20 are in or adjacent to the protected region. U33 was not affected in protection experiments. In addition, since tRNAs with an intron in its anticodon loop can be exported by exportin-t, Lipowsky *et al.* argued that anticodon probably does not contribute to exportin-t binding (Lipowsky *et al.*, 1999). The acceptor arm and TΨC arm are viewed as the major contact region of tRNA and exportin-t (Arts *et al.*, 1998b). However, a minihelix consisting of only the acceptor arm and TΨC arm showed no detectable binding to exportin-t and Ran·GTP (Arts *et al*., 1998b). D loop is likely to be important for exportin-t binding. The role of anticodon loop in this interaction requires further evidence. From the primer extension experiment, U33 is a contact site between $tRNA^{Phe}_{T.th}$ and exportin-t, and it is the weakest one. It is probable that anticodon loop helps exportin-t recognize mature tRNA.

U47 of $tRNA^{Phe}_{T.th}$ was interesting to us, because it seemed to be a major contact site of tRNA to exportin-t. A point mutation into of $tRNA^{Phe}_{T.th}$ gene was introduced by

replacing uridine 47 with an adenosine. The mutant was able to bind exportin-t, but a little weaker than normal $tRNA^{Phe}_{T.th}$ transcript (Fig. 4.16). Substitution of U47 by A did not affect the tRNA tertiary structure significantly. However, after incorporating s^4U into the tRNA transcript, the mutant $(s^4U)tRNA^{Phe}_{T.th}$ could not crosslink to exportin-t efficiently (Fig. 4.17). Therefore, U47 is supposed to be a major contact site between $tRNA^{Phe}_{T.th}$ and exportin-t.

$tRNA^{Phe}_{T.th}$ has been intensively studied in its interaction with *Thermus thermophilus* phenylalanyl-tRNA synthetase (PheRS). The crystal structure of PheRS complexed with cognate $tRNA^{Phe}$ was obtained (Goldgur *et al.*, 1997). From the X-ray structure, U47 of $tRNA^{Phe}_{T.th}$ is unstacked, and does not base pair with other nucleotides. It seems that U47 is not involved in tertiary structure forming. However, Steinberg *et al.* (1996) found that in most tRNAs nucleotide 47 might play a role in contribution to the tertiary structure. Using computer modeling they discovered a correlation between the absence of a nucleotide at position 47 in the extra loop and the presence of a U13:G22 base pair in the D-stem. If a Watson-Crick pair C13:G22 is present, the tRNA has to have a nucleotide at position 47 to accommodate the C13:G22 base pair to maintain the functional structure. This rule is valid for most cytoplasmic tRNAs, but not for mitochondrial tRNAs, which have C13:G22 base pair but no nucleotide 47. U47 is highly conservative among $tRNA^{Phe}$ species, and some of them even have modified uridine residues. The native $tRNA^{Phe}_{E.c}$ has a modified acp^3U47. Osswald *et al.* (1995) reported that the native $tRNA^{Phe}_{E.c}$ with its acp^3U47 modified by azido reagents could crosslink to the A, P, E sites of ribosome after irradiation at 350 nm. In general situations modified nucleotides play an important role in structure maintenance or act as tRNA determinants. U47 being modified manifests its importance for the tRNA structure from another respect.

Moor *et al*. (2001) also made use of photoaffinity crosslinking of randomly s^4U-monosubstituted $tRNA^{Phe}_{E.c}$ transcripts to study the interaction between $tRNA^{Phe}_{E.c}$ and *Thermus thermophilus* phenylalanyl-tRNA synthetase. $tRNA^{Phe}_{E.c}$ has the highest structural resemblance to $tRNA^{Phe}_{T.th}$ and could be efficiently aminoacylated by *T. thermophilus* PheRS. Therefore, the results from Moor *et al.* are a wonderful reference to us. In their crosslink experiments 7 contact sites were found, namely nucleotides 8, 12, 20, 33, 39, 45, 47. Exportin-t recognizes the common feature of all tRNAs, whereas PheRS

has to discern $tRNA^{Phe}$ from other tRNAs. U47, U20, U33 are the common crosslinking sites between tRNA-eportin-t and tRNA-PheRS, inferring that these nucleotides might be important for maintaining a readable tRNA structure. U39, a contact site to PheRS, showed no crosslinking to exportin-t. It is near anticodon nucleotides (34, 35, 36), the major determinants of $tRNA^{Phe}$. The contact between U39 and PheRS is $tRNA^{Phe}$ specific, not a shared feature of tRNAs. The similarities and differences of these two interactions imply that some nucleotides important for its identity as a $tRNA^{Phe}$ are also important for its identity as a tRNA.

5.4 Fractionation of calf liver $tRNA^{Bulk}$ by affinity chromatography on immobilized exportin-t

5.4.1 Aminoacylation is dispensable but a mature 3′-CCA end of tRNA is critical to exportin-t binding

Calf liver $tRNA^{Bulk}$ bound to immobilized exportin-t in a Ran·GTP-dependent way and the interaction could be disrupted by increasing the salt concentration to 500 mM KCl. It is suggested that the interaction between exportin-t and tRNA is mainly of electrostatic attraction.

After proofing of 3′-CCA end by NTase, nearly all tRNA molecules in $tRNA^{Bulk}$ could bind exportin-t. From the affinity chromatography (Fig. 4.20), a mature 3′-CCA end was critical to the interaction, which is consistent with the finding of Kutay *et al.* (1998). Aminoacylation was not necessary to the binding. It confirmed the results of Arts *et al.* (1998b), though nuclear aminoacylation was suggested to promote efficient export in *X. laevis* (Lund *et al.*, 1998). It is noteworthy that nuclear aminoacylation has not been certified in all species, and tRNA export pathway is likely to be species-specific. It is found that in yeast the major tRNA export is aminoacylation dependent (Steiner-mosonyi *et al.*, 2004), whereas in mammalian cells nuclear aminoacylation is still an unsettled issue (Gunasekera *et al.*, 2004). The role of aminoacylation in tRNA export in vertebrates requires further evidence.

5.4.2 Different tRNAs bind exportin-t with different affinities

By step-wise elution two fractions of tRNA with different affinity to exportin-t were obtained (4.21). Not all tRNA bound exportin-t with the same affinity. Northern hybridization was applied to identify tRNAs, a suitable method by which all tRNAs of *E.coli* were determined on the 2D urea polyacrylamide gel (Dong *et al.*, 1996). However, in our case, it is a little more complicate. Firstly, $tRNA^{Bulk}$ in the experiments came from calf liver, but there are only a few bovine tRNAs sequenced. This problem was solved by using human tRNA gene database (http://www.trna.uni-bayreuth.de) instead, because mammalian tRNA genes are very highly homologous. Secondly, there are more than 300 human tRNA gene sequences in the database, it would be time-assuming and uneconomical if primers complementary to all of them were purchased and tested. Fortunately the tRNA gene database has a great advantage, which can test a tDNA sequence by a typical secondary structure frame. If a tRNA genes had a different nucleotide other than the conservative one, it was much likely to be a pseudogene. Those pseudo-tRNA genes were winnowed away by checking the conservative nucleotides at specific positions. But even after this data handling, the amount of tRNA gene candidates was still daunting. Therefore, only those tRNAs for Ser, Leu, Arg, Pro were tested. The relative affinities of the 7 tRNAs to exportin-t was ranked as $tRNA^{Leu}_{CAG} > tRNA^{Ser}_{GCU}$, $tRNA^{Leu}_{CAA}$, $tRNA^{Ser}_{UGA} > tRNA^{Ser}_{AGA}$, $tRNA^{Leu}_{AAG} > tRNA^{Arg}_{ACG}$.

Different tRNAs binding to exportin-t with different affinity is an interesting phenomenon. In the experiments $tRNA^{Leu}_{CAG}$ is the strongest bindable tRNA and the most abundant $tRNA^{Leu}$ species. But being a major tRNA is not the reason of being bound preferentially by exportin-t, because $tRNA^{Arg}_{ACG}$ is also the most abundant $tRNA^{Arg}$, and it bound to exportin-t the weakest. Think of it from a theoretically angle, in mammalian cells, after all tRNAs are transcribed, matured, and waiting for export, which tRNAs should be transported into cytoplasm first? It depends on the demand of the cell. In the protein synthesis machinery of ribosome, codons in mRNAs are being decoded rapidly by tRNAs acylated with appropriate amino acids. The assembly line would stop at the codon that cannot get an aa-tRNA to read it. That means if a codon is the more used in genes, and the corresponding aa-tRNA is the less provided, this tRNA would be the

fastest consumed and thus most required by the cell. Presumed that aminoacylation efficiency and recognition by eEF1A of all aa-tRNAs are the same, it is not the tRNA concentration, but the ratio of tRNA concentration to the codon frequency in the genome, that decides the preference in tRNA export. To test this hypothesis, the ratio of tRNA gene number to codon frequency was calculated (the data are from human genome analysis (Lander *et al.*, 2001)), which theoretically indicates the requirement of the tRNA by a cell. It was compared with the relative affinity of the tRNA to exportin-t measured in the affinity chromatography experiments.

Tab 5.1 Comparison the ratios of tRNA amount to codon frequency (indicating the extent of requirement by cell) with the tRNA quantity ratio between in 250 mM KCl and 500 mM KCl (indicating the relative affinity to exportin-t)

Spot (tRNA)	the ratio of the numbers of tRNA gene to codon frequency per 10,000 codons (A)	the tRNA quantity ratio between in 250 mM KCl and 500 mM KCl (B)
1 ($tRNA^{Ser}_{AGA}$)	**0.031**	**3.0**
2 ($tRNA^{Ser}_{UGA}$)	0.042	1.9
3 ($tRNA^{Ser}_{GCU}$)	0.025	1.5
4 ($tRNA^{Leu}_{CAA}$)	0.048	1.5
5 ($tRNA^{Leu}_{CAG}$)	**0.015**	**0.4**
6 ($tRNA^{Leu}_{AAG}$)	0.041	4.6
8 ($tRNA^{Arg}_{ACG}$)	**0.058**	**8.4**

The data incompatible with our hypothesis are labeled out with gray color.
The major tRNAs are emphasized with bold character.

From the data shown in Tab. 5.1, it was found that among 7 tRNAs tested, 5 tRNAs, namely, $tRNA^{Leu}_{CAG}$, $tRNA^{Ser}_{AGA,}$ $tRNA^{Arg}_{ACG}$ (the three major tRNAs for the amino acids) and $tRNA^{Ser}_{GCU}$, $tRNA^{Leu}_{AAG}$ fit in our hypothesis. The other 2 tRNAs, ($tRNA^{Ser}_{UGA}$ and $tRNA^{Leu}_{CAA}$) bound to exportin-t with higher affinities than expected. This incompatibility may be due to the following three possible reasons. 1. It was presumed that the aminoacylation efficiency and recognition by eEF1A of all tRNAs are the same; it is too simplistic for the real events in cells. Now the sequencing of bovine genome is under the way. 2. There might be some regulatory tRNAs in cells, which are exported with priority and accomplish their functions in the cytoplasm. 3. The numbers of tRNA genes and codon frequency used were from the database of human, but the

tRNAs used in the experiments were of bovine origin. Though a very close homology exists between the two species, some difference might be neglected by us.

Up to date, different roles of different tRNA species are mostly studied in the prokaryotic system. It is interesting to find that in *E.coli*, the tRNAs with the smallest ratio of tRNA amount to codon frequency are the most sensitive to amino acid starvation and their codons are used in regulatory elements (Elf *et al.*, 2001); whereas in mammalian cells, the tRNAs with the smallest ratio of tRNA amount to codon frequency are likely to be the fastest exported out into cytoplasm. $tRNA^{Leu}_{CAG}$, the major tRNA both in *E.coli* and in mammalian cells, was tested to be sensitive to amino acid starvation (Dittmar *et al.*, 2005) and also was the strongest bindable tRNA to exportin-t among tRNAs tested.

5.5 AFM imaging of exportin-t-esterase and its interaction with tRNA and Ran·GppNHp

Atomic force microscopy is receiving more and more attention among biologists because it provides a platform to study proteins and other biological molecules in their native and undisturbed state on a scale of nanometer. The technical difficulty lies in the immobilization of bio-molecules on the surface, without which the random movement of the molecules would greatly compromise the image resolution.

In our lab a method of immobilizing proteins to the TFK-modified mica surface via the interaction of TFK and esterase was used. TFK is an inhibitor of esterase and binds to the enzyme very strongly with a K_D of 6 nM. In the present study they were shown to be excellent partners for immobilizing proteins on mica surface. The purified NADOX-esterase was immobilized on the TFK-modified mica surface and produced sharp images under AFM.

Unfortunately, though the gene of exportin-t-esterase was inserted in a plasmid with success, the target protein could not be expressed in *E.coli*. We had to use this plasmid containing exportin-t-esterase gene as template in *in vitro* translation, and the recombinant protein was produced and showed esterase activity, inferring that the protein had a complete sequence of exportin-t because it was located at the N terminus of

esterase. In the experiments, the particles of exportin-t-esterase sample were determined to be 15 ± 2 nm. $tRNA^{Arg}_{E.c}$ and Ran·GppNHp were added to the immobilized exportin-t-esterase. The complex was shown to increase its diameter by about 1 nm.

Fukuhara *et al.* (2004) used X-ray scattering to study the shape of exportin-t and the ternary complex of exportin-t·tRNA·Ran·GTP. In their experiments exportin-t was of 16 ± 2 nm, the complex was of 11 ± 1 nm. In their experiments, the diameter of exportin-t·tRNA·Ran·GTP complex did not increase, but decreased by 5 nm, compared with free exportin-t. This is in variance with our results. We have tried to separate the ternary complex exportin-t·tRNA·Ran·GTP from exportin-t by gel permeation chromatography, but they were inseparable, inferring that they had similar dimensions. If the diameter of the complex decreased by 5 nm (nearly 31% of the original sized of exportin-t) as claimed by Fukuhara *et al.*, it should be separated from the free exportin-t by gel permeation chromatography. There was another discrepancy, because Fukuhara *et al.* reported to have separated the exportin-t·tRNA·Ran·GTP from free exportin-t by gel permeation chromatography. Anyway, after binding its cargo tRNA, exportin-t seemed to change to a more compact conformation, which showed a similar diameter even after the molecular mass of the complex was increased by 50 kDa, nearly half of exportin-t itself. The conclusion was also confirmed by Fukuhara *et al.* (2004). The conformation of exportin-t must be very elastic in solution, because the efforts to crystallize exportin-t or the complex of exportin-t·tRNA·Ran·GTP never succeed in several research groups. Other novel methods and more experiments are required to illuminate the structure of exportin-t.

6 Summary

In this thesis the ternary complex of tRNA·exportin-t·Ran·GTP was studied by biochemical and biophysical methods. Firstly, photocrosslinking was used to determine the contact sites between tRNA and exportin-t. 4-Thiouridine (s^4U) was introduced into $tRNA^{Phe}_{T.th}$ by *in vitro* transcription with T7 RNA polymerase and crosslinked to exportin-t by irradiation at 312 nm. The crosslinking was Ran·GTP dependent and could be competitively inhibited by other tRNA species, showing that the crosslinking was the consequence of the formation of a tRNA·exportin-t·Ran·GTP complex. The crosslinked complex of (s^4U)$tRNA^{Phe}_{T.th}$-exportin-t after proteinase K digestion was incubated with a primer complementary to the 3′end of the $tRNA^{Phe}_{T.th}$ in the primer extension reaction. The elongation of the reverse transcriptase was forced to halt at s^4Us crosslinked to peptides, namely, U55, U47, U33, U20. Among them, U47 and U55 were shown to be the major crosslinking sites. U47A mutation was introduced into $tRNA^{Phe}_{T.th}$ to test the role of U47. The mutant $tRNA^{Phe}_{T.th}$ transcript was still able to bind exportin-t, though a little weaker than normal $tRNA^{Phe}_{T.th}$ transcript. In contrast, s^4U containing mutant $tRNA^{Phe}_{T.th}$ U47A exhibited a much poorer capability to crosslink exportin-t. It is concluded that U47 may be a major contact site between $tRNA^{Phe}_{T.th}$ and exportin-t.

Secondly, the binding abilities of different tRNA species in calf liver $tRNA^{Bulk}$ to exportin-t was examined by affinity chromatography on immobilized exportin-t. With a stepwise elution of 250 mM and 500 mM KCl, $tRNA^{Bulk}$ was fractionated into 2 peaks. Therefore, Different tRNAs bound to exportin-t with different affinity. Among 7 tRNAs tested, the relative affinity to exportin-t ranked as $tRNA^{Leu}_{CAG} > tRNA^{Ser}_{GCU}$, $tRNA^{Leu}_{CAA}$, $tRNA^{Ser}_{UGA} > tRNA^{Ser}_{AGA}$, $tRNA^{Leu}_{AAG} > tRNA^{Arg}_{ACG}$. To interpret the different affinity of tRNAs to exportin-t, it is proposed that exportin-t preferentially exports tRNAs that are required the stronger by the protein synthesis machine. The extent of requirement of a specific tRNA by cells is supposed as the ratio between the tRNA concentration in a cell and its codon frequency in the genome, if all tRNAs are supposed to be aminoacylated and transported to ribosome equally. It was found that among 7 tRNAs identified on the

2D urea PAGE, the theoretical estimation of 5 tRNA species upon their requirement by cell ranked the same as their relative affinity to exportin-t.

Finally, atomic force microscopy was used to observe exportin-t and its interaction with tRNA in a native and undisturbed state directly. Exportin-t-esterase, immobilized to trifluoromethyl ketone (TFK) modified mica surface, showed a diameter of 15 ± 2 nm. After binding tRNA and Ran·GppNHp, the diameter of the complex somewhat increased to 16 ± 2 nm.

7 Zussamenfassung

In dieser Doktorarbeit wurde die ternäre Komplexbildung von tRNA mit Exportin-t·Ran·GTP durch biochemische und biophysikalische Methoden untersucht. Zunächst wurden die Kontaktstellen zwischen tRNA und Exportin-t durch Licht-induzierte Quervernetzung (Photocrosslinking) bestimmt. Hierzu wurde 4-Thiouridin (s^4U) über *in vitro* Transkription mit T7 RNA Polymerase in $tRNA^{Phe}_{T.th}$ eingebaut und mit Licht bei 312 nm bestrahlt. Die Quervernetzung war Ran·GTP abhängig und konnte durch andere tRNA kompetitiv inhibiert werden. Beides unterstreicht die spezifische und produktive Komplexbildung unter den Meßbedingungen. Proteinase K Verdau des (s^4U)$tRNA^{Phe}_{T.th}$ Komplexes und Reverse Transkriptase-abhängige Primer-Verlängerung erlaubte die Positionen quervernetzter Nukleotide zu ermitten. Der Transkriptionsarrest erfolgte an den Positionen U55, U47, U33 und U20, wobei U47 und U55 die Hauptprodukte darstellten. Mutation von U47 zu A (U47A) sollte die Bedeutung dieser Position klären, wobei das mutierte Transkript von Exportin-t ohne große Affinitätseinbußen gebunden wurde. Die gesamte Quervernetzungsausbeute des U47A-Transkripts verringerte sich aber bei durchgängiger s^4U-Modifikation deutlich. Die Position 47 erscheint daher als wichtige Kontaktstelle für die Bindung an Exportin-t.

Als Zweites wurden die Bindungsstärken verschiedener tRNA Spezies aus Kalbsleber durch Affinitätschromatographie mittels immobiliserten Exportin-t untersucht. Die stufenweise Elution mit 250 mM und 500 mM KCl erlaubte die Fraktionierung der Total-tRNA in zwei Hauptgruppen. Es scheinen daher deutlich unterschiedliche Bindungsaffinitäten für verschiedene tRNA vorzuliegen. Bei den untersuchten tRNA nimmt die relative Affinität für Exportin-t in der Reihenfolge $tRNA^{Leu}_{CAG} > tRNA^{Ser}_{GCU}$, $tRNA^{Leu}_{CAA}$, $tRNA^{Ser}_{UGA} > tRNA^{Ser}_{AGA}$, $tRNA^{Leu}_{AAG} > tRNA^{Arg}_{ACG}$ ab. Als mögliche Erklärung der Unterschiede kann darin liegen, daß Exportin-t preferentiell diejenigen tRNA aus dem Kern transportiert die am Notwendigsten für die Aufrechterhaltung der Proteinbiosynthese sind. Als Maß der tRNA-Bedeutung wurde das Verhältnis zwischen der zellulären Konzentration einer bestimmten tRNA und ihrer Codon-Häufigkeit im Genom gewählt. Unter der Vorraussetzung das in erster Näherung alle tRNA gleich

aminoacyliert und gleiche Affinität zum Ribosom aufweisen, korrellierten 5 der 7 tRNAs mit der experimentell durch Zweidimensionale-PAGE beobachteten Abstufung.

In einem dritten Arbeitsbereich wurde die Rasterkraftmikroskopie verwendet um Exportin-t und seine Wechselwirkung mit tRNA in einem nativen Zustand direkt zu untersuchen. Exportin-t-Esterase wurde auf Trifluoromethylketone(TFK)-modifizierter Silika immobilisiert und zeigte einen Partikeldurchmesser von 15±2 nm in der freien Form und 16±2 nm im Komplex mit tRNA und Ran·GppNHp.

8 Literature

Adam SA, Marr RS, Gerace L. (**1990**). Nuclear protein import in permeabilized mammalian cells requires soluble cytoplasmic factors.. *J. Cell Biol.* **111**, 807-16

Arts GJ, Fornerod M, Mattaj IW. (**1998a**). Identification of a nuclear export receptor for tRNA. *Curr. Biol*. **8**, 305-14

Arts GJ, Kuersten S, Romby P, Ehresmann B, Mattaj IW. (**1998b**). The role of exportin-t in selective nuclear export of mature tRNAs. *EMBO J.* **17**, 7430-41

Askjaer P, Jensen TH, Nilsson J, Englmeier L, Kjems J. (**1998**). The specificity of the CRM1-Rev nuclear export signal interaction is mediated by RanGTP. *J Biol. Chem*. **273**, 33414-22

Baron C, Bock A. (**1991**). The length of the aminoacyl-acceptor stem of the selenocysteine-specific $tRNA^{Sec}$ of *Escherichia coli* is the determinant for binding to elongation factors SELB or Tu. *J Biol Chem.* **266**, 20375-9

Bischoff FR, Görlich D. (**1997**). RanBP1 is crucial for the release of RanGTP from importin beta-related nuclear transport factors. *FEBS Lett*. **419**, 249-54

Björk GR. (**1992**). The role of modified nucleosides in tRNA interactions, in *Transfer RNA in Protein Synthesis.* eds Hatfield DL, Lee BJ, Pirtle RM. CRC Press, Boca Raton, Fla

Bohnsack MT, Czaplinski K, Görlich D. (**2004**). Exportin 5 is a RanGTP-dependent dsRNA-binding protein that mediates nuclear export of pre-miRNAs. *RNA* **10**, 185-91

Carazo-Salas RE, Guarguaglini G, Gruss OJ, Segref A, Karsenti E, Mattaj IW. (**1999**). Generation of GTP-bound Ran by RCC1 is required for chromatin-induced mitotic spindle formation. *Nature* **400**, 178-81

Cermakian N, McClain WH, Cedergren R. (**1998**). tRNA nucleotide 47: an evolutionary enigma. *RNA* **4**, 928-36

Chook YM, Blobel G. (**2001**). Karyopherins and nuclear import. *Curr. Opin. Struc. Biol.* **11**, 703-15

Cingolani G, Lashuel HA, Gerace L, Müller CW. (**2000**). Nuclear import factors importin alpha and importin beta undergo mutually induced conformational changes upon association. *FEBS Lett.* 484, 291-8

Cullen BR. (**2003**). Nuclear RNA export. *J. Cell Sci.* **116**, 587-97

Derwenskus KH, Fischer W, Sprinzl M. (**1984**). Isolation of tRNA isoacceptors by affinity chromatography on immobilized bacterial elongation factor Tu. *Anal. Biochem*. **136**, 161-7

Dingwall C, Sharnick SV, Laskey RA. (**1982**). A polypeptide domain that specifies migration of nucleoplasmin into the nucleus. *Cell* **30**, 449-58

DirHeimer G, Keith G, Dumas P, Westhof E. (**1995**). tRNA: Structure, Biosynthesis, and Function. © 1995 American Society for Microbiology

Dittmar KA, Sorensen MA, Elf J, Ehrenberg M, Pan T. (**2005**). Selective charging of tRNA isoacceptors induced by amino-acid starvation. *EMBO Rep.* **6**, 151-7.

Dong H, Nilsson L, Kurland CG. (**1996**). Co-variation of tRNA abundance and codon usage in Escherichia coli at different growth rates. *J Mol. Biol.* **260**, 649-63

Drake B, Prater CB, Weisenhorn AL, Gould SA, Albrecht TR, Quate CF, Cannell DS, Hansma HG, Hansma PK. (**1989**). Imaging crystals, polymers, and processes in water with the atomic force microscope. *Science*. **243**,1586-9

Dube SK, Marcker KA, Clark BEC, Cory S. (**1968**). Nucleotide sequence of N-formyl-methionyl-transfer RNA. *Nature* **218**, 232-3

Edqvist J, Straby KB, Grosjean H. (**1993**). Pleiotrophic effects of point mutations in yeast tRNA(Asp) on the base modification pattern. *Nucleic Acids Res*. **21**, 413-7

Ehresmann B, Imbault P, Weil JH. (**1973**). Spectrophotometric determination of protein concentration in cell extracts containing tRNAs and rRNAs. *Biochem.* **54**, 454–463

Elf J, Nilsson D, Tenson T, Ehrenberg M. (**2003**). Selective charging of tRNA isoacceptors explains patterns of codon usage. *Science*. **300**,1718-22

Engel A, Muller DJ. (**2000**). Observing single biomolecules at work with the atomic force microscope. *Nat Struct Biol.* 7, 715-8

Fahrenkrog B, Stoffler D, Aebi U. (**2001**). Nuclear pore complex architecture and functional dynamics. *Curr. Top. Microbiol. Immunol*. **259**, 95-117

Faulhamer HG, Joshi RL. (**1987**). Structural features in aminoacyl-tRNA binding and peptide bond formation in *Escherichia coli* translation. *J. Mol. Biol.* **211**, 739-49

Favre A. (1990) 4-Thiouridine as an intrinsic photoaffinity probe of nucleic acid structure and interactions. in *Bioorganic Photochemistry: Photochemistry and the Nucleic Acids.* eds Morrison H, Wiley. New York

Favre A, Saintome C, Fourrey JL, Clivio P, Laugâa P. (**1998**). Thionucleobases as intrinsic photoaffinity probes of nucleic acid structure and nucleic acid-protein interactions. *J Photochem. Photobiol. B.* **42**, 109-24

Forchhammer K, Leinfelder L, Böck A. (**1989**). Identification of a novel translation factor necessary for the incorporation of selenocysteine into protein. *Nature* 342, 453-6

Fornerod M, Ohno M, Yoshida M, Mattaj IW. Crm 1 is an export receptor for leucin-rich nuclear export signals. (**1997**). *Cell* **90**:1051-60

Förster C, Ott G, Forchhammer K, Sprinzl M. (**1990**). Interaction of a selenocysteine-incorporating tRNA with elongation factor Tu from *E.coli*. *Nucleic Acids Res.* **18**, 487-91

Fukuhara N, Fernandez E, Ebert J, Conti E, Svergun D. (**2004**). Conformational variability of nucleo-cytoplasmic transport factors. *J Biol. Chem*. ;279, 2176-81

Gadal O, Strauss D, Kessl J, Trumpower B, Tollervey D, Hurt E. (**2001**). Nuclear export of 60s ribosomal subunits depends on Xpo1p and requires a nuclear export sequence-containing factor, Nmd3p, that associates with the large subunit protein Rpl10p. *Mol Cell Biol*. **21**, 3405-15

Gehrke CW, Kuo KC. (**1989**). Ribonucleoside analysis by reversed-phase high-performance liquid chromatography. J Chromatogr. 471, 3-36

Giegé R, Puglisi JD, Florentz C. (**1993**). tRNA structure and aminoacylation efficiency. *Prog Nucleic Acid Res Mol Biol.* **45**, 129-206

Goldfarb DS, Gariepy J, Schoolnik G, Kornberg RD. (**1986**). Synthetic peptides as nuclear localization signals *Nature* **322**:641-4

Goldgur Y, Mosyak L, Reshetnikova L, Ankilova V, Lavrik O, Khodyreva S, Safro M. (**1997**). The crystal structure of phenylalanyl-tRNA synthetase from *thermus thermophilus* complexed with cognate $tRNA^{Phe}$. *Structure*. **5**, 59-68

Gunasekera N, Lee SW, Kim S, Musier-Forsyth K, Arriaga E. (**2004**). Nuclear localization of aminoacyl-tRNA synthetases using single-cell capillary electrophoresis laser-induced fluorescence analysis. *Anal Chem*. **76**, 4741-6

Görlich D, Mattaj IW. (**1996**). Nucleocytoplasmic transport. *Science* **271**, 1513-8

Görlich D. (**1998**). Transport into and out of the cell nucleus. *EMBO J*. **17**, 2721-7

Grosshans H, Hurt E, Simos G. (**2000**). An aminoacylation-dependent nuclear tRNA export pathway in yeast. *Genes. Dev*. **14**, 830-40

Hajnsdorf E, Favre A, Expert-Bezancon A. (**1986**). Multiple crosslinks of proteins S7, S9, S13 to domains 3 and 4 of 16S RNA in the 30S particle. *Nucleic Acids Res.* **14**, 4009-23

Harrington KM, Nazarenko IA, Dix DB, Thompson RC, Uhlenbeck OC. (**1993**). In vitro analysis of translational rate and accuracy with an unmodified tRNA. *Biochemistry* **32**, 7617-22

Hellmuth K, Lau DM, Bischoff FR, Kunzler M, Hurt E, Simos G. (**1998**). Yeast Los1p has properties of an exportin-like nucleocytoplasmic transport factor for tRNA. *Mol. Cell Biol.* **18**, 6374-86

Holley RW, Apgar J, Everett GA, Madison JT, Marquisee M, Merrill SH, Penswick JR, Zamir A. (**1965**). Structure of a ribonucleic acid. *Science* **19**,147:1462-5

Helm M, Attardi G. (**2004**). Nuclear control of cloverleaf structure of human mitochondrial $tRNA^{Lys}$. *J Mol. Biol*. 337, 545-60

Hurt DJ, Wang SS, Lin YH, Hopper AK. (**1987**). Cloning and characterization of LOS1, a Saccharomyces cerevisiae gene that affects tRNA splicing. *Mol. Cell Biol*. **7**, 1208-16

Ikemura T. (**1981**). Correlation between the abundance of Escherichia coli transfer RNAs and the occurrence of the respective codons in its protein genes: a proposal for a synonymous codon choice that is optimal for the E. coli translational system. *J Mol. Biol*. **151**, 389-409

Ikemura T, Ozeki H. (**1983**). Codon usage and transfer RNA contents: organism-specific codon-choice patterns in reference to the isoacceptor contents. *Cold Spring Harb Symp Quant Biol.* **47** Pt 2, 1087-97

Izaurralde E, Kutay U, von Kobbe C, Mattaj IW, Görlich D. (**1997**). The asymmetric distribution of the constituents of the Ran system is essential for transport into and out of the nucleus. *EMBO J.* **16**, 6535-47

Jarmolowski A, Boelens WC, Izaurralde E, Mattaj IW. (**1994**). Nuclear export of different classes of RNA is mediated by specific factors. *J Cell Biol*. **124**, 627-35

Kang Y, Cullen BR. (1999). The human Tap protein is a nuclear mRNA export factor that contains novel RNA-binding and nucleocytoplasmic transport sequences. *Genes. Dev.* **13**, 1126-39

Kalderon D, Roberts BL, Richardson WD, Smith AE. (**1984**). A short amino acid sequence able to specify nuclear location. *Cell* **39**, 499-509

Kim SH, Quigley GJ, Suddath FL, McPherson A, Sneden D, Kim JJ, Weinzierl J, Rich A. (**1973**).Three-dimensional structure of yeast phenylalanine transfer RNA: folding of the polynucleotide chain. *Science* **179**, 285-8

Kim SH. (**1979**). Crystal structure of yeast tRNAPhe and general structural features on other tRNAs. Transfer RNA: Structure, properties, and recognition © 1979 by Cold Spring Harbor Laboratory

Kiseleva E, Goldberg MW, Allen TD, Akey CW. (**1998**). Active nuclear pore complexes in Chironomus: visualization of transporter configurations related to mRNP export. *J. Cell. Scl*. **111(Pt2)**, 223-6

Komine Y, Adachi T, Inokuchi H, Ozeki H. (**1990**). Genomic organization and physical mapping of the transfer RNA genes in Escherichia coli K12. *J Mol Biol*. **212**, 579-98

Kroll H. (**1951**). The Participation of Heavy Metal Ions in the Hydrolysis of Amino Acid esters. *J Am. Chem. Soc.* **74**, 2036-2039

Kruse C, Willkomm DK, Grunweller A, Vollbrandt T, Sommer S, Busch S, Pfeiffer T, Brinkmann J, Hartmann RK, Müller PK. (**2000**). Export and transport of tRNA are coupled to a multi-protein complex. *Biochem J.* **346**, 107-15

Kuersten S, Arts GJ, Walther TC, Englmeier L, Mattaj IW. (**2002**). Steady-state nuclear localization of exportin-t involves RanGTP binding and two distinct nuclear pore complex interaction domains. *Mol. Cell Biol*. **22**, 5708-20

Kumar RK, Davis DR. (**1997**). Synthesis and studies on the effect of 2-thiouridine and 4-thiouridine on sugar conformation and RNA duplex stability. *Nucleic Acids Res*. **25**, 1272-80

Kutay U, Lipowsky G, Izaurralde E, Bischoff FR, Schwarzmaier P, Hartmann E, Görlich D. (**1998**). Identification of a tRNA-specific nuclear export receptor. *Mol. Cell* **1**, 359-69

Kuwabara T, Warashina M, Sano M, Tang H, Wong-Staal F, Munekata E, Taira K. (**2001**). Recognition of engineered tRNAs with an extended 3′ end by Exportin-t (Exportin-t) and transport of tRNA-attached ribozymes to the cytoplasm in somatic cells. *Biomacromolecules* 2, 1229-42

Laemmli UK. (**1970**). Cleavage of structural proteins during the assembly of the head of bacteriophage T4. *Nature* **227**, 680–685

Lander ES, Linton LM, Birren B, Nusbaum C, Zody MC, Baldwin J,Devon K, Dewar K, Doyle M, FitzHugh W, Funke R et al. (**2001**). Initial sequencing and analysis of the human genome. *Nature* **409**, 860-921

Leinfelder W, Zehelein E, Mandrand-Berthelot mA, Bock A. (**1988**). Gene for a novel tRNA species that accepts L-serine and contranslationally inserts selenocysteine. *Nature* **331**, 723-5

Leibundgut M, Frick C, Thanbichler M, Bock A, Ban N. (**2005**). Selenocysteine tRNA-specific elongation factor SelB is a structural chimaera of elongation and initiation factors. *EMBO J*. **24**, 11-22

Lipowsky G, Bischoff FR, Izaurralde E, Kutay U, Schafer S, Gross HJ, Beier H, Görlich D. (**1999**). Coordination of tRNA nuclear export with processing of tRNA. *RNA* **5**, 539-49

Lipsett MN. (**1965**). The isolation of 4-thiouridylic acid from the soluble ribonucleic acid of *Escherichia coli*. *J Biol. Chem.* **240**, 3975-8

Lund,E. and Dahlberg,J.E. (1998). Proofreading and aminoacylation of tRNAs before export from the nucleus. *Science* **282,** 2082-2085.

Macara IG. (**2001**). Transport into and out of the nucleus. *Micro. Mol. Biol. Rev.* **65**, 570-94

Maglott EJ, Deo SS, Przykorska A, Glick GD. (**1998**). Conformational transitions of an unmodified tRNA: implications for RNA folding. *Biochemistry* **37**, 16349-59

Mattaj IW, Englmeier L. (**1998**). Nucleocytoplasmic transport: the soluble phase. *Annu. Rev. Biochem*. **67**, 265-30

McClain WH, Foss K, Jenkins RA, Schneider J. (**1991**). Rapid determination of nucleotides that define $tRNA^{Gly}$ acceptor identity. *Proc. Natl. Acad, Sci. USA* **88**, 6147-51

McGregor A, Rao MV, Duckworth G, Stockley PG, Connolly BA. (**1996**). Preparation of oligoribonucleotides containing 4-thiouridine using Fpmp chemistry. Photo-crosslinking to RNA binding proteins using 350 nm irradiation. *Nucleic Acids Res*. **24**, 3173-80

Melton DA, Robertis EM, Cortese R. (**1980**). Order and intracellular location of the events involved in the maturation of a spliced tRNA. *Nature* **284**, 143-8

Miller J. (**1972**). *Experiments in molecular genetics.* Cold Spring Harbour Laboratory Press, Cold Spring Harbor

Milligan JF, Uhlenbeck OC. (**1989**). Synthesis of small RNAs using T7 RNA polymerase. *Methods Enzymol*. **180**, 51-62

Moor NA, Favre A, Lavrik OI. (**1998**). Covalent complex of phenylalanyl-tRNA synthetase with 4-thiouridine-substituted tRNA(Phe) gene transcript retains aminoacylation activity. *FEBS Lett.* 427, 1-4.

Moor NA, Ankilova VN, Lavrik OI, Favre A. (**2001**). Determination of tRNA(Phe) nucleotides contacting the subunits of Thermus thermophilus phenylalanyl-tRNA synthetase by photoaffinity crosslinking. *Biochim. Biophys. Acta*. **1518**, 226-36

Mosammaparast N, Pemberton LF. (**2004**). Karyopherins: from nuclear-transport mediators to nuclear-function regulators. *Trends Cell Biol*. **14**, 547-56

Moy TI, Silver PA. (**1999**). Nuclear export of the small ribosomal subunit requires the ran-GTPase cycle and certain nucleoporins. *Genes Dev*. **13**, 2118-33

Muhlhausser P, Muller EC, Otto A, Kutay U. (**2001**). Multiple pathways contribute to nuclear import of core histones. *EMBO Rep*. **2**, 690-6

Nakanishi K, Nureki O. (**2005**). Recent progress of structural biology of tRNA processing and modification. *Mol Cells.* **19**, 157-66

Nemergut ME, Mizzen CA, Stukenberg T, Allis CD, Macara IG. (**2001**). Chromatin docking and exchange activity enchancement of RCC1 by histones H2A and H2B. *Science* **292**, 1540-3

Nissen P, Kjeldgaard M, Thirup S, Polekhina G, Reshetnikova L, Clark BF, Nyborg J. (**1995**). Crystal structure of the ternary complex of Phe-tRNAPhe, EF-Tu, and a GTP analog. *Science* **270**, 1464-72

Nordin BE, Schimmel P. (**2002**). Plasticity of recognition of the 3'-end of mischarged tRNA by class I aminoacyl-tRNA synthetases. *J Biol. Chem.* **277**, 20510-7

Ohno M, Segref A, Bachi A, Wilm M, Mattaj IW. (**2000**). PHAX, a mediator of U snRNA nuclear export whose activity is regulated by phosphorylation. *Cell* **101**, 187-98

Osswald M, Doring T, Brimacombe R. (**1995**). The ribosomal neighbourhood of the central fold of tRNA: cross-links from position 47 of tRNA located at the A, P or E site. *Nucleic Acids Res*. **23**, 4635-41.

Piehler J, Brecht A, Valiokas R, Liedberg B, Gauglitz G. (2000). A high-density poly(ethylene glycol) polymer brush for immobilization on glass-type surfaces. Biosens Bioelectron. 2000;15(9-10):473-81

Quimby BB, Dasso M. (2003). The small GTPase Ran: interpreting the signs. *Curr. Opin. Cell Biol.* **15**, 338-44

Reichelt R, Holzenburg A, Buhle EL Jr, Jarnik M, Engel A, Aebi U. (**1990**). Correlation between structure and mass distribution of the nuclear pore complex and of distinct pore complex components. *J. Cell. Biol*. **110**, 883-94

Rodriguez MS, Dargemont C, Stutz F. (**2004**). Nuclear export of RNA. *Biol. Cell* **96**, 639-55

Sambrook J, Russel DW. Molecular Cloning: A Laboratory Manual. Cold Spring Harbor Laboratory Press.

Schlenstedt G, Wong DH, Koepp DM, Silver PA. (**1995**). Mutants in a yeast Ran binding protein are defective in nuclear transport. *EMBO J*. **14**, 5367-78

Schofield P, Zamecnik PC. (**1968**). Cupric ion catalysis in hydrolysis of aminoacyl-tRNA. *Biochim Biophys Acta.* **155**, 410-6

Shaheen HH, Hopper AK. (**2005**). Retrograde movement of tRNAs from the cytoplasm to the nucleus in *Saccharomyces cerevisiae*. *Proc. Natl. Acad. Sci. U S A.* **102**, 11290-5

Sharp PM, Matassi G. (**1994**). Codon usage and genome evolution. *Curr. Opin. Genet. Dev.* **4**, 851-60

Sherman JM, Rogers MJ, Söll D. (**1992**). Competition of aminoacyl-tRNA synthetases for tRNA ensures the accuracy of aminoacylation. *Nucleic Acids Res.* **20**, 1547-52

Shi PY, Maizels N, Weiner AM. (**1998**). CCA addition by tRNA nucleotidyltransferase: polymerization without translocation? *EMBO J*. **17**, 3197-206

Sontheimer EJ, Steitz JA. (**1993**). The U5 and U6 small nuclear RNAs as active site components of the spliceosome. *Science* **262**, 1989-96

Sprinzl M, Vassilenko KS. (**2005**). Compilation of tRNA sequences and sequences of tRNA genes. *Nucleic Acids Res*. **33**, D139-40

Sprinzl M, Meissner JMF, Hartmann T. (**1993**). Elongation factor Tu from *Thermus thermophilus*, strucutre, domain and interactions. in *The Translation Apparatus*, eds. Nierhaus, KH., Franceschi F, Subramanian AR, Erdmann VA. & Wittmann-Liebold, B. (Plenum, New York)

Sprinzl M, Gauss DH. (**1984**). Compilation of sequences of tRNA genes. *Nucleic Acids Res.* **12 Suppl**, r59-131

Sprinzl M, Sternbach H. (**1979**). Enzymic modification of the C-C-A terminus of tRNA. *Methods Enzymol.* **59**, 182-90

Steinberg S, Cedergren R. (**1994**). Structural compensation in atypical mitochondrial tRNAs. *Nat Struct Biol*. **1**, 507-10

Steinberg S, Ioudovitch A. (**1996**). A role for the bulged nucleotide 47 in the facilitation of tertiary interactions in the tRNA structure. *RNA* **2**, 84-87

Steiner-Mosonyi M, Mangroo D. (**2004**). The nuclear tRNA aminoacylation-dependent pathway may be the principal route used to export tRNA from the nucleus in Saccharomyces cerevisiae. *Biochem J.* **378**, 809-16

Takano A, Endo T, Yoshihisa T. (**2005**). tRNA actively shuttles between the nucleus and cytosol in yeast. *Science* **309**, 140-2

Wiese C, Wilde A, Moore MS, Adam SA, Merdes A, Zheng Y. (**2001**). Role of importin-beta in coupling Ran to downstream targets in microtubule assembly. *Science* **291**, 653-6

Wollenzien P, Expert-Bezancon A, Favre A. (**1991**). Sites of contact of mRNA with 16S rRNA and 23S rRNA in the Escherichia coli ribosome. *Biochemistry* **30**, 1788-95

Yamaguchi R, Newport J. (**2003**). A role for Ran-GTP and Crm1 in blocking replication. *Cell* **113**, 115-25

Yoshida K, Blobel G. (**2001**). The karyopherin Kap142p/Msn5p mediates nuclear import and nuclear export of different cargo proteins. *J Cell Biol*. **152**, 729-40

Zagryadskaya EI, Kotlova N, Steinberg SV. (**2004**). Key elements in maintenance of the tRNA L-shape. *J Mol. Biol.* **340**, 435-44

Zasloff M. (**1983**). tRNA transport from the nucleus in a eukaryotic cell: carrier-mediated translocation process. *Proc Natl Acad Sci U S A* **80**, 6436-40

9 Acknowledgement

First of all, I would like to thank Prof. Dr. M. Sprinzl, who gave me the opportunity to work in his group, from whom I have learnt so much.
And I would like to thank Dr. Alexandra Wolfrum, who led me into this study and gave me generous support.
And I would like to thank Antje Doppel, Norbert Grillenbick, Petra Zippelius, Yiran Wang, Dr. Yiwei Huang, Dong Han for their invaluable help.
And I would like to thank all colleagues in Lehrstuhl für Biochemie. This is a wonderful research group.
Finally I would like to thank my parents who are always backing me, whatever I do and wherever I am.

Erklärung

Hermit erkläre ich, dass ich die Arbeit selbstständig verfasst und keine anderen als die angegebenen Quellen und Hilfsmittel benutzt habe.

Ferner erkläre ich, dass ich anderweitig mit oder ohne Erfolg nicht versucht habe, eine Dissertation einzureichen oder mich der Doktorprüfung zu unterziehen.

Bayreuth, 12. June, 2006

Sheng Li